TECHNICAL REPORT STANDARD TITLE PAGE

1. Report No.	2. Government Accession No.	3. Recipient's Catalog No.
Research Report 168-1F		

4. Title and Subtitle	5. Report Date
Torsional Stresses in Prestressed Concrete Bridge Beams	April 1973
	6. Performing Organization Code
7. Author(s)	8. Performing Organization Report No.
Eugene Buth	
9. Performing Organization Name and Address	10. Work Unit No.
Texas Transportation Institute Texas A&M University College Station, Texas 77843	11. Contract or Grant No. Research Project 2-5-72-168
	13. Type of Report and Period Covered
12. Sponsoring Agency Name and Address	Final--September 1971 April 1973
Texas Highway Department 11th and Brazos Austin, Texas 78701	14. Sponsoring Agency Code

15. Supplementary Notes

Research performed in cooperation with DOT, FHWA
Research Study Title: "Combined Torsion and Flexure in Prestressed Concrete Bridge Beams"

16. Abstract

The behavior of the Texas Highway Department 54-in. prestressed concrete bridge beam under combined torsional and transverse loads was studied. Elastic theory and maximum tensile stress failure criterion were used to develop a theoretical failure envelope. Deflection, rotation and strain measurements were made on edge beams in two structures during placement of the deck. Load induced strains were of such small magnitude in comparison to other transient strain responses that the effective loads actually carried by the beam could not be determined with reasonable accuracy from the data.

17. Key Words	18. Distribution Statement
Prestressed concrete, beam, concrete bridge, torsion, shear, bending and combined loadings	

19. Security Classif. (of this report)	20. Security Classif. (of this page)	21. No. of Pages	22. Price
Unclassified	Unclassified	113	

Form DOT F 1700.7 (8-69)

TORSIONAL STRESSES IN PRESTRESSED CONCRETE BRIDGE BEAMS

by

Eugene Buth
Assistant Research Engineer

Research Report 168-1F

Combined Torsion and Flexure in
Prestressed Concrete Bridge Beams

Research Project 2-5-72-168

Sponsored by

The Texas Highway Department
in Cooperation with
The U.S. Department of Transportation Federal Highway Administration

April 1973

Texas Transportation Institute
Texas A&M University
College Station, Texas

TABLE OF CONTENTS

ACKNOWLEDGMENTS

The information contained in this report was developed on a cooperative research study sponsored jointly by the Texas Highway Department and the Federal Highway Administration. Liaison was maintained through Mr. Charles Covill, contact representative for the Texas Highway Department.

The contents of this report reflect the views of the author who is responsible for the facts and the accuracy of the data presented herein. The contents do not necessarily reflect the official views or policies of the Federal Highway Administration. This report does not constitute a standard, specification or regulation.

ABSTRACT

The behavior of the Texas Highway Department 54-in. prestressed concrete bridge beam under combined torsional and transverse loads was studied. Elastic theory and maximum tensile stress failure criterion were used to develop a theoretical failure envelope. Deflection, rotation and strain measurements were made on edge beams in two structures during placement of the deck. Load induced strains were of such small magnitude in comparison to other transient strain responses that the effective loads actually carried by the beam could not be determined with reasonable accuracy from the data.

Key words: Prestressed concrete, beam, concrete bridge, torsion, shear, bending and combined loadings.

SUMMARY

The behavior of the Texas Highway Department 54-in. prestressed bridge beam under combined torsional and bending loads was studied. Reported research on concrete members of various cross sections was used to develop theoretical predictions of the behavior of the THD 54-in. beam. An interaction surface diagram for this beam was developed. The diagram describes the three-way interaction between bending moment, shear and torque. The occurrence of initial cracking in the concrete was considered to constitute failure and the interaction diagram was developed by determining the various combined loadings required to produce a principal tensile stress equal to the tensile strength of the concrete.

Edge beams in two structures under construction were instrumented to determine deflections, rotations, and strains occurring during forming operations and deck placement. Load induced strains were comparable in magnitude to those produced by environmental effects and difficulty was experienced in obtaining meaningful data.

IMPLEMENTATION STATEMENT

A theoretical study of combined torsional and flexural stresses in THD 54-in. beams and an attempt to provide experimental data on this subject are reported. The theoretical interaction surface that is reported includes the effects of torsion, shear, and bending. It can be used to predict the combinations of these three types of loading that will cause cracking in the concrete.

Two 54-in. beams in a bridge under construction were instrumented with strain, deflection, and rotation gages to determine values of these parameters that occur during construction under actual conditions in the field. Although the strain readings did not indicate any excessively large values, they were not such that they could be used to accurately validate the theory. The strains measured do not indicate that any changes in the present design and construction practices are warranted.

The behavior of prestressed beams subjected to combined loadings should be more thoroughly verified before significant design considerations are based on the theory that is presented.

INTRODUCTION

In an earlier study (1), two 50-ft long, Type B beams were tested to failure in the torsional mode to determine the torsional stresses produced under conditions of a torque applied at each end and to determine the torque which would produce cracking in the concrete. The results of these two tests were presented and compared with elastic theory in an attempt to establish a procedure for analytically determining the value of a torque to produce cracking (1).

This report presents the results of a study of the behavior of the Texas Highway Department 54-in. prestressed concrete bridge beam when subjected to combined torsional and transverse loads. In the present study, literature is reviewed and examined with the objective of selecting the most appropriate method of analysis and failure criterion for THD 54-in. prestressed beams. Elastic theory and the maximum tensile stress failure criterion are used to develop a theoretical failure envelope for this beam.

Field measurements were made to determine the magnitude of torsional stresses that are actually developed in edge beams under conventional construction procedures and to obtain an estimate of the margin of safety against cracking. Edge beams in two structures were instrumented to determine deflections, rotations, and strains that occurred during construction.

BACKGROUND AND REVIEW OF LITERATURE

The Problem

In recent years, a significant amount of research has been devoted to the subject of torsion in concrete members. Most of this work has been devoted to plain and reinforced concrete subjected to either pure torsion or combined torsion and bending with little effort being devoted to prestressed concrete members.

The problem of analysis and/or design of a concrete member under a generalized loading including bending and torsion can be grouped into the following major divisions.

(1) The selection or establishment of design loads which represent the expected service loads,

(2) The computation of internal stresses resulting from the design loads, and

(3) A reliable failure criterion with which to compare the values of internal stresses.

These three items cannot be approached independently, because of the influence of one upon the other. The particular failure criterion that is employed dictates the kinds of internal stresses that are computed and the manner in which they are computed.

Failure Criteria

The first step in the development or establishment of a failure criterion is to define failure. In concrete members, two general concepts of failure are of interest. The first concept involves initial cracking of the concrete and the second involves the ultimate load that the member may carry. In this study of THD 54-in. prestressed concrete bridge beams, the occurrence of cracking in the concrete is of greatest interest and the subject is approached with the intent of searching for a failure criterion to reliably predict the occurrence of cracking in the concrete.

A number of failure criteria have been proposed for concrete members subjected to combined loadings (2) but there is no general acceptance among engineers of any one of them, excluding all others. Various criteria appear to be more reliable than others for a given type of member and again certain criteria appear to be more suitable for certain combinations of loadings than they are for other combinations.

Zia (2) summarized and compared a number of commonly used failure criteria. These criteria are presented graphically in Figure 1. It is noted that for a state of pure shear, represented by the smaller circle, all criteria yield the same result. That is, failure will occur when the maximum principal tensile stress reaches the tensile strength of the concrete. All the failure criteria in Figure 1 are also noted to be identical for the other extreme of pure compression. Failure will result when the compressive stress reaches the compressive strength of the concrete. All the failure criteria in Figure 1 are also noted to be identical for the other extreme of pure compression. Failure will result when the compressive stress reaches the compressive strength of the concrete. Differences exist, however, at intermediate states of stress where shear and normal stresses are both present.

Chandler et. al. (3) in discussing failure criteria for concrete made the following statement:

> Experimental evidence has clearly demonstrated that Coulomb's theory is not valid for concrete. It is valid for materials failing by yielding but not by brittle fracture. Any one of the remaining theories may correlate with the torsional experimental results reasonably well depending on the method used to measure the tensile strength on the concrete. Although various direct and indirect methods of measuring the tensile strength of concrete have been proposed in the past, it is very difficult to measure the tensile strength of concrete accurately.

The most popular failure criterion also happens to be the simplest one and that is the maximum tensile strength failure criterion (Rankine). When cracking of the concrete rather than ultimate strength of the member is of interest, the tensile strength rather than the compressive strength generally controls in actual installations. The maximum tensile strength failure criterion states

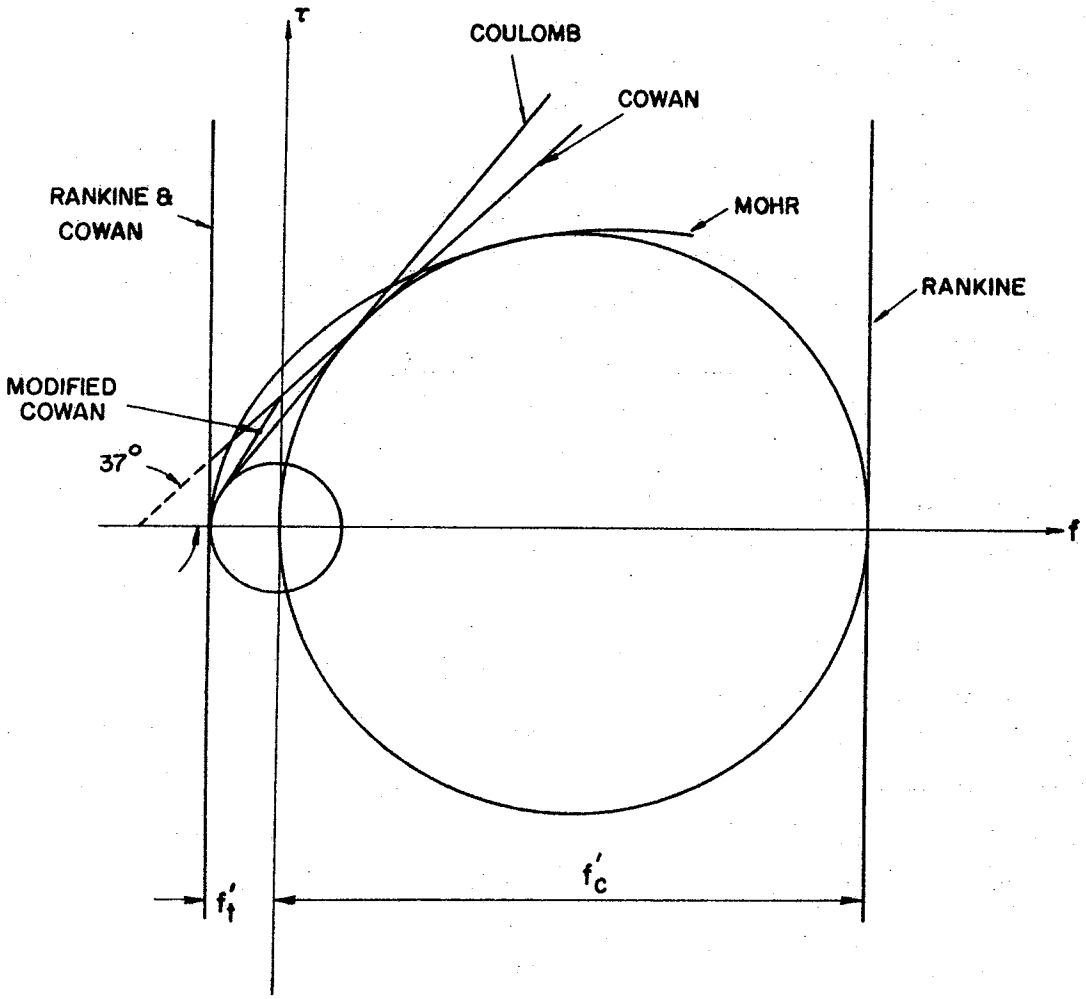

Figure 1. Failure theories for concrete under combined stress. After Zia (2).

that failure will occur when the principal tensile stress at any point reaches the tensile strength of the concrete. The effects of other normal and shear stresses at the point are included only through their influence on the principal tensile stress. A reasonable amount of success in comparisons between this theory and experimental results has been demonstrated by researchers.

If one accepts the maximum tensile stress failure criterion, the only problems that remain are to predict the tensile strength of the concrete and to determine the appropriate relationship between externally applied torque and internal stress. Once the latter problem is solved and the appropriate torque-stress relationship determined, prediction of the tensile strength of the concrete is relatively simple. An appropriate measure of the tensile strength that will bring the theory in line with experimental results, perhaps with some degree of conservatism, can be chosen.

Torque-Stress Relationships

The fact that concrete is neither perfectly elastic or perfectly plastic but somewhere in between has resulted in difficulty in establishing appropiate torque-stress relationships for various shapes of members. The problem is further complicated by the influence of concrete strength on the degree of plasticity that is exhibited. Proposed torque-stress relationships have been based on elastic theory, plastic theory, and on combinations of the two theories. However, it is generally agreed that elastic theory is more reliable for higher strength concrete such as is used in prestressed beams and plastic theory is more reliable for lower strength concrete.

Hsu (4) in his study of plain concrete rectangular sections subjected to pure torsion deviated from the classical theoretical approach and developed a theory based on skew-bending behavior. The expression for ultimate torque from skew-bending theory does not contain a shape factor and is identical to that for classical theory when $y/x \to \infty$, that is:

$$T_u = \frac{b^2 h}{3} f_t \qquad (1)$$

Where:

T_u = ultimate torque for the section.

b,h = length of shorter and longer sides of the cross section, respectively.

f_t = tensile strength of the concrete.

However, in Saint-Venant's equation, Hsu uses values obtained from direct tensile strength tests as the ultimate tensile strength of the concrete. In the skew-bending equation, he uses an adjusted value of modulus of rupture as the ultimate tensile strength. Hsu discounts the application of Saint-Venant's theory to concrete members in favor of the skew-bending theory on the basis of these comparisons. The author does not agree with this conclusion. The two theories are fundamentally the same. The real question is not a comparison of theories, but the appropriate choice of the value of ultimate tensile strength of the concrete.

It is appropriate at this point to review and develop information describing the behavior of concrete members with less complex cross sections before discussing the behavior of the THD 54-in. prestressed beam. The following sections are included for that purpose.

Behavior of Sections Subjected to Pure Torque

Plain rectangular cross section: For a rectangular cross section, the torque-stress relationship from Saint-Venant's elastic theory is (5):

$$T = \alpha b^2 h \tau \qquad (2)$$

Where:

T = the torque, in-lbs.

b = length of shorter side of cross section, in.

h = length of longer side of cross section, in.

τ = the maximum torsional shear stress (occurs on outer surface at the mid point of the longer side), psi.

α = a constant whose value depends on the ratio of b/h.

The value of α ranges from 0.208 for b/h = 1 to 0.333 as b/h increases infinitely. A conservative approximation is sometimes made by setting $\alpha = 0.333$. It is emphasized that in equation 2, τ is the maximum torsional shear stress for the condition of pure torque. It occurs at the mid point of the longer side of the cross section. This is the point where the maximum principal tensile stress occurs and the point where cracking will initiate when a pure torque is applied. The state of stress at this point is one of pure shear, and the maximum principal tensile stress is numerically equal to the shear stress in equation 2. For a plain concrete section, the crack producing torque will also be the failure torque.

It has been found that, in general, elastic theory used in conjunction with the maximum principal tensile stress failure criterion results in predicted torsional capacities that are significantly lower than experimental values. This was found to be true for the two tests conducted earlier (1). Two possible reasons for this lack of agreement are: (1) inappropriate application of elastic theory to concrete, and/or (2) inability to evaluate the tensile strength of the concrete.

Attempts have been made to apply plastic and semi-plastic theories to concrete members to obtain better predictions of torsional capacity (2). Chandler et. al. (3) observed that prediction equations proposed for plain concrete members can all be written in the basic form:

$$T_c = K^{\lambda} b^{\delta} h \quad \eta f_c'^{\xi} \quad [f_c'(b/h)] \tag{3}$$

They performed a statistical analysis using test results available in the literature to evaluate the constants and arrived at the following prediction equation:

$$T_c = b^2 h \ (5 \sqrt{f_c'}) \quad [0.4731 \ (1 - 0.5924 \ b/h + 0.2763 \ b^2 h^2)] \tag{4}$$

The effective shape factor in this equation falls between elastic and plastic shape factors but much closer to that of plastic theory. Comparison between this equation and test results from 117 tests from eleven different sources was good. Most of the test results were within $\pm$ 15 percent of the predictive equation.

Reinforced rectangular cross section:

If a minimum amount of appropriately arranged reinforcement is provided, the torsional capacity of a cracked section can be made to exceed the cracking torque. This will provide both ductility and reserve capacity. Whether the presence of reinforcement serves to increase the torque at which cracking occurs is a question that has not been resolved. Zia (2) states,

> It is generally agreed that in reinforced concrete subject to torsion, the reinforcement has no appreciable effect on the stiffness before cracking. Similarly, the longitudinal or transverse reinforcement acting alone provides little additional strength beyond the capacity of plain concrete. However, if the longitudinal and the transverse steels are combined, the torque corresponding to first cracking is usually somewhat increased. After cracking, the stiffness is markedly reduced but considerable increase in strength and a large amount of plastic detrusion are possible, depending on the amount and disposition of the reinforcement.

The presence of only longitudinal steel provides very little, if any, additional torsional capacity beyond that which causes initial cracking. Hsu (6) observed that it tended to increase the torque at cracking and that this increase could be expressed by:

$$T_{cr} = (1.00 + 0.04\ p_t)\ T_{up} \tag{5}$$

There was a large amount of data scatter and some individual data points indicated no increase in strength for percentages of reinforcement as great as 3. It is generally agreed that any increase in cracking strength due to reinforcement is small and unpredictable and it is usually neglected.

However, the presence of both longitudinal steel and closed stirrups will significantly increase the ultimate torsional capacity of a rectangular section (7). The most popular expressions for ultimate torque of a reinforced section are of the form:

$$T_u = T_o + \alpha_y x_1 y_1 \frac{A_t f_y}{s} \tag{6}$$

Where:

T_u = ultimate torque of the reinforced section.

T_o = in general, the contribution of the concrete to the torsional strength. Its value depends on the theory used. This parameter is discussed below.

α_t = a factor or constant expressing the influence of reinforcement on the strength. Its value depends on the theory used. This parameter is discussed below.

x_1 = smaller center-to-center dimension of the closed rectangular stirrup.

y_1 = larger center-to-center dimension of the closed rectangular stirrup.

A_t = cross sectional area of one leg of the stirrup.

f_y = yield strength of stirrups.

s = spacing of stirrups.

The qualitative influence of reinforcement in the form of closed stirrups accompanied by the required amount of longitudinal steel is shown in Figure 2 . The horizontal portion of the curve represents the ultimate torque (same as cracking torque) of an unreinforced section. A certain amount of reinforcement is required before any increase in torsional strength can be realized, although reinforcement in lesser amounts will provide some ductility. The straight line sloping portion of the relationship gives the influence of reinforcement in the range where under-reinforced failures occur. The intercept of this line extended back to the torque axis gives T_o in Equation 6. In ACI 318-71, v_{tc} is limited to $2.4\sqrt{f'_c}$ and according to Hsu (7), $T_o = 0.4\ T_{up}$. This implies that the accepted tensile strength of the concrete is $\frac{2.4}{0.4}\sqrt{f'_c}$ or $6\sqrt{f'_c}$.

The slope of the line is expressed by:

$$\alpha_t = 0.66 + 0.33\frac{y_1}{x_1} \leq 1.50 \qquad (7)$$

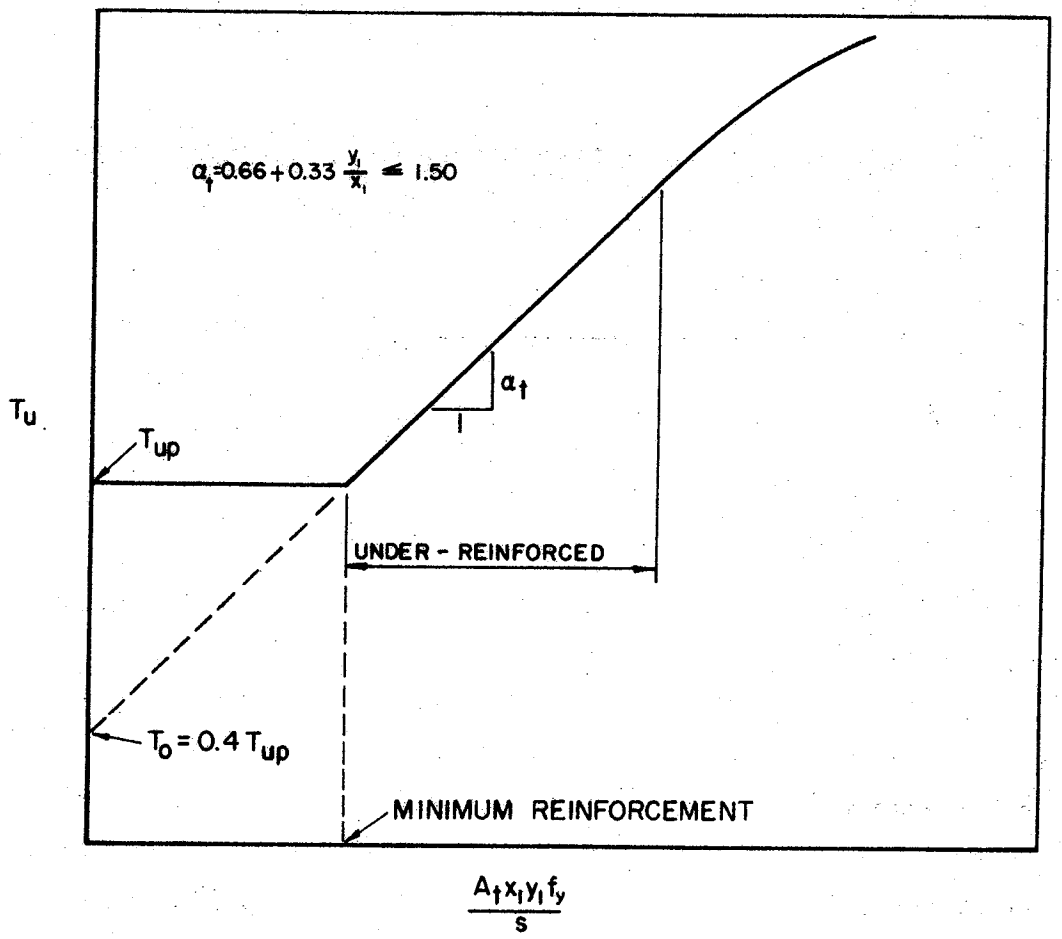

Fig 2 . Effect of closed stirrup reinforcement on the ultimate strength of rectangular beams. After Hsu (6)

Concentrically prestressed rectangular cross section:

Hsu (6) proposed that the ultimate strength of a concentrically prestressed rectangular section be computed by the following equation:

$$T_u = T_{up} \sqrt{1 + 10 \frac{\sigma}{f'_c}} \tag{8}$$

Where:

T_u = ultimate strength of the prestressed section.

T_{up} = ultimate strength of a non prestressed section of identical dimensions.

σ = uniform prestress.

f'_c = compressive strength of the concrete.

The factor $\sqrt{1 + 10 \frac{\sigma}{f'_c}}$ is said to account for the effect of prestress. This relationship can be readily obtained using elementary strength of materials relationships.

Consider the state of stress at a point in a member where shear and axial normal stresses exist. The shear stress could arise from an applied torque, an applied flexural loading, or a combination of the two. The axial normal stress could result from a prestressed force a flexural load or a combination of these two. The state of stress at this point can be described from elementary strength of materials as follows:

$$\sigma_{1,2} = \frac{\sigma_x}{2} \pm \sqrt{\left(\frac{\sigma_x}{2}\right)^2 + (\tau_{xy})^2} \tag{9}$$

or;

$$\tau_{xy} = \sigma_1 \sqrt{1 - \frac{\sigma_x}{\sigma_1}} \tag{10}$$

If σ_x, the normal stress is considered to be positive when compressive, equation 10 is written:

$$\tau_{xy} = \sigma_1 \sqrt{1 + \frac{\sigma_x}{\sigma_1}} \tag{11}$$

The maximum principal tensile stress, σ_1, was approximated by Hsu (6) as $f'_c/10$ and in this case equation 11 becomes:

$$\tau_{xy} = f'_c/10 \sqrt{1 + 10 \frac{\sigma_x}{f'_c}} \qquad (12)$$

If τ_{xy} is considered to be produced by a torque only, then for a rectangular section (or one made up of a number of rectangles) the expression for the ultimate torsional capacity may be written:

$$T_u = \frac{\Sigma x^2 y}{3} \frac{f'_c}{10} \sqrt{1 + 10 \frac{\sigma_x}{f'_c}} \qquad (13)$$

This equation governs as long as the failure is tensile. There exists a limiting value of prestress, σ_x, above which the mode of failure changes from tensile to compressive in nature. Equation 13 is not valid for members having a prestress above this limiting value. This value can be determined theoretically by determining the value of σ_x in Equation 9 that will cause the principal compressive stress to reach the compressive strength of the concrete before the principal tensile stress reaches the tensile strength of the concrete. This operation requires the use of a relationship between the tensile and compressive strength of the concrete. Many such relationships of the form $f'_t = C\sqrt{f'_c}$ with various values of C have been proposed. If f'_t is chosen to be $5\sqrt{f'_c}$ as has been suggested by some authors, the limiting value of prestress that will cause the mode of failure to change from tensile to compressive will depend on the strength of the concrete but is about $0.9\sqrt{f'_c}$. Zia (9) states that the limiting value is between $0.46\sqrt{f'_c}$ and $0.9\sqrt{f'_c}$. Many authors discount the possibility of a compressive failure by noting that prestress is normally less than the limiting values. While this is generally true for a prestressed beam subjected to a pure torque, an applied bending moment produces normal stresses that will add to the prestress in certain portions of the cross section and thereby create the conditions necessary for a compressive mode of failure. This condition is very probable when a relatively large bending moment exists in combined bending and torsional loads and should not be overlooked.

Eccentrically Prestressed Rectangular Cross Section:

A total of 71 rectangular beams were tested and evaluated by Chandler, Kemp and Wilhelm (3). The experiment included post-tensioned beams both with and without conventional reinforcement and pretensioned reinforced beams with and without eccentricity of prestressing. The observed behavior of these tests verified a number of phenomena predicted by classical theory as indicated by the following statements (3):

> The cracking initiated in all the test specimens at the center of the longer side. Plain prestressed beams failed suddenly at the formation of this first crack and the failure was explosive in nature due to compressive action of the prestressing force. The crack was inclined to the longitudinal axis of the beam at an angle which was always less than 45° to the horizontal. The angle of inclination of the crack was a function of degree of prestress and became flatter with increasing degree of prestress. This inclined crack developed in the shape of a helix on the two short sides and one of the longer sides but the helix was unable to develop on the second longer side. The direction of the crack on the second longer side was dictated by the extremities of the helical crack on the other three sides.

Prestressed specimens that were reinforced in the longitudinal direction only failed in a brittle manner immediately after initial cracking. Longitudinal reinforcement did not appear to influence the torque at which initial cracking occurred.

They found that prestressing did not affect the torsional stiffness of the beams. Results of the two tests conducted in Study 150 also indicated this to be true (1).

The concentrically and eccentrically prestressed beams tested by Chandler et al. behaved alike (3). No difference was found in the cracking strength and the ultimate strength of these specimens. No significant difference in torsional stiffness and strength between pretensioned and post-tensioned beams was indicated. It should be noted that all specimens were of rectangular cross section and that initial cracking occurred at the middle of the longer side. It is further noted that eccentricity was less than the kern limit in all cases.

Classical elastic theory predicts that cracking should initiate at the middle of the longer side of a plain rectangular section. As an increasing amount of concentric prestressing is added up to a certain limit, the location of initial cracking will remain at the middle of the longer side, but an increasing amount of torque will be required to cause cracking. As the eccentricity of prestress (along the longer axis of the cross section) is increased, no effect on torsional behavior is predicted until a certain value of eccentricity is reached. This value is that which will cause the location of the critically stressed point to change from the middle of the longer side to the middle of the shorter side with the lesser prestress.

The magnitude of the torsional shearing stress at the middle of the shorter side may be related to that at the middle of the longer side by the approximate relationship (8).

$$\tau_B = \tau_A \frac{b}{h} \tag{14}$$

Where:

τ_B = torsional shear stress at the middle of the shorter side, psi

τ_A = torsional shear stress at the middle of the longer side, psi

b = length of the shorter side, in.

h = length of the longer side, in.

For Chandler's 4 x 12 in. and 4 x 9 in. cross sections, this equation becomes $\tau_B = 1/3\ \tau_A$ and $\tau_B = 4/9\ \tau_A$ respectively. Equation 13 is applicable to both points on the cross section if the appropriate value of prestress, σ_p, is used. This equation written for the two points A and B under the limiting conditions necessary to cause location of the critically stressed point to change from A to B becomes:

For A:

$$T_A = \frac{b^2 h}{3} \quad f_t \sqrt{1 + \frac{\sigma pA}{f_t}} \tag{15}$$

For B:

$$T_B = \frac{b^2 h}{3} \quad (h/b) \quad f_t \sqrt{1 + \frac{\sigma pB}{f_t}} \tag{16}$$

The critically stressed point will occur at B, the middle of the shorter side if $(h/b) \sqrt{1 + \frac{\sigma pB}{f_t}}$ is less than $\sqrt{1 + \frac{\sigma pA}{f_t}}$. Almost all of Chandler's beams were such that theory predicts the critically stressed point to be at the middle of the longer side. For those few beams in which the critically stressed point is predicted to be on the shorter side, it is only by a very small margin.

Chandler et al. extended the equation for plain rectangular sections to account for prestressing using the principal tensile stress failure criteria. Their equation in this case becomes:

$$T = b^2 h \, \tau [0.4731 \quad (1 - 0.5924 \, b/h + 0.2763 \, b^2/h^2)] \tag{17}$$

Where:

$$\tau = f_t' \sqrt{1 + \sigma_p / f_t}$$

and f_t' is again taken to be $5\sqrt{f_c'}$. A number of test results from seven different sources were compared with this predictive equation and the comparison was very good. Almost all of the data were within $\pm$ 20 percent of the predictive equation and only a few data were outside of $\pm$ 15 percent.

Eccentrically Prestressed I-beams: Only a relatively small amount of effort has been devoted to the study of torsion in this type of beam. Most researchers have logically devoted their efforts to developing an understanding of torsion in less complex shapes before attempting to study eccentrically prestressed I-beams.

Zia (9), in 1961, reported on a study of torsion in prestressed members. The members tested in his study were of rectangular, T, and I-sections. The T and I-sections were such that they would be composed of a number of rectangular sections and in this respect they differ somewhat from the THD standard cross sections.

More recently, this subject was studied at the University of Washington (10, 11). Prestressed I-beams of standard cross section used by the State of Washington were studied in this program. The cross section of these beams more closely resembled those of the THD standard beams than did those studied by Zia. In the tests conducted by the University of Washington, the beams contained web reinforcement and were eccentrically prestressed with bonded strand. In pure torsion tests (10), elastic theory in connection with the maximum principal tensile stress failure criterion very accurately predicted the location on the cross section where initial cracking occurred. However, the measured cracking torque was 25 to 75 percent greater than that predicted by elastic theory using the splitting tensile strength from cylinders as the tensile strength of the concrete. Measured and predicted values of torsional stiffness compared very well. These results are in agreement with those obtained in tests on THD Type B beams conducted in Study 150 (1).

Combined Loadings

The effect of combined loadings depends upon the location of the critically stressed point on the cross section. If, in a member subjected to a torque in combination with bending and shear, the critically stressed point occurs near the neutral surface of the member, there will be a minimum amount of interaction between torsional and bending stresses. In this case there will be a maximum of interaction between torsional stresses and shear stresses. If the critically stressed point occurs on either the top or bottom flange, the maximum interaction between torsional and bending stresses would occur, and minimum interaction between torsional and shear stresses would occur. The problem is further complicated in concrete members because of the two different types of shear

(diagonal tension) cracking that occur in concrete beams. Wyss and Mattock (11) in their study of interaction of torsion, shear and bending in I-section girders, tested two series of girders. One series had a moment-to-shear ratio of 4 ft and the other 9 1/2 ft. These two values resulted in diagonal tension cracking without flexural cracking and diagonal tension cracking in the presence of flexural cracking respectively.

For those girders which exhibited flexural cracking prior to diagonal tension cracking in the web, the occurrence of diagonal tension cracking (rather than flexural cracking) was chosen to be the condition which constituted cracking failure. The effects of torsional stresses on the cracking moment were considered in the theoretical calculations. The ratio of torsion to shear ranged from pure torsion to pure transverse load. In a pure torsion test, cracking first occurred in the top flange of the girder; but under combined loading conditions, cracking first occurred in the web.

The actual tensile strength of the concrete was calculated from test results using: (1) elastic stress distribution for both transverse shear and torsional stresses, and (2) elastic stress distribution for transverse shear and plastic stress distribution for torsional stresses. In the first case, the actual tensile strength was found to range from $5.93\sqrt{f'_c}$ to $13.99\sqrt{f'_c}$. In the latter case, it was found to range from $5.54\sqrt{f'_c}$ to $8.62\sqrt{f'_c}$. This suggests that plastic theory for the distribution of torsional stresses may be more appropriate in the general case of combined loadings. However, the use of plastic theory for torsional stress distribution and elastic theory for transverse shear stress distribution leaves something to be desired.

Very little experimental data are available for members having relatively deep, narrow cross sections and the extent to which existing theory can be applied is not known. Wyss et. al. (10) tested some deep narrow rectangular sections (5 in. by 24 in.) and the experimentally obtained cracking torques were found to be

consistently less than the calculated cracking torques. They did not explain the reason for this. The THD 54-in beam is relatively deep and narrow, and its behavior under torsional loads has not been determined experimentally.

Theory for Texas Highway Department 54-in. Beam

Torque-stress and torque-rotation relationships were developed for the 54-in. beam using elastic theory for noncircular sections (1). The relationship between applied torque and angle of twist per unit length is given by:

$$T = KG\,\Theta \tag{18}$$

where:

- T = applied torque, in-lb.,
- K = torsional stiffness constant, $in.^4$,
- G = shearing modulus of elasticity, psi, and
- Θ = angle of twist, radians/in.

The value of the torsional stiffness, K, was computed by a relationship developed from the membrane analogy (1). The relationship is:

$$K = \frac{2\int_{Area} \phi da}{G} \tag{19}$$

where:

- ϕ = ordinate to membrane
- Area = cross sectional area of beam

This procedure requires the computation of values of the ordinate, ϕ, to the membrane. Those valves for the 54-in. beam, in terms of $G\Theta$, are given in Table 1. Cross sectional dimensions of the 54-in. beam are given in Figure 3 and the locations of grid points are given in Table 4. The value of the torsional stiffness constant, K, was computed to be 10,110 in^4. The torque-stress relationship is a function of the position on the cross section, and values for selected points are given in Figure 4.

Wyss and Mattock (11) presented a procedure by which families of interaction curves could be constructed for prestressed I-beams subjected to combined loadings. Their procedure defines the interaction between torque and shear for various ratios of moment to shear. Flexural cracking prior to diagonal tension cracking

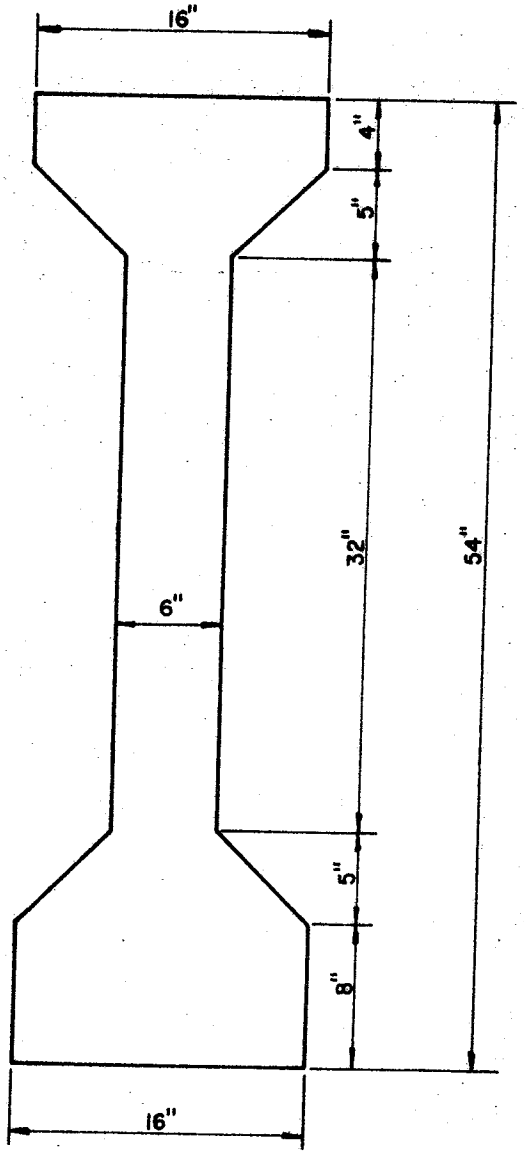

Figure 3. Geometry of cross section of THD 54-in. beam.

Table 1. VALUES FOR ϕ AT THE VARIOUS GRID POINTS IN A THD 54-IN. PRESTRESSED CONCRETE GIRDER

* Grid Point	Value of ϕ	Grid Point	Value of ϕ	Grid Point	Value of ϕ	Grid Point	Value of ϕ
1	8.25 GΘ	18	22.29 GΘ	35	9.01 GΘ	52	6.75 GΘ
2	12.82	19	26.34	36	5.00	53	11.67
3	15.18	20	15.48	37	9.01	54	11.39
4	15.93	21	23.42	38	5.00	55	15.13
5	12.32	22	8.20	39	9.00	56	9.01
6	19.81	23	14.75	40	5.00	57	15.69
7	23.98	24	6.08	41	9.01	58	18.05
8	25.34	25	11.18	42	5.01	59	6.59
9	13.18	26	5.38	43	9.02	60	12.34
10	22.13	27	9.81	44	5.02	61	16.30
11	27.60	28	5.14	45	9.05	62	17.71
12	29.47	29	9.30	46	5.07	63	6.01
13	10.28	30	5.05	47	9.14	64	9.46
14	19.94	31	9.11	48	5.19	65	11.48
15	26.80	32	5.02	49	9.39	66	12.17
16	29.35	33	9.04	50	5.55		
17	12.56	34	5.01	51	10.04		

*See Figure 4 for grid point locations. Values of ϕ are symmetric about the vertical centerline of the cross section.

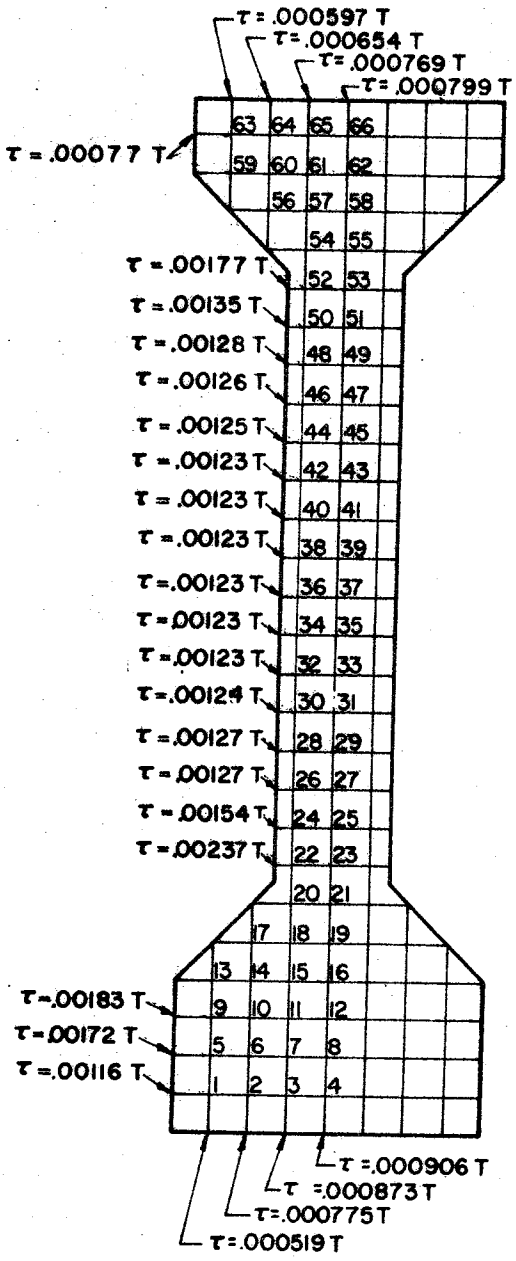

Figure 4. Relationships between torsional shear stresses and applied torque for THD 54-in. beam.

in the web is not considered to constitute cracking failure. Cracking failure is defined by the occurrence of tensile cracking in the top flange or the web whichever occurs first. Therefore, the interaction curves relate torque to shear and are influenced by the moment-to-shear ratio.

The interaction relationship involving torque, shear and moment is actually a surface rather than a curve and can be defined by a three-axis system in which the axis represent the three types of loads (torque, shear and moment). Such a procedure was followed in constructing an interaction surface for the THD 54-in. beam.

The following values are assumed:

f'_c = 5000 psi

f'_t = $6\sqrt{f'_c}$ = 424 psi

f_{pt} = 0 psi (prestress at top face)

f_{pb} = 2000 psi (prestress at bottom face)

A point on the top flange is expected to be the critically stressed point in the 54-in. beam when it subjected to a pure torque. However, the location of the critically stressed point is not known until the torques required to produce cracking at each point on the cross section are calculated and compared.

If the critically stressed point is located on the surface of the top flange, the state of stress will be determined by the torsional stress, prestress and flexural stress. The transverse shear stress is zero at this point and will have no influence. The applicable relationship is

$$\tau = f'_t \sqrt{1 + \frac{\sigma}{f'_t}} \qquad (20)$$

where:

τ = the shear stress due to the applied torque, psi.

f'_t = tensile strength of the concrete, psi.

σ = normal stress in the longitudinal direction of the girder (due to prestress and any other sources) psi.

The relationship between applied torque and torsional shear stress at this point, as shown in Figure 4 , is:

$$\tau = .000799T \tag{21}$$

Using $\sigma = 0$ psi and $\tau = 424$ psi, the cracking torque, T, is found to be 530 in.-kips.

If the critically stressed point is located at the neutral axis, the bending stresses have no influence. Actually, the torsional stress distribution on the boundary of the cross section varies very little over the vertical dimension of the web and is reasonably constant near the neutral surface (Figure 4). Also, bending stresses are small in the vicinity of the neutral surface. Therefore, if the critically stressed point is not exactly on the neutral surface but in close proximity, little error will be involved in applying the relationships at the neutral surface to determine the cracking torque. Torsional and transverse shear stress will be in the same direction on one side of the web and of opposite directions on the other side. The point on the side of the web where they are additive will control and the relationship is:

$$\tau + v = f_t' \sqrt{1 + \frac{\sigma}{f_t'}} \tag{22}$$

Where:

v = shear stress due to transverse load, psi.

and all other terms are as defined before.

The prestress at the neutral surface is 1054 psi. This gives (Equation 22) a total shear stress, $\tau + v$, of 793 psi. Any combination of torque and transverse load that will produce this total shear stress will cause cracking at this point. Assume, for the moment, that the shear stress due to transverse load is zero, then the cracking torque is given by:

$$\tau = .00123T \tag{23}$$

For the given value of τ, this expression gives a cracking torque of 644 in-kips.

For transverse shear stresses other than zero, the two shear stresses must be combined as in Equation 23. The corresponding relationship between torque and transverse load is a linear relationship.

If the critically stressed point is located on the outer surface of the bottom flange, the state of stress includes the combined effects of torque, prestress, and flexural stress at that point. The transverse shear stress is zero at this point and therefore, has no effect. In this case Equation 21 is applicable if σ is taken to be the sum of the prestress and flexural stress at that point.

Another possible location of the critically stressed point is one of the re-entrant corners at the web flange juncture. However, Wyss and Mattock found in their tests on prestressed I-beams that significant cracking did not occur until the tensile stress over most of the depth of the web had reached the tensile strength of the concrete. Therefore, any effects of stress concentrations at these corners were not included in constructing the interaction surface for the 54-in. beam.

The resulting interaction surface is shown in Figure 5 and the same relationships are presented in two-dimensional curves for various values of M/M_o in Figure 6. It is noted that, in the construction of this interaction surface, failure was defined to be the initial occurence of cracking. Portions of the surface which represent tensile cracking in the top flange, in the web, and in the bottom flange are indicated on the figure. Construction of this surface differs in concept from that proposed by Wyss and Mattock in that they did not consider tensile cracking in the bottom flange to constitute failure. They considered the effects of combined loads on flexural cracking in the bottom flange and then considered the effect of this cracking on the shear capacity of the web. The construction of the interaction surface for the 54-in. beam is more conservative than the method proposed by Wyss and Mattock.

The theoretical interaction surface for the THD 54-in. beam presented herein has not been verified by experimental results. The surface was developed from theoretical considerations and reported experimental data from tests on prestressed I-beams that were somewhat similar in cross

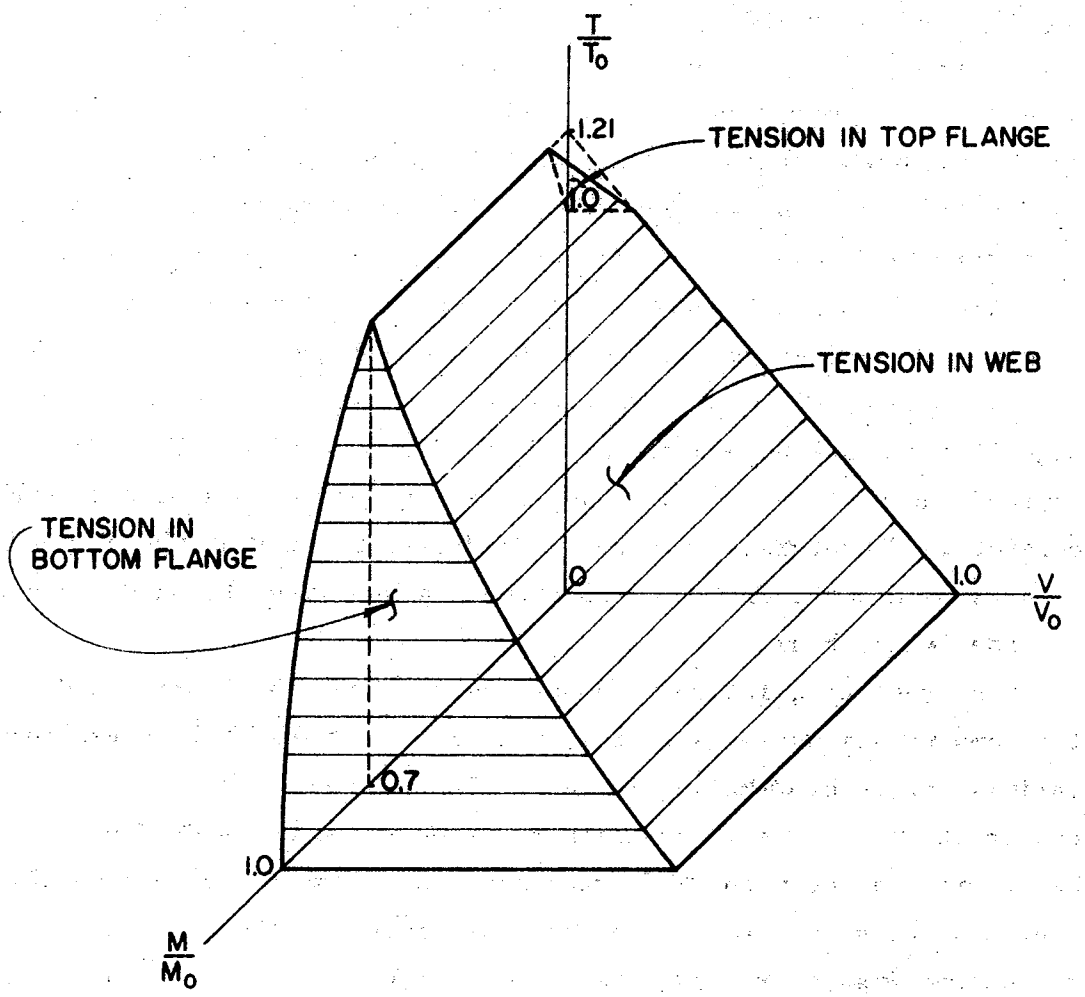

Figure 5. Interaction surface for THD 54-in. beam.

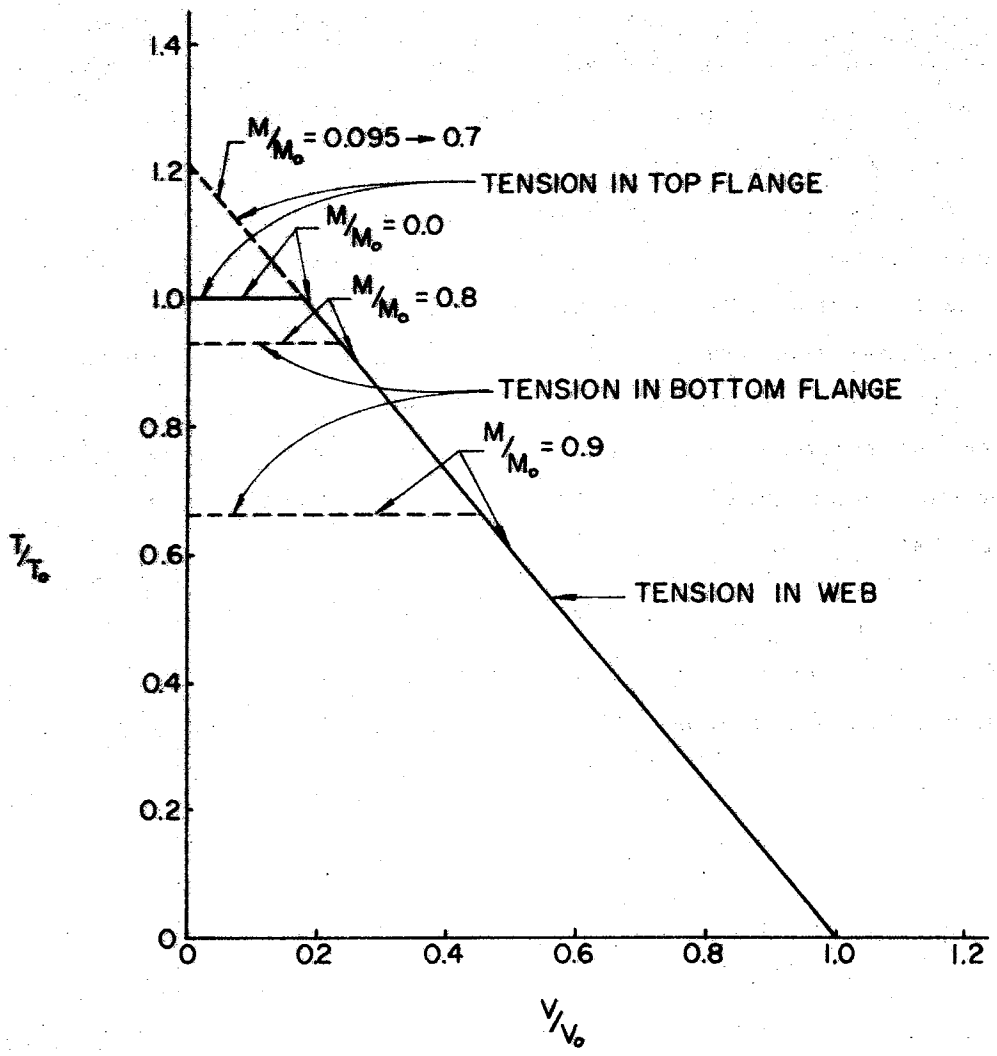

Figure 6. Nondimensional torque-shear interaction curves for various moment-to-cracking moment ratios for THD 54-in. beam.

section. Some of the values used were selected as those thought to be most appropriate for this situation and they have not been verified by experimental data. The unconditional use of this theory before it is experimentally verified is not recommended.

The torque-stress relationship was also developed for the 54-in. beam assuming completely plastic behavior. Under this assumption, all points of the cross section are stressed to their ultimate strength. This theory is not fundamentally applicable to a concrete member because deformation of the outer fibers of sufficient magnitude to create a completely plastic section do not occur. However, favorable comparisons with experimental results have been obtained (3). The sand heap analogy was employed to accomplish the calculations. This analogy is the counterpart to the membrane analogy for elastic theory. The torsional shear stress at any point on the cross section is related to the slope of the surface of the sand heap and the torque is proportional to the volume of the sand heap. Photographs of the sand heap for the 54-in. beam are shown in Figure 7. The relationship between torque and stress is:

$$T_p = 1870\ \tau \tag{24}$$

This relationship is applicable to any point on the cross section and is the counterpart to those for elastic theory given in Figure 4.

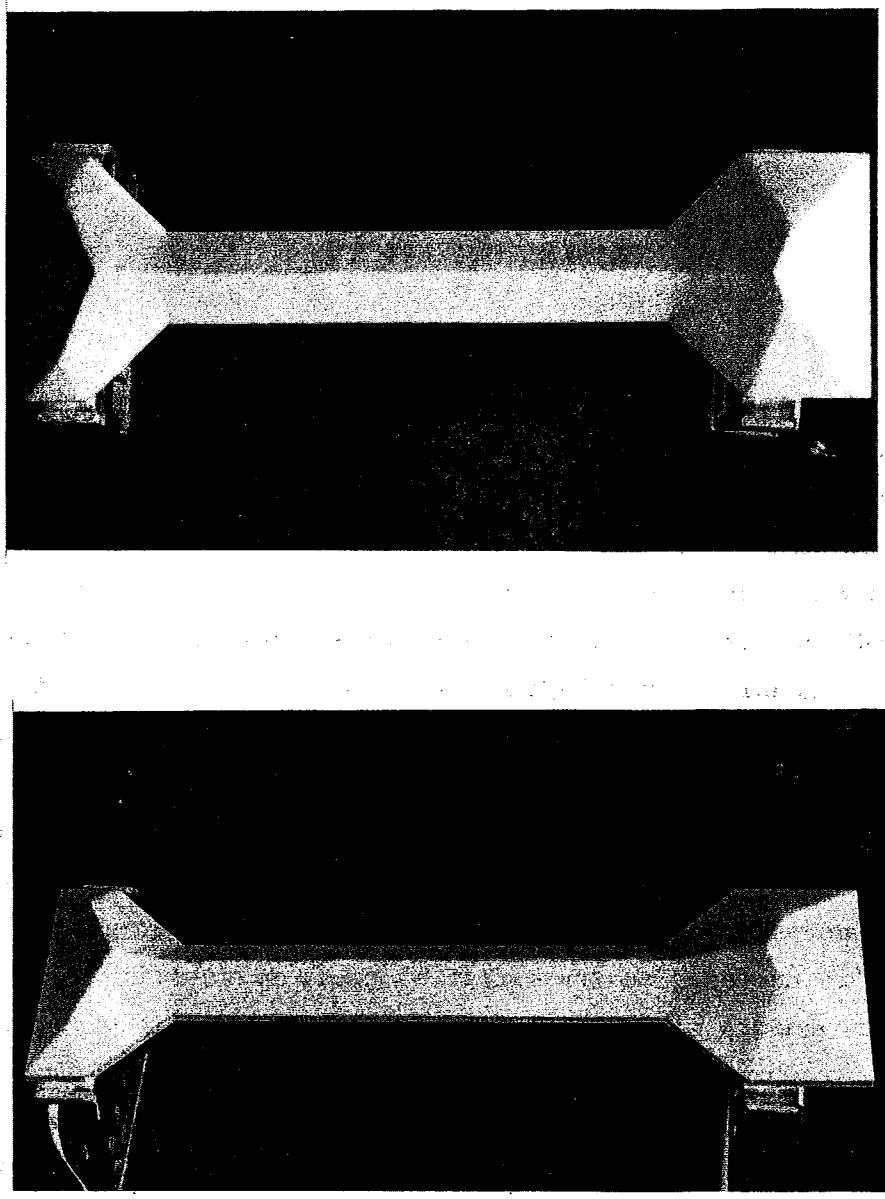

Figure 7. Photographs of sand heap for THD 54-in. beam.

EXPERIMENTAL PROGRAM

General

The experimental program was planned to provide information about magnitudes and directions of stresses that occur in THD 54-in. beams during construction under given conditions. Instrumentation was planned that would give a measure of the effects of diaphragms on the stress patterns in the beams. It was intended that the derived data would be used to describe typical behavior of these beams and would be valuable in developing methods of analysis and design of such beams. Reliable data would provide insight into the amount of torsional and other loads that an edge beam actually experiences and the relative amount of restraint offered by the diaphragms. This then, would allow one to more readily assign design loads to such beams. However, the experimental program was not successful in this respect. It is documented herein and the results are used to the extent of their reliability.

Measurements of deflection, rotation, and strain were made prior to starting the deck placement operation, at specified intervals during placement, and after completion of deck placement. At both sites, placement of the deck began on one end and proceeded to the other. No delays were experienced and placement proceeded at a regualr pace.

Test beams

Two edge beams in structures with overhanging slabs were selected for study in this program. Both were THD 54-in. beams. One was in the Airport Boulevard overpass on IH 35 and the other was in the Columbus Drive overpass in Austin, Texas.

The spacing between the edge beam and the adjacent interior beam in the Airport Boulevard structure varies. The edge beam is skewed slightly less than 3 degrees. The span length is nominally 87.5 ft. The overhanging portion of the slab is 7.5 in. thick and the interior

portion is 7.75 in. thick. The overhanging span varies from 2.32 ft on the north end to 2.1 ft on the south end. Center-to-center spacing to the adjacent interior beam on the north end is 6.1 ft and on the south end is 7.0 ft.

The span in the Columbus Drive structure is skewed 10° and the span length is nominally 92 ft. The slab is 7.25 in. thick and overhangs 3 ft 5.5 in. Center-to-center spacing of the beams is 7 ft.

Deflection and Rotation Gages

Measurements of deflections and rotations were made with scales hanging from cross bars attached to the lower flange of the prestressed beams. The cross bars were attached at the positions indicated in Figures 8 and 9. The center-to-center distance between scales on each cross bar was 6.877 ft. Vertical displacements of the scales were determined with a precision surveyor's level. This arrangement allowed determination of vertical deflections as well as rotational displacements of the beam.

Strain Gages

Electrical resistance strain gages were installed on the surface of the two beams at the locations indicated in Figures 10 and 11. The gages were the same type as those used in Study 150 (1) and in other applications where their use has been reasonably successful. Temperature compensation gages were mounted on a slab that was placed on a scaffold adjacent to the bridge beam.

The beam in the Airport Boulevard structure was the first to be instrumented. This beam was adjacent to an existing structure which continued to carry traffic. The traffic was only a few feet from the instrumented beam and caused significant disturbance, possibly contributing to some of the problems experienced. Strain readings were not made during a long period of time when there was no activity on and around the structure. Therefore, there is no assurance that the entire instrumentation system was stable.

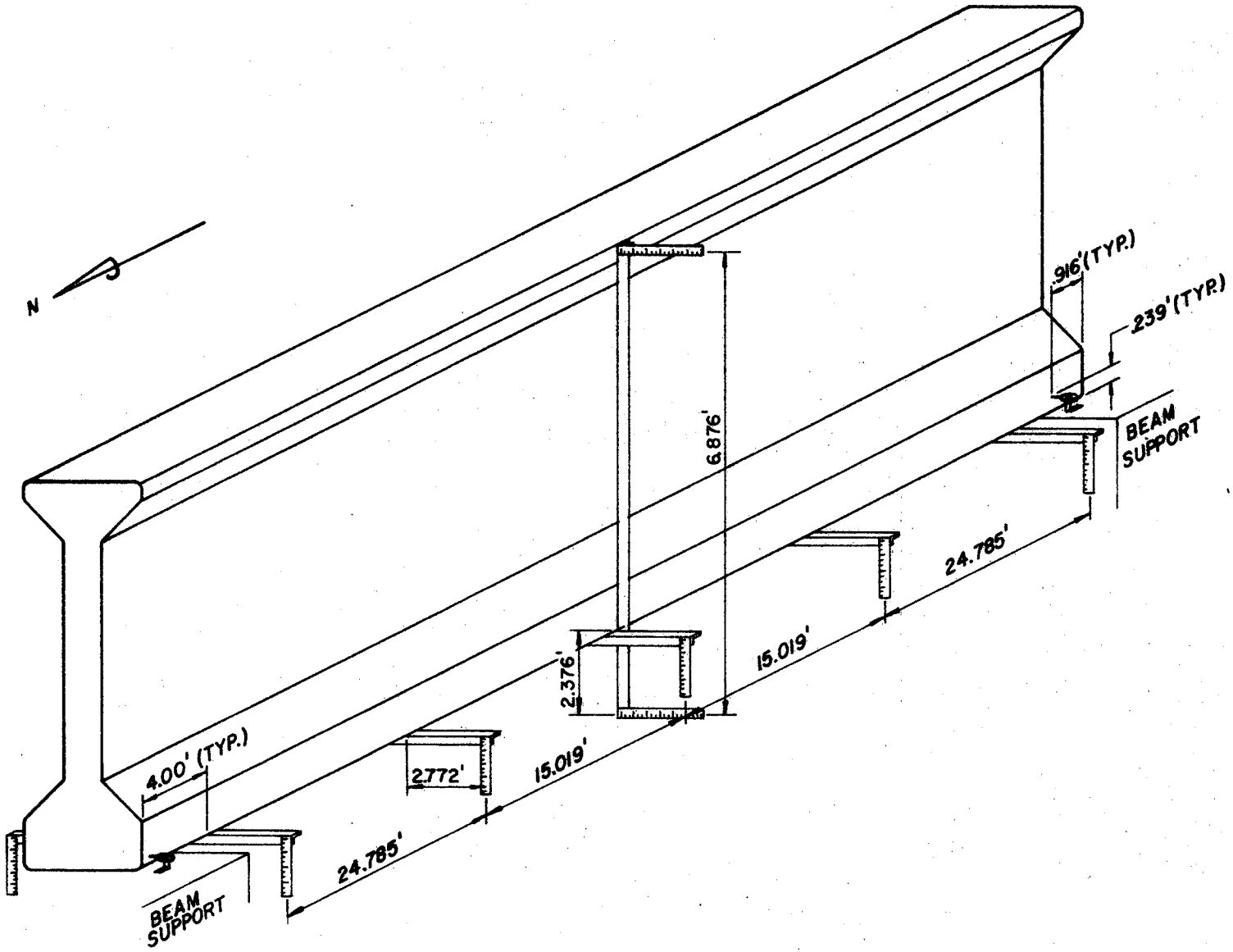

Figure 8. Location of deflection and rotation gages on Airport Blvd.

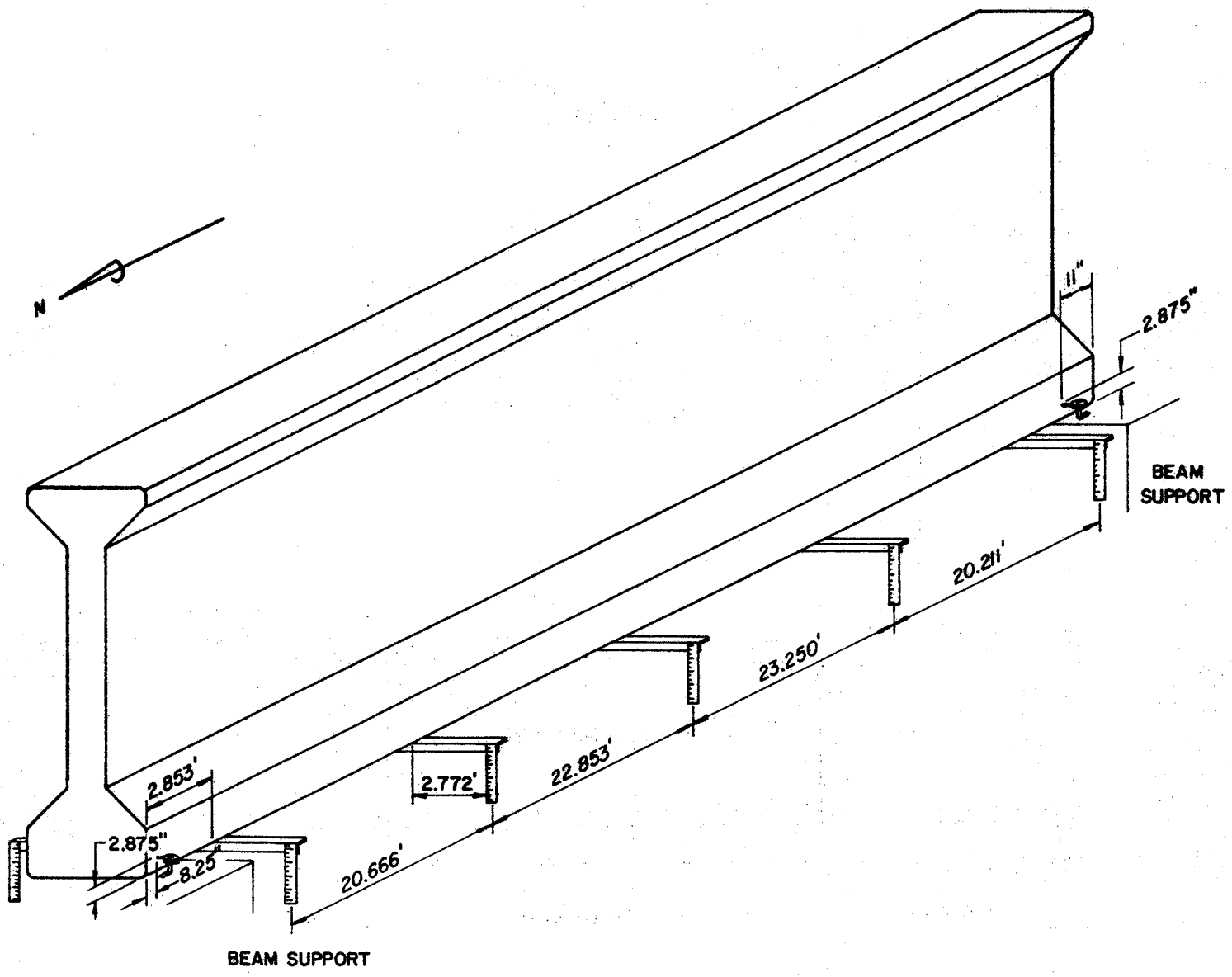

Figure 9. Location of deflection and rotation gages on Columbus Drive.

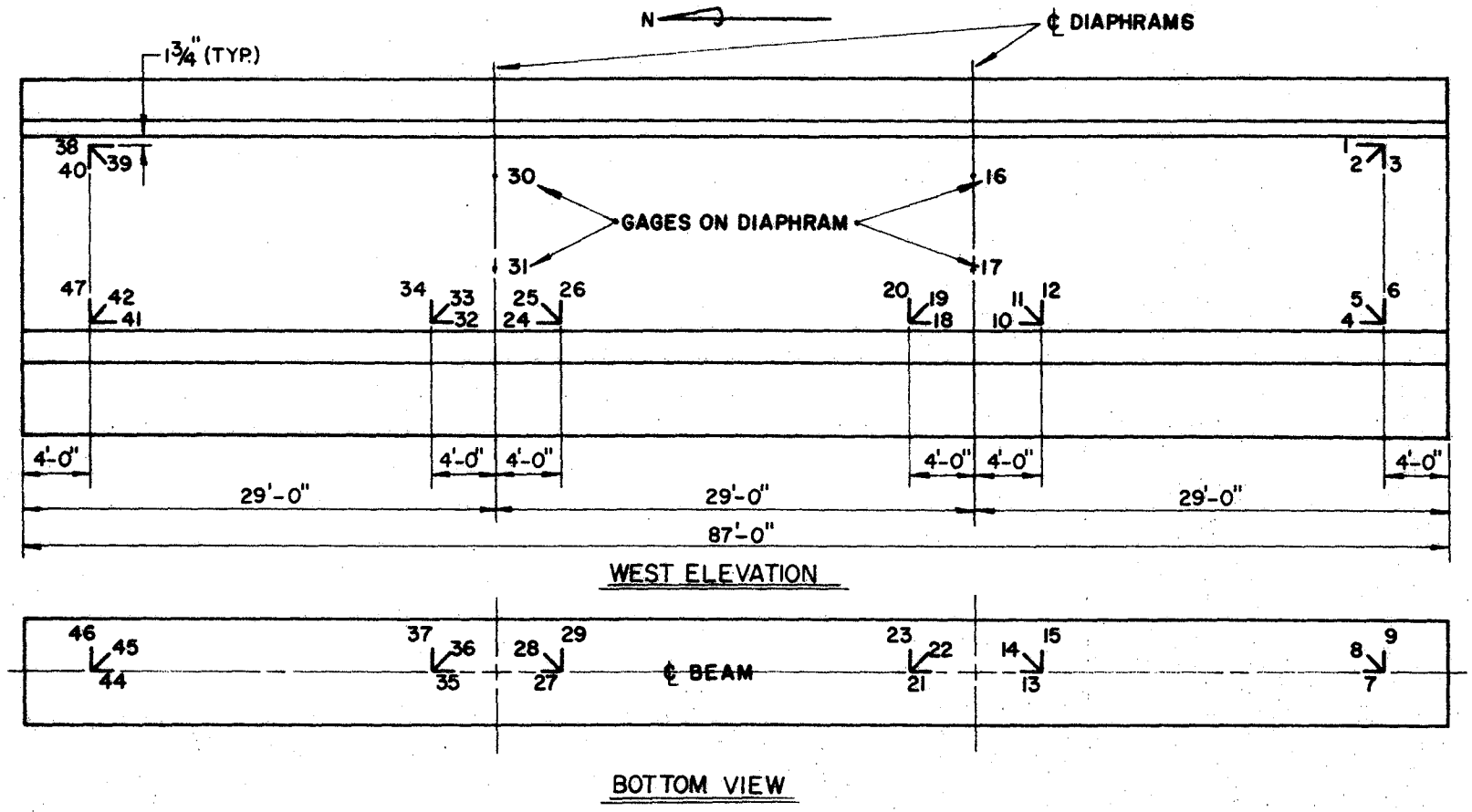

Figure 10. Locations of electrical resistance strain gages on Airport Blvd.

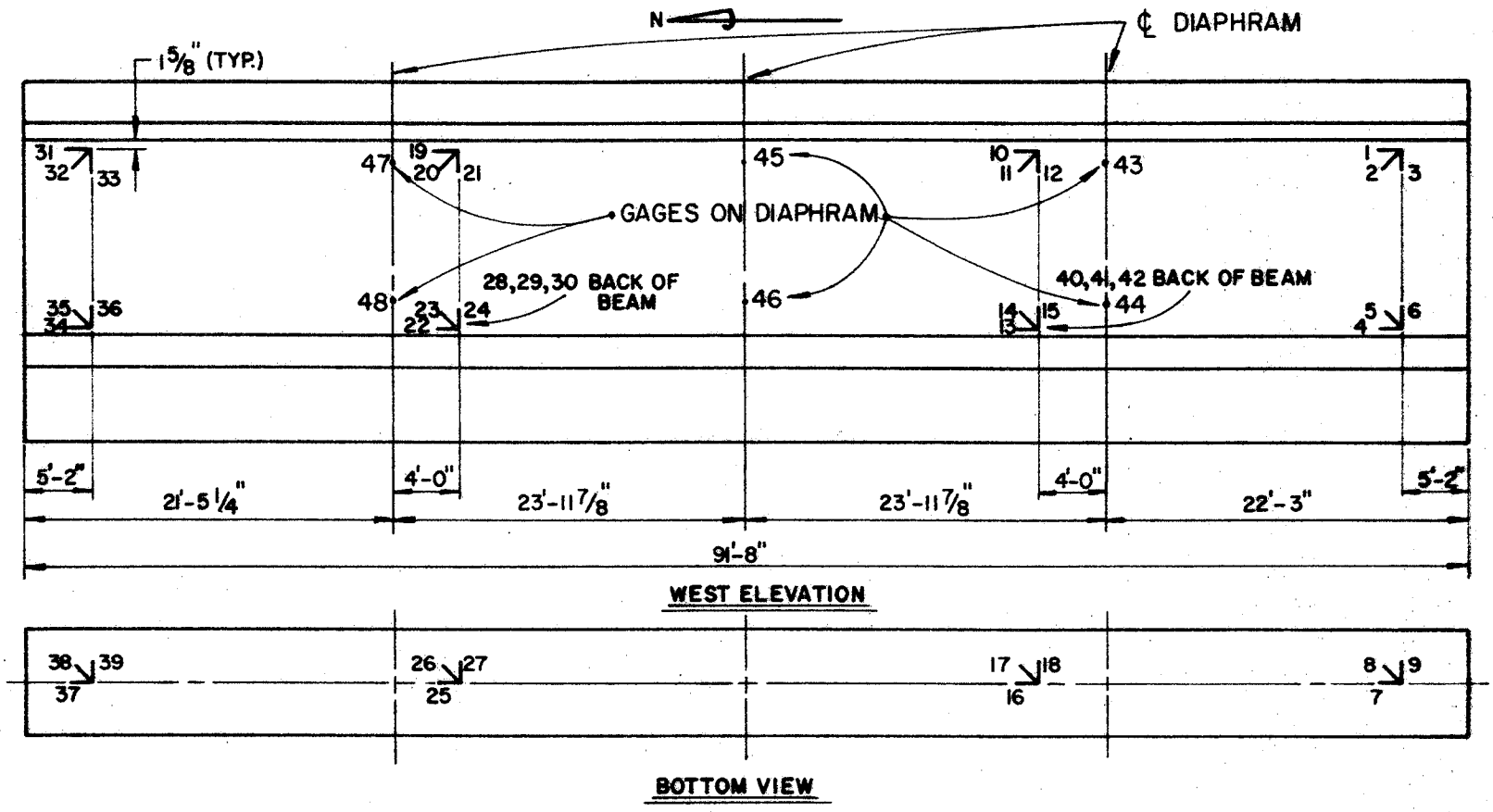

Figure 11. Locations of electrical resistance strain gages on Columbus Drive.

The second beam to be instrumented was in the Columbus Drive overpass. This structure was in a secluded area with a minimum amount of possible disturbances. Strain readings made, both before and after placement of the deck concrete during periods of time when there was no activity on the structure, show that the instrumentation system was stable (Figures A-15 through A-31 in the Appendix).

Results and Discussion

Vertical deflections of the two beams at various amounts of deck placement are presented in Figures 12 and 13 and rotational displacements during deck placement are shown in Figures 14 and 15. The loading on the beam during deck placement consisted of the weight of the forms, the in-place concrete, the screed, and other finishing equipment. The forms and in-place concrete are uniformly distributed loads but the screed and finishing equipment are more closely approximated by concentrated loads. Vertical deflections caused by these loads are not of primary interest here and analysis of these data are not carried to a high degree of refinement; however, the values obtained lend confidence to the data from these gages.

The value of a uniformly distributed load that would cause a midspan deflection of 0.75 in. was computed using the following relationship:

$$\Delta = \frac{5\ (w\ell)\ \ell^3}{384\ EI} \tag{25}$$

with:

$$I = 164{,}023\ \text{in.}^4$$

$$E = 57{,}000\ \sqrt{f'_c} = 5 \times 10^6\ \text{psi}$$

The value of uniform load from this calculation is about 725 lbs/ft which compares with the estimated load on the beam.

Gage locations and rotational displacement data for the two beams are given in Figures 14 and 15. On the Airport Boulevard beam, the rotation gages were located near the ends of the beam, at the two diaphragms, and at midspan. Relative amounts of rotation between cross sections at any of these locations are obtained by taking the difference between gages at the cross sections of interest. It is first noted, however, that all of the rotations are positive (outside

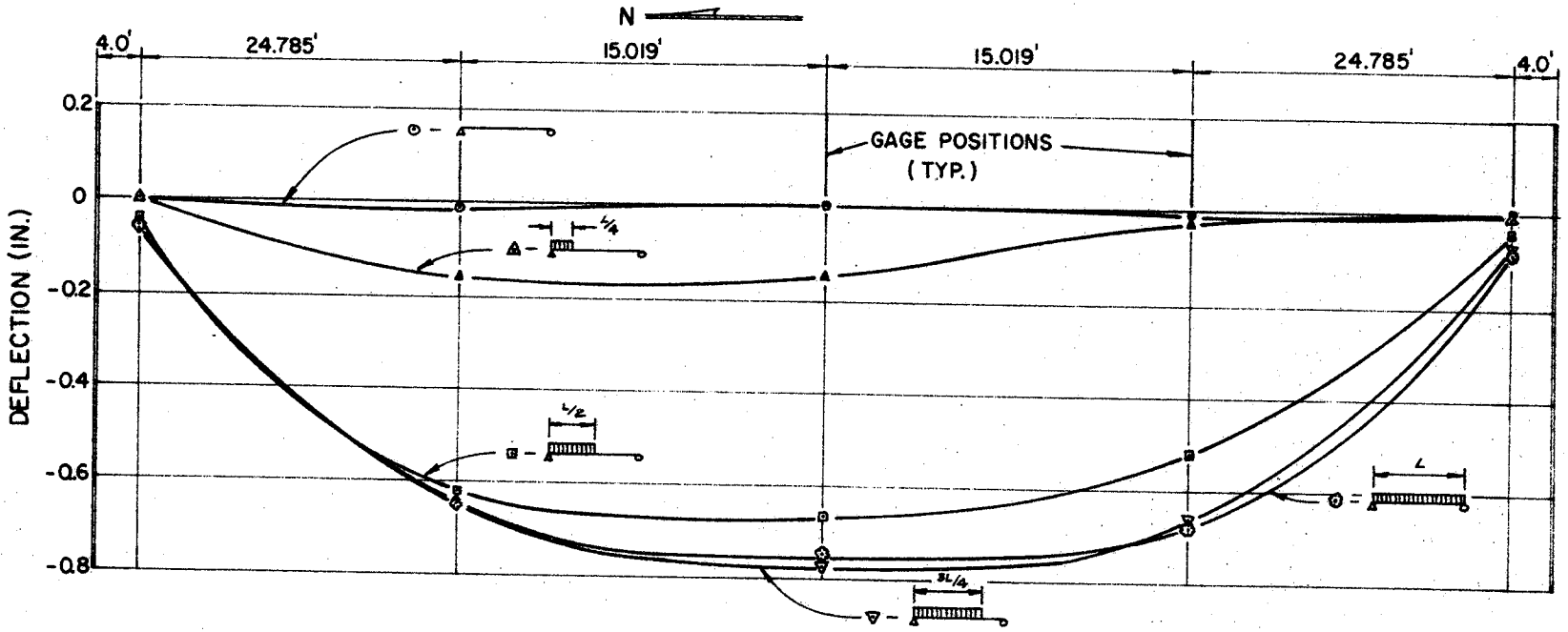

Figure 12. Vertical deflections of beam in Airport Blvd. structure at various stages of deck placement.

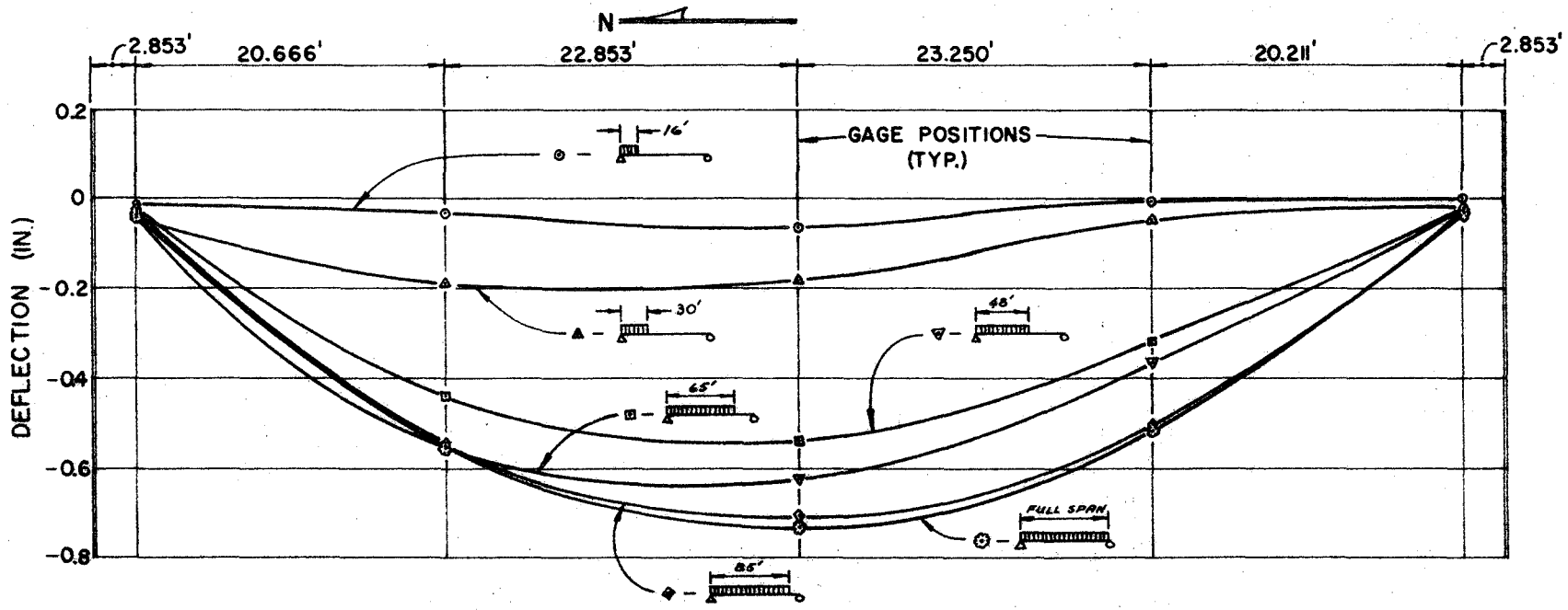

Figure 13. Vertical deflections of beam in Columbus Drive structure at various stages of deck placement.

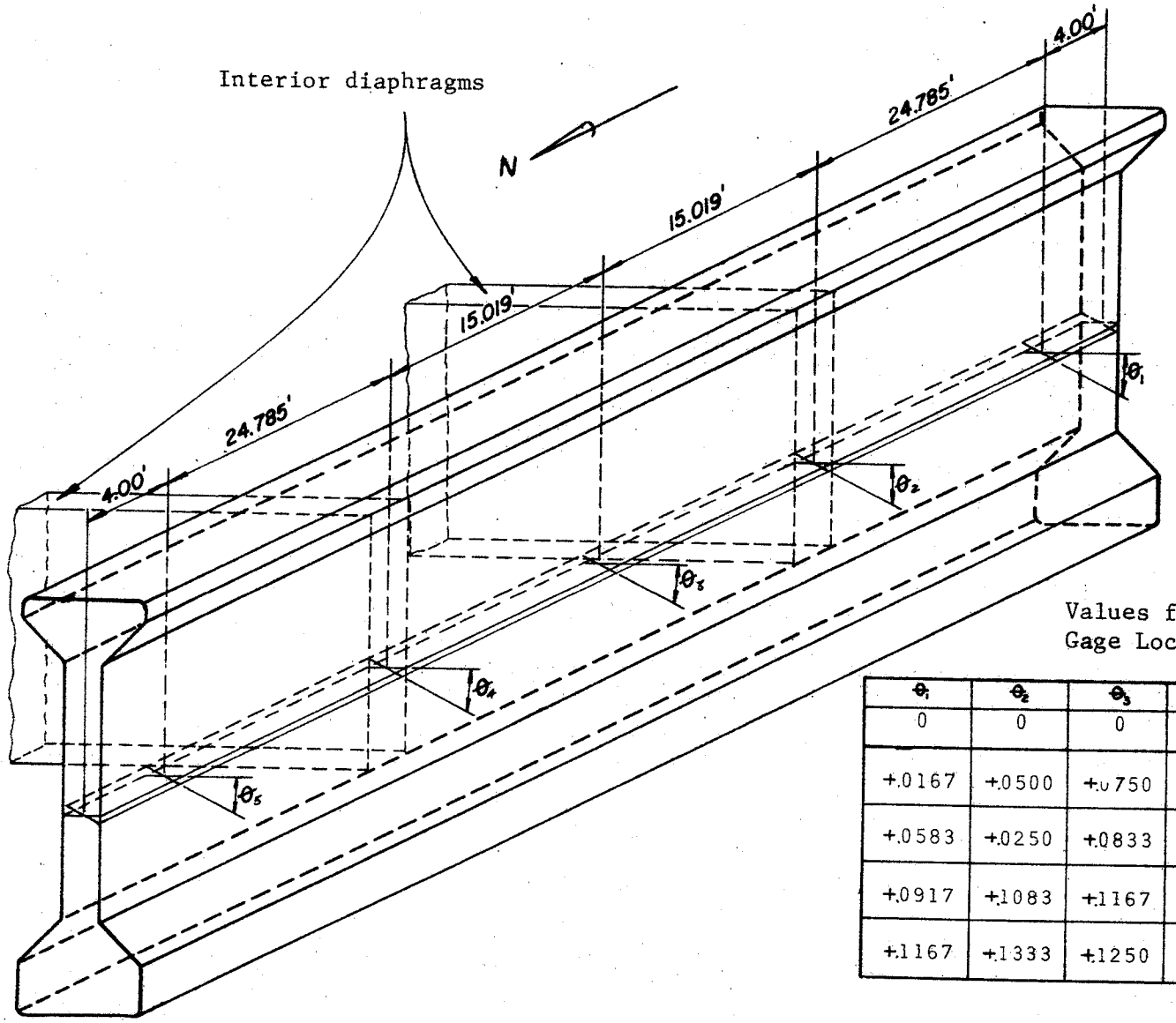

Values for θ (Degrees) at Gage Locations on Beam

θ_1	θ_2	θ_3	θ_4	θ_5	LOAD ← N
0	0	0	0	0	NO LOAD
+.0167	+.0500	+.0750	+.0417	+.0667	L/4
+.0583	+.0250	+.0833	+.1167	+.0530	L/2
+.0917	+.1083	+.1167	+.0833	+.0917	3L/4
+.1167	+.1333	+.1250	+.1167	+.0833	L

Figure 14. Rotational displacements of beams in Airport Blvd. structure.

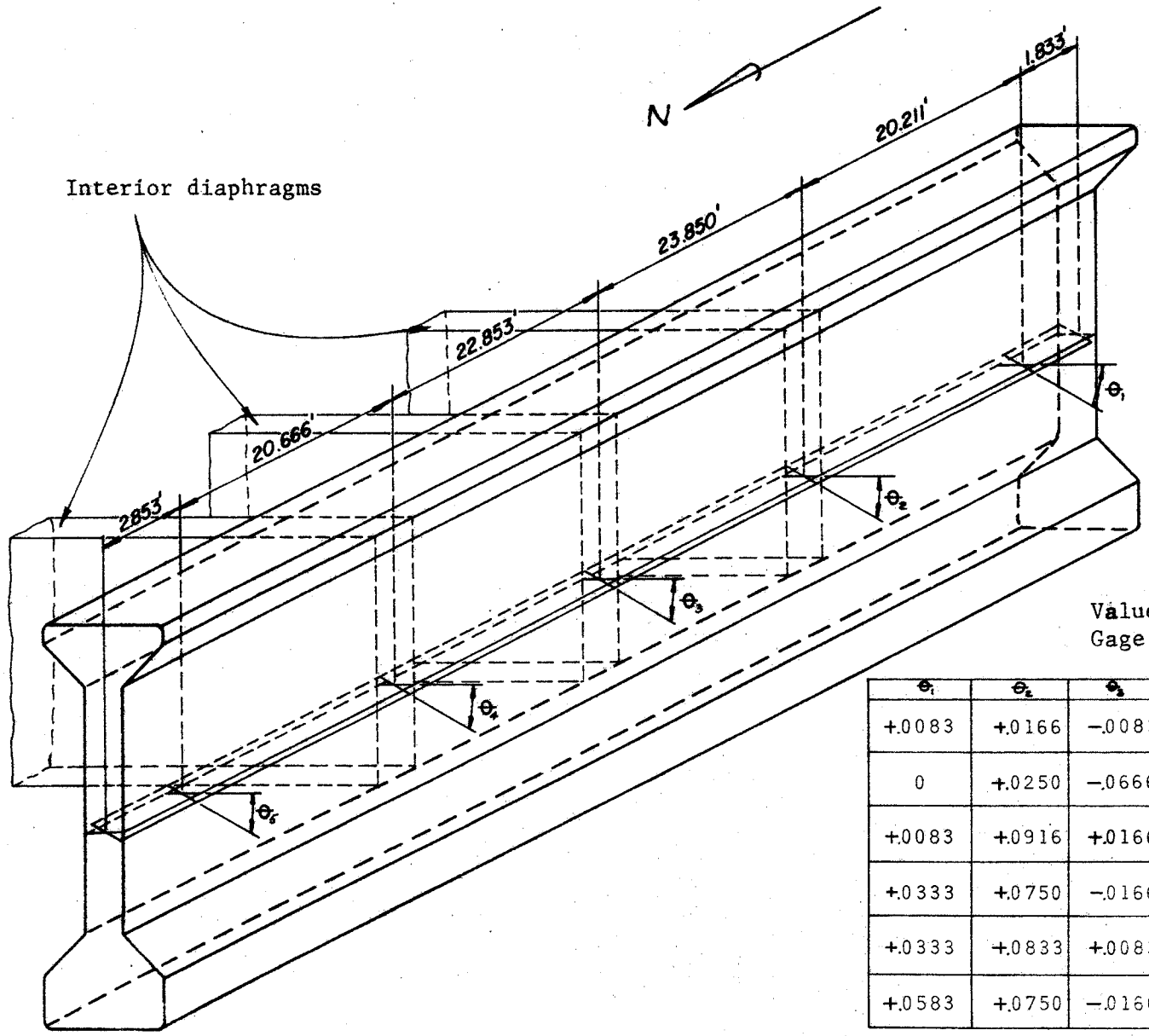

Values for θ (Degrees) at Gage Locations on Beam

θ_1	θ_2	θ_3	θ_4	θ_5	LOAD POSITION
+.0083	+.0166	−.0083	+.0166	−.0250	16'
0	+.0250	−.0666	+.0500	0	30'
+.0083	+.0916	+.0166	+.1083	+.0166	48'
+.0333	+.0750	−.0166	+.1167	+.0583	65'
+.0333	+.0833	+.0083	+.1167	+.0417	85'
+.0583	+.0750	−.0166	+.1000	+.0417	

Figure 15. Rotational displacements of beam in Columbus Drive structure.

of beam down) and somewhat comparable in magnitude. Differences between θ_1 and θ_2, θ_2 and θ_4, and θ_4 and θ_5 will give the relative twist in the beam between adjacent diaphragms. Comparisons between θ_3 and the average value of θ_2 and θ_4 gives the amount of relative rotation that occurred at midspan of the free spanning portion between interior diaphragms.

Plots of strain readings from each of the strain gages on both beams are given in the Appendix. An indication of the validity of these strains can be obtained by examining strains from longitudinal gages at various cross sections. Figure 16 shows longitudinal strain diagrams for the Airport Boulevard beam obtained by taking the difference between readings made immediately before and immediately after placement of the deck concrete. Similar diagrams for the Columbus Drive structure are given in Figure 17. The inconsistent strain results in the simple bending mode leads one to conclude that these strain readings reflect variations due to causes other than externally applied loads and therefore, should not be used in an analysis of load induced strains. The planned program to provide experimental data on the effective amount of torque that such a beam must carry under actual construction conditions cannot be accomplished with the data obtained.

Most of the problems experienced with the strain gage data were probably caused by temperature changes that were not compensated for by the arrangement used. Temperature changes were not uniform over the entire beam and were probably different in the beam than they were in the compensating gages. This was further complicated by the small magnitudes of the load induced strains that were experienced. Data scatter due to transient temperature changes and other effects tended to overshadow the load induced strains.

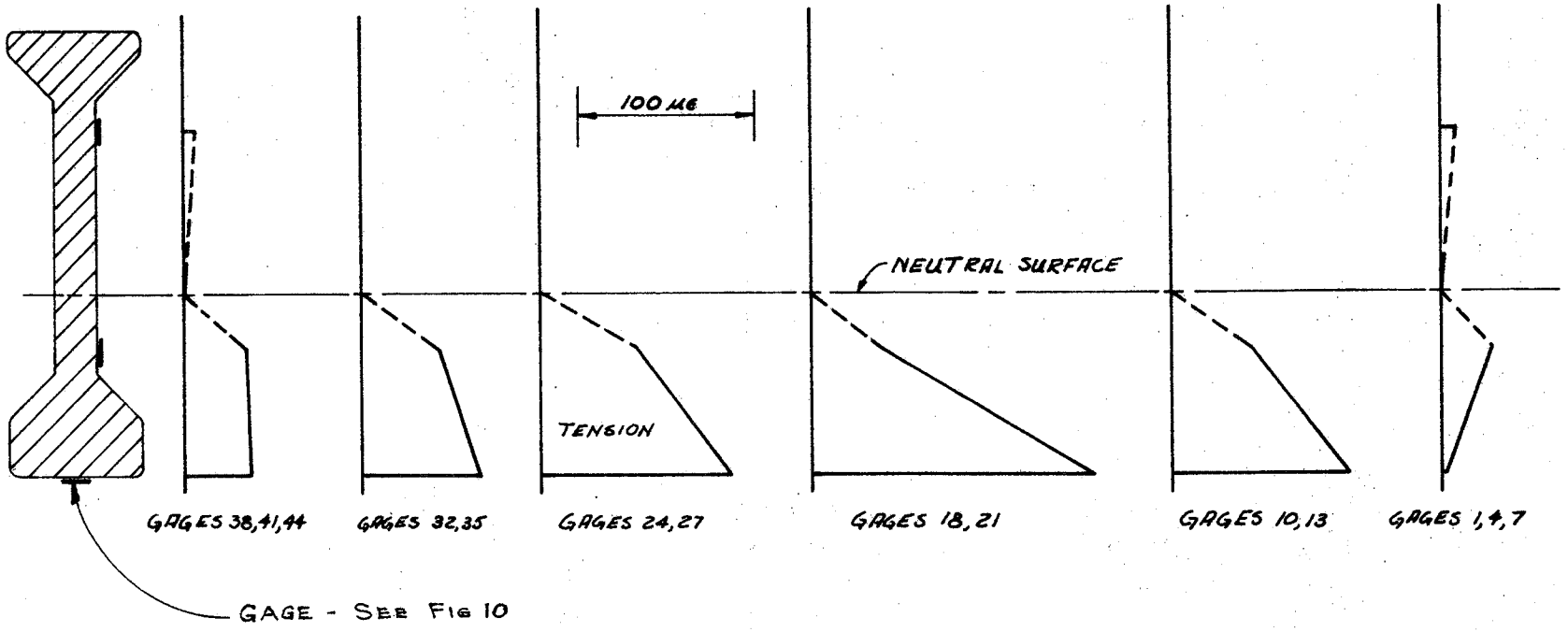

Figure 16. Diagrams of bending strains occurring during placement of deck, Airport Blvd.

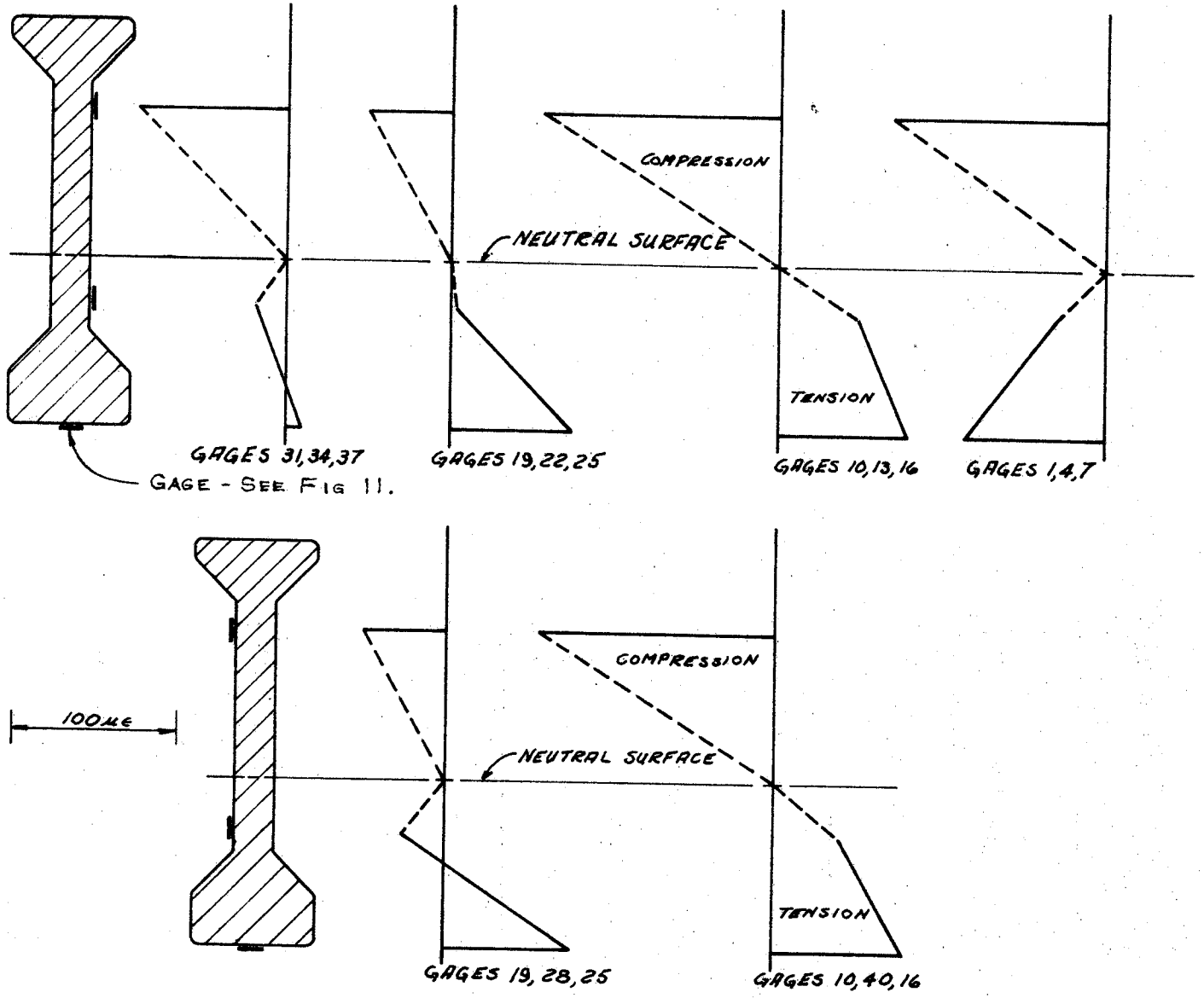

Figure 17. Diagrams of bending strains occurring during placement of deck, Columbus Drive.

SUMMARY AND CONCLUSIONS

Research reported in the literature on the behavior of concrete members subjected to torsional, and combined torsional and transverse loads has resulted in a number of phenomena that are reasonably well understood and verified by experimental data. Some of the more significant findings that have been reported are summarized below:

1. The torsional stiffness of a concrete member can be predicted by elastic theory with reasonable accuracy. Torsional stiffness of an uncracked concrete member is not significantly affected by the presence of reinforcement, either prestressed or nonprestressed.
2. Experimentally obtained torque-stress relationships are usually somewhere between those predicted by elastic theory and those predicted by plastic theory. Elastic theory in connection with measured tensile strength predicts values of torsional strength that are lower than experimental values. Plastic theory tends to overpredict torsional strength.
3. Neither longitudinal nor transverse reinforcement alone will increase the torsional capacity of a concrete member; however, appropriately arranged, equal proportions of the two will increase the torsional strength and ductility over that of plain concrete members.
4. Compressive prestressing will increase the cracking torque of a concrete member. This increase can be accounted in theory by considering the two-dimensional state of stress at the critically stressed point. For concentrically prestressed rectangular sections subjected to a pure torque, this can be accomplished by multiplying the cracking torque for a plain section by the factor $\sqrt{1 + \frac{\sigma_p}{f'_t}}$. This factor results from consideration of the state of stress at the critically stressed point on the cross section of the member.

The following conclusions are drawn from the research reported herein:

(1) A nondimensional interaction diagram relating torque, shear and bending moment has been constructed for the THD 54-in. beam. The diagram is based on elastic theory in connection with the maximum tensile stress failure criterion and assumes that the beam has failed when cracking occurs in the concrete. Although sufficient experimental data on beams similar to the THD 54-in. beam are not available, the theory presented represents the state-of-the-art on prestressed concrete members subjected to combined loads.

(2) An attempt was made to experimentally determine the magnitudes and directions of concrete strains that occur in two typical 54-in. edge beams during deck placement operations. Extraneous variations in the strain gage data due to transient temperature changes and other effects were of such magnitude that they overshadowed load induced strains. In order to obtain meaningful and reliable experimental data, it will be necessary to employ a more sophisticated instrumentation system and/or more closely controlled conditions.

RECOMMENDATIONS

The following recommendations are made on the basis of reported research on concrete members subjected to torsional and to combined loadings:

(1) It is recommended that elastic theory for torsional stress distribution and the maximum tensile stress failure criterion be used.

(2) The ultimate tensile strength of the concrete should be $5\sqrt{f'_c}$ or less if a more conservative analysis is desired.

(3) In cases where previously developed relationships between applied loads and the critical internal stress are not available, the problem should be approached by considering the states of stress (due to all loads) at all points in the member and seeking the most critically stressed point to arrive at a load stress relationship. The effects of prestressing can be handled in this manner. However, for some members such as a concentrically prestressed rectangular section, prestressing can be accounted for by simply multiplying the cracking torque by the prestressing factor, $\sqrt{1 + \frac{\sigma_p}{f_t}}$.

(4) It is recommended that laboratory tests be conducted on full-scale 54-in. beams to determine the validity of the theory presented for these beams. It would be necessary to conduct these tests under laboratory conditions so that reliable experimental data might be obtained.

NOTATION

A_t = cross sectional area of one leg of a stirrup (in.^{2})

b = shorter dimension of a rectangular cross section (in.)

E = modulus or elasticity of concrete (psi)

f_t = tensile strength of concrete (psi)

f_y = yield strength of stirrups (psi)

f_{sy} = yield strength of steel (psi)

f'_c = compressive strength of concrete (psi)

f'_t = tensile strength of concrete (psi)

G = shear modulus of elasticity for concrete (psi)

h = longer dimension of a rectangular cross section (in.)

I = moment of inertia for selected cross section (in.^{4})

K = torsional stiffness constant (in.^{4})

M = bending moment (in. -lbs)

M_o = pure moment which will produce cracking in beam in the absence of other loads (in. - lbs)

P_t = total percentage of steel (%)

s = spacing of stirrups (in.)

T = torque (in. - lbs)

T_c = torsional capacity (in. - lbs)

T_{cr} = cracking torque (in. - lbs)

T_o = contribution of concrete to torsional strength (in. -lbs)

T_p = plastic torsional capacity of the member (in. - lbs)

T_u = ultimate torque (in. - lbs)

T_{up} = ultimate torsional strength of a non-prestressed section (in. - lbs)

V = transverse shear stress (psi)

V_o = transverse shear stress which will produce cracking in the web of the beam in the absence of other loads (psi)

V_{tc} = torsional shear stress of concrete (psi)

x_1 = shorter center-to-center dimension of closed rectangular stirrup (in.)

y_1 = longer center-to-center dimension of closed rectangular stirrup (in.)

α = a constant determined by the b/h ratio

α_t = constant reflecting the effect of reinforcement of stirrups

Δ = deflection of beam (in.)

θ = angle of twist (radians/in.)

ϕ = ordinate to membrane (in.)

σ = normal stress (psi)

σ_x = normal stress in x-direction (psi)

σ_p = amount of prestressing (psi)

τ = torsional shear stress (psi)

τ_a = torsional shear stress at the mid point of the longer leg (psi)

τ_b = torsional shear stress at the mid point of the shorter leg (psi)

τ_{xy} = torsional shear stress on the x, y plane (psi)

REFERENCES

1. Buth, Eugene and Furr, H. L., "Torsional Strength of Prestressed Concrete Bridge Girders," Research Report 150-1F, Texas Transportation Institute, Texas A&M University, College Station, Texas, August 1971.
2. Zia, Paul, "Torsion Theories for Concrete Members," Torsion of Structural Concrete, Special Publications no. 18, American Concrete Institute, 1966.
3. Chandler, H., Kemp, E. L., and Wilhelm, W. J., "Behavior of Prestressed Concrete Rectangular Members Subjected to Pure Torsion," Report no. 2007, Department of Civil Engr., West Virginia University, 1970.
4. Hsu, Thomas T. C., "Torsion of Structural Concrete - Plain Concrete Rectangular Sections," Torsion of Structural Concrete Special Publication no. 18, American Concrete Institute, 1966.
5. Timoshenko, S. and Goodier, J. M., Theory of Elasticity, Second Edition, McGraw Hill, New York, 1951.
6. Hsu, Thomas, T. C., "Torsion of Structural Concrete.- A Summary on Pure Torsion," Torsion of Structural Concrete, Special Publication no. 18, American Concrete Institute, 1966.
7. Hsu, Thomas, T. C., "Torsion of Structural Concrete - Behavior of Reinforced Concrete Rectangular Members," Torsion of Structural Concrete, Special Publication no. 18, American Concrete Institute, 1966.
8. Seeley, F. B., and Smith, J. O., Advanced Mechanics of Materials, Second Edition, John Wiley and Sons Inc., 1967.
9. Zia, Paul, "Torsional Strength of Prestressed Concrete Members," Journal of the American Concrete Institute, vol. 32, no. 10, April 1961.
10. Wyss, A. N., Garland, J. B., and Mattock, A. H., "A Study of the Behavior of I-Section Prestressed Concrete Girders Subject to Torsion," Structures and Mechanics Report SM 69-1, University of Washington, Seattle, Washington, March 1969.
11. Wyss, A. N., and Mattock, A. H., "A Study of I-Section Prestressed Concrete Girders Subject to Torsion, Shear and Bending," Final Report Research Project No. Y-1180, University of Washington, Dept. of Civil Engr., Seattle, Washington, June 1971.
12. Hsu, Thomas T. C., and Kemp, E. L., "Background and Practical Application of Tentative Design Criteria for Torsion," ACI Journal, Proceedings v. 66, no. 1, January 1969.
13. Swamy, N., "The Behavior and Ultimate Strength of Prestressed Concrete Hollow Beams Under Combined Bending and Torsion," Magazine of Concrete Research (London), vol. 14, no. 40, March 1962.

APPENDIX

STRAIN GAGE READINGS

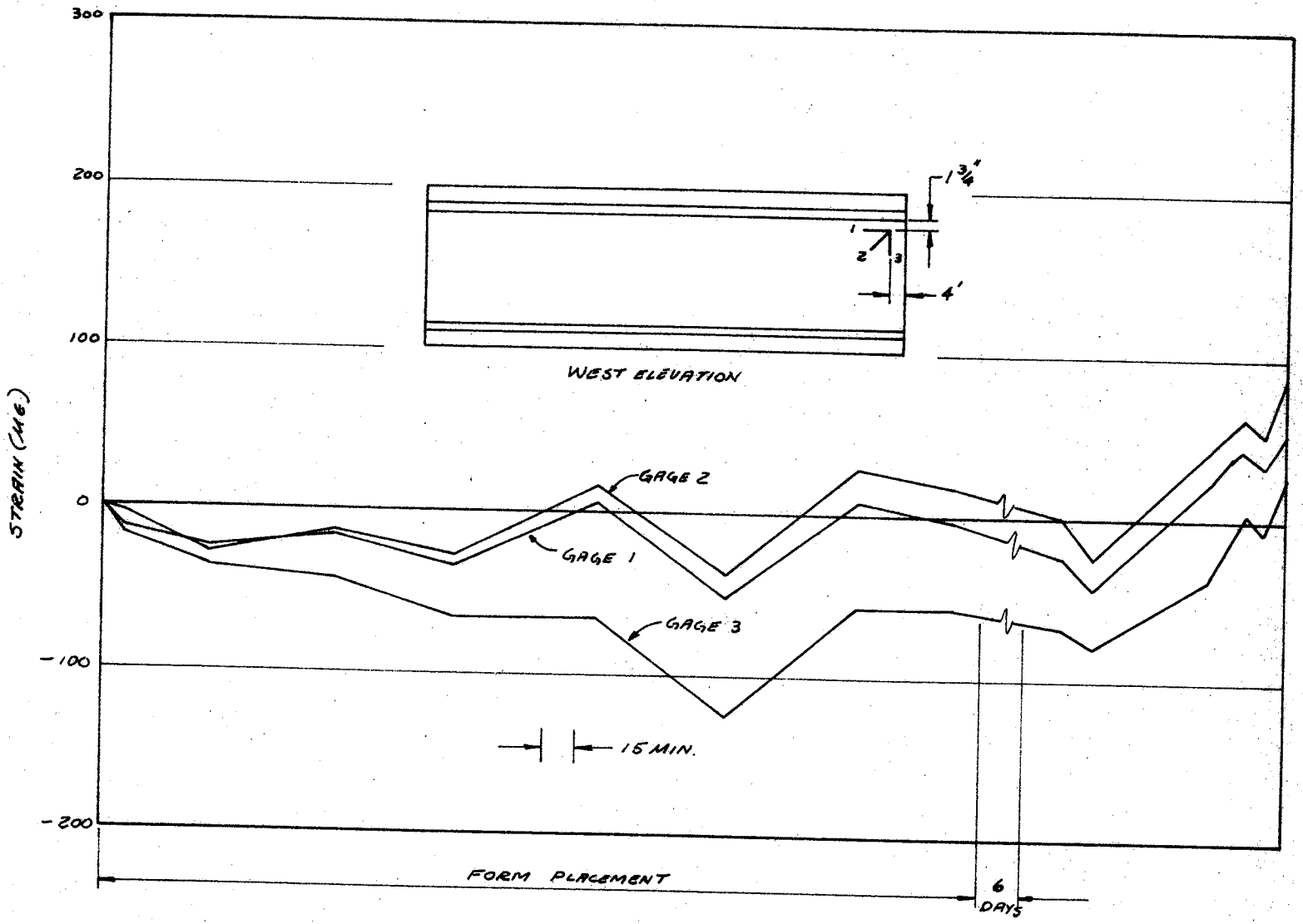

Figure A1. Strain readings, Airport Blvd. Gages 1, 2, and 3.

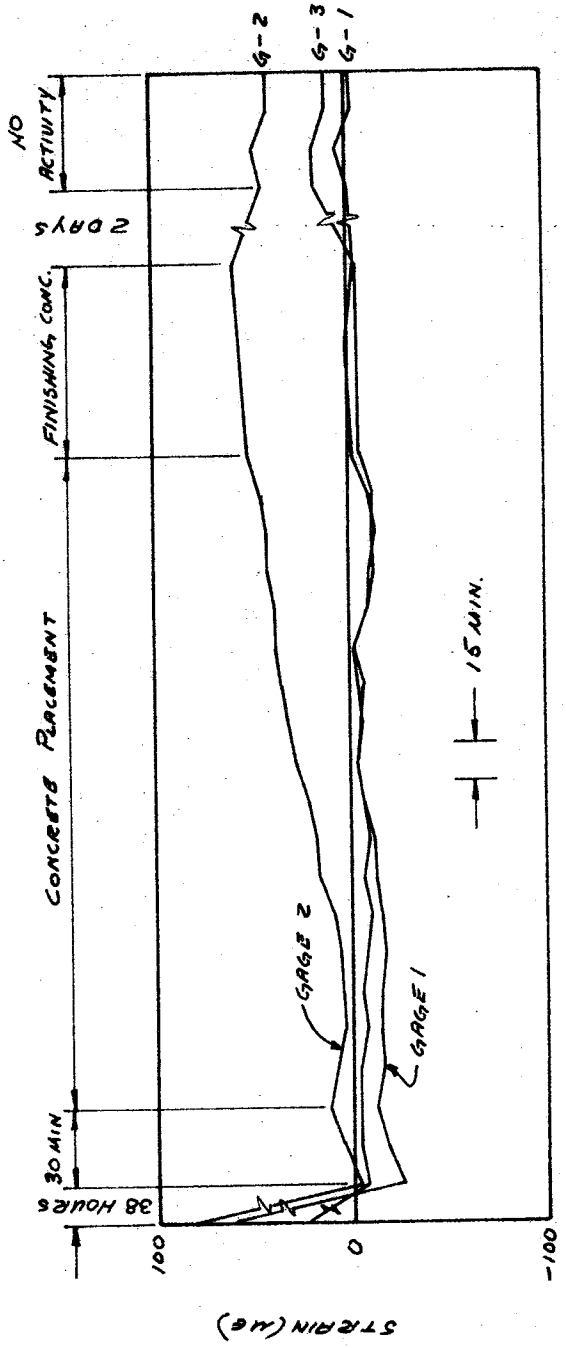

Figure A1. Cont'd.

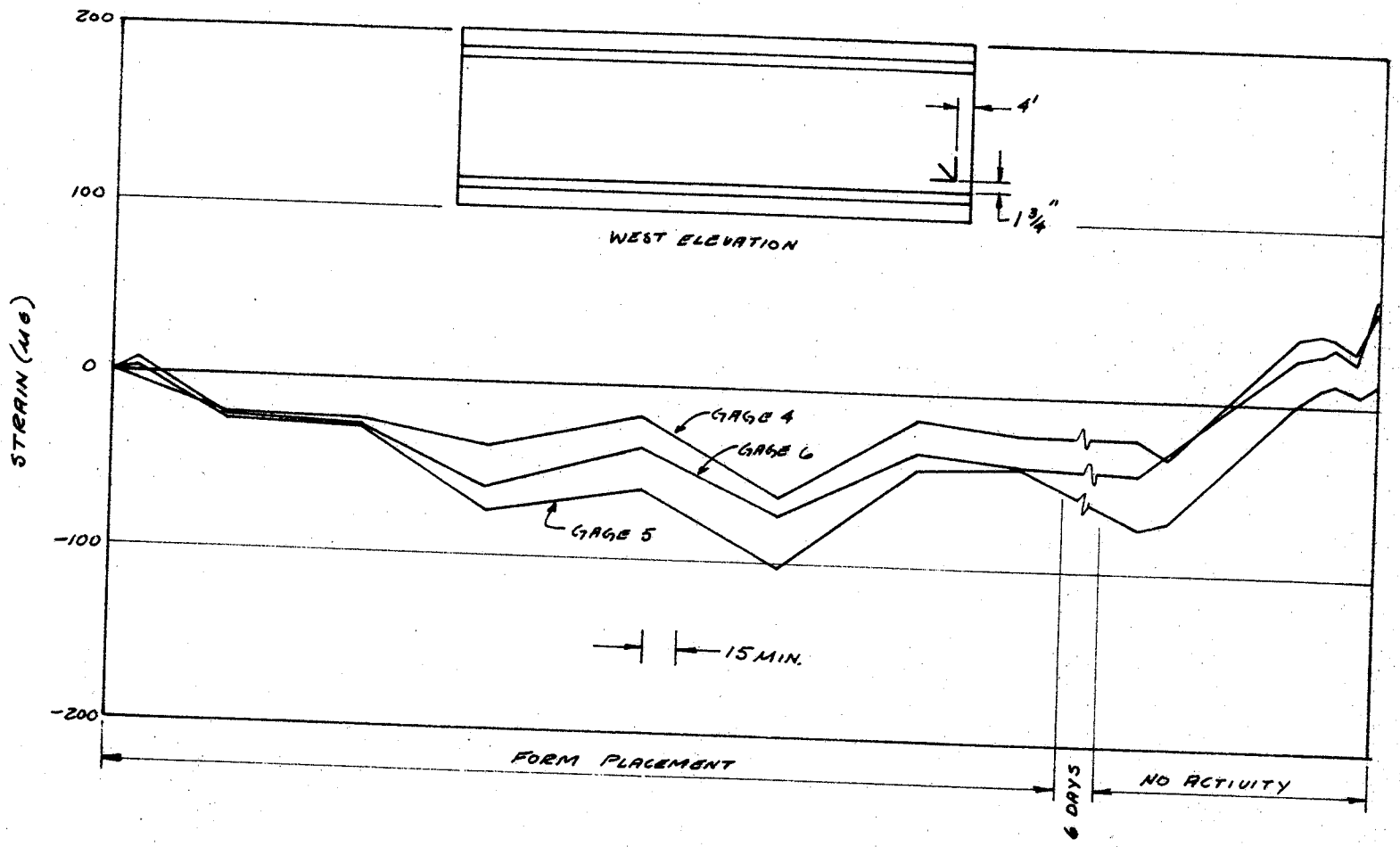

Figure A2. Strain readings, Airport Blvd. Gages 4, 5, and 6.

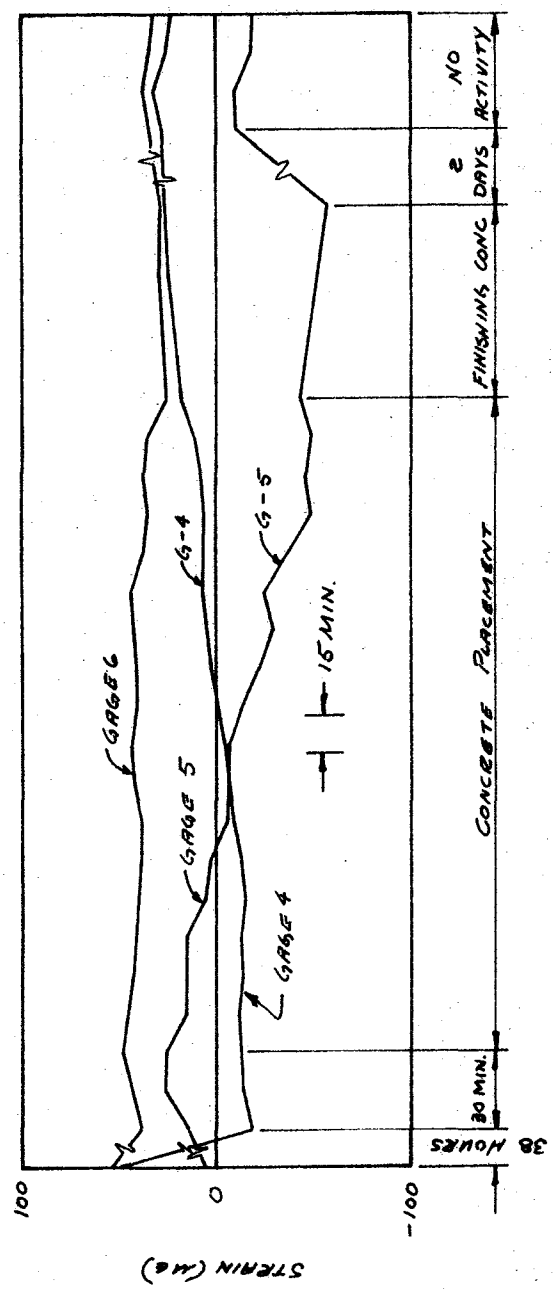

Figure A2. Cont'd.

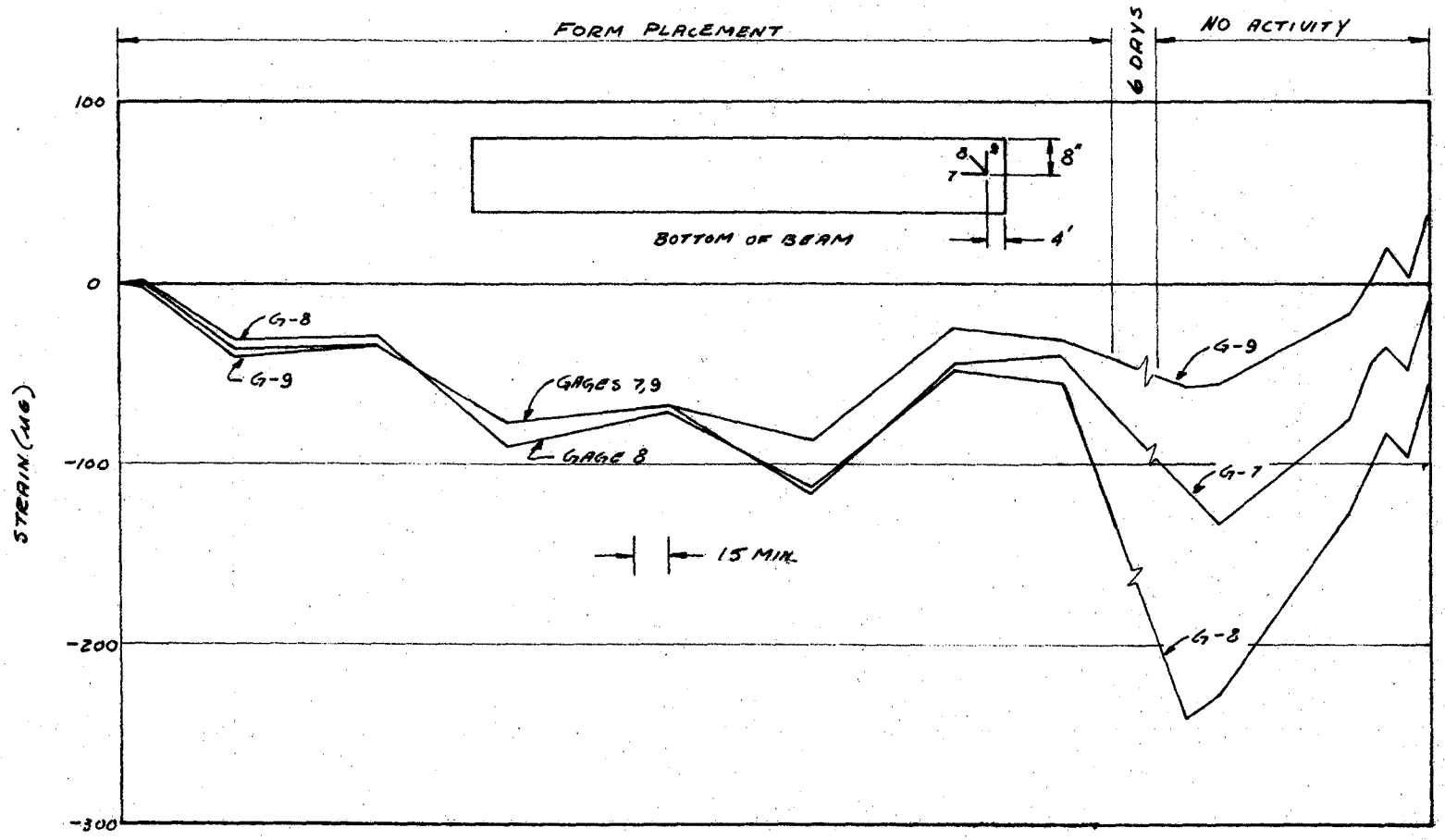

Figure A3. Strain readings, Airport Blvd. Gages 7, 8, and 9.

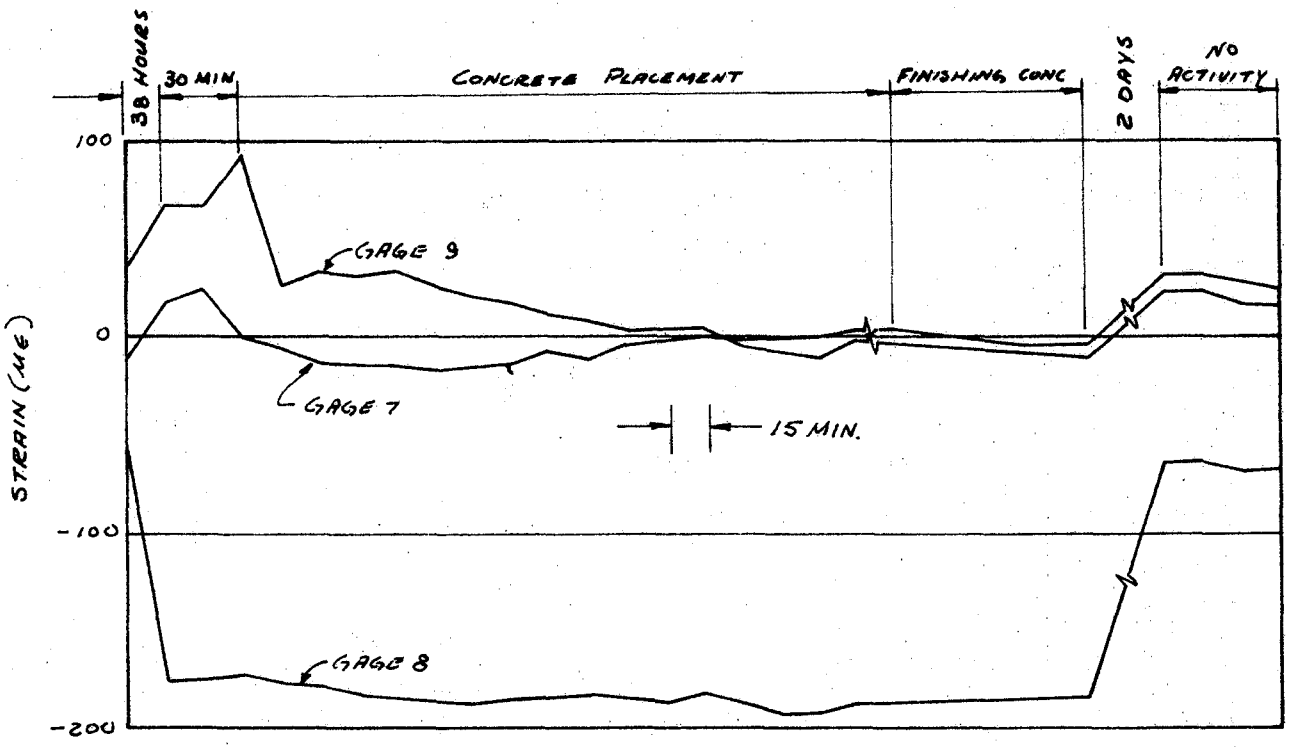

Figure A3. Cont'd.

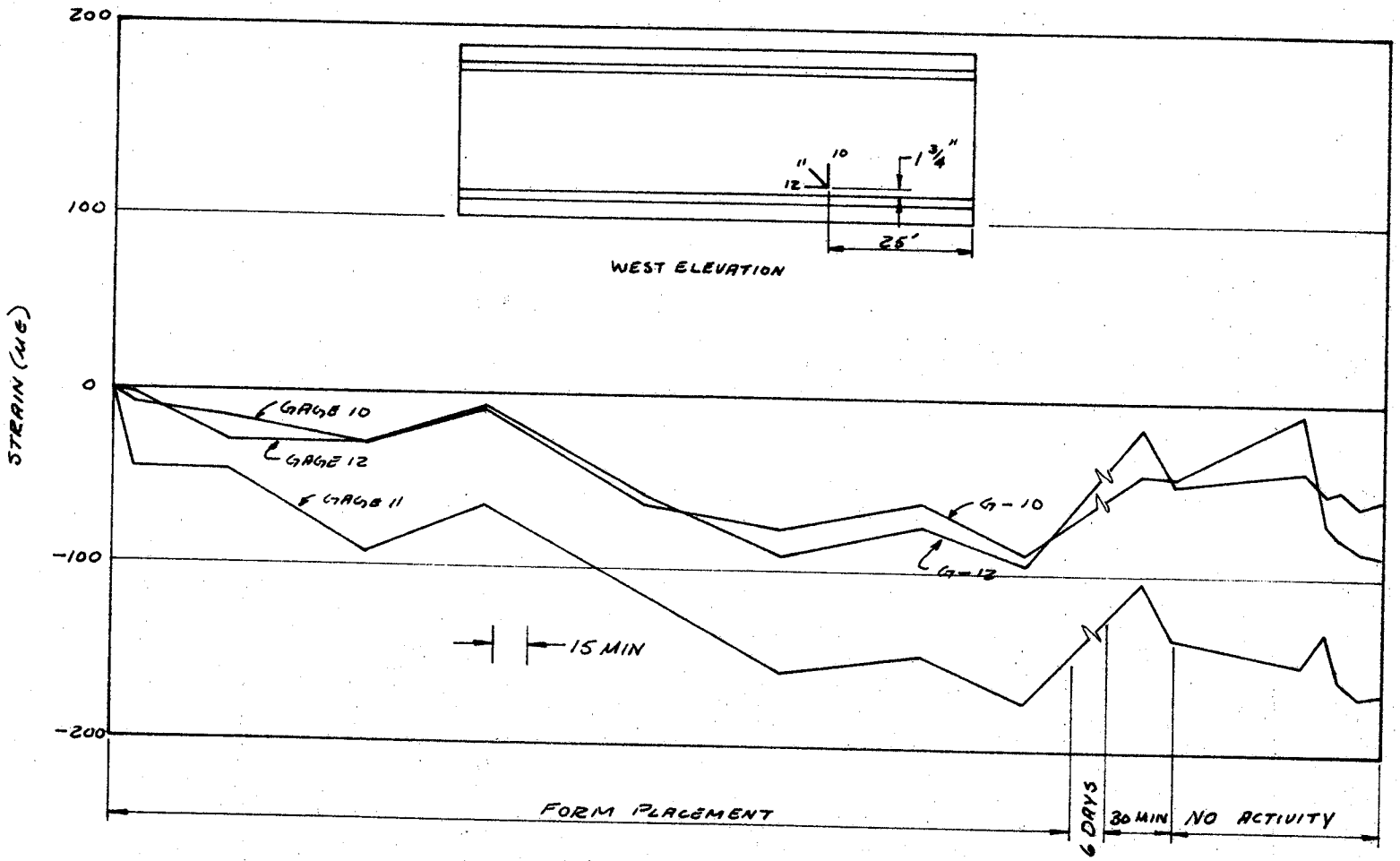

Figure A4. Strain readings, Airport Blvd. Gages 10, 11, and 12.

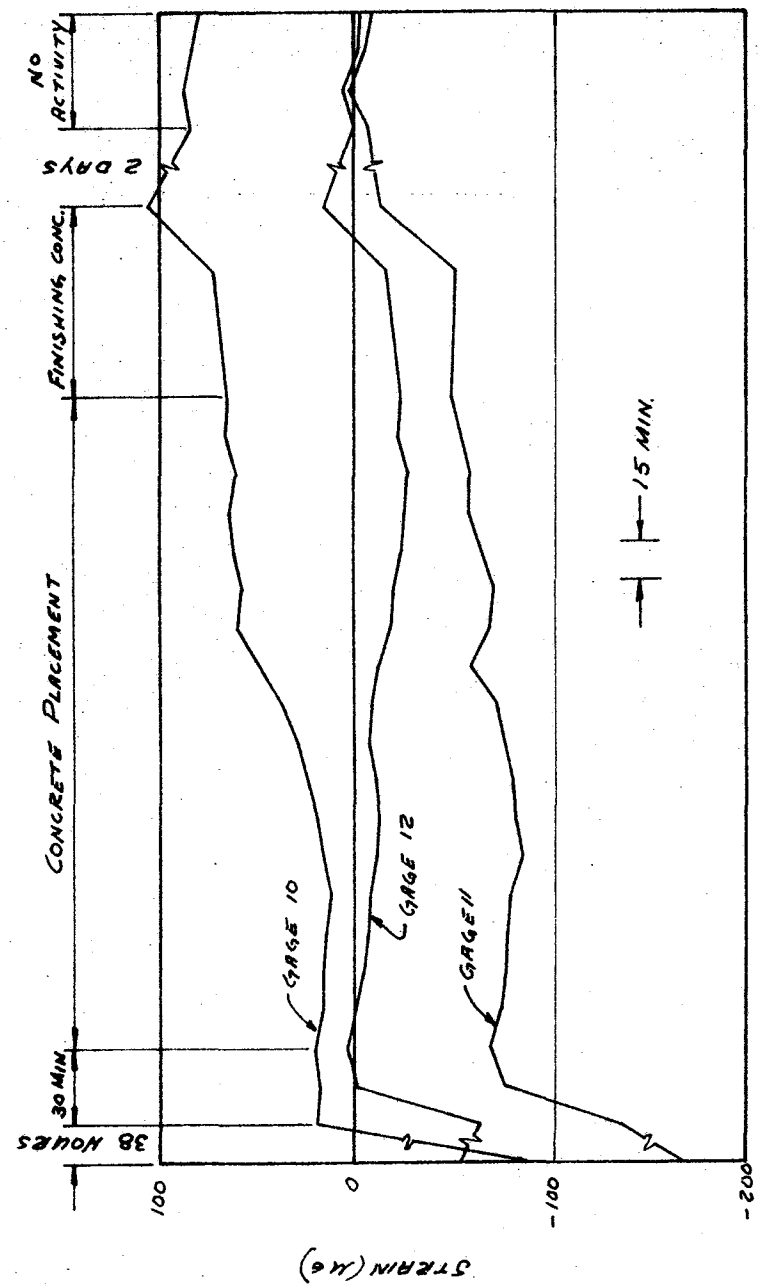

Figure A4. Cont'd.

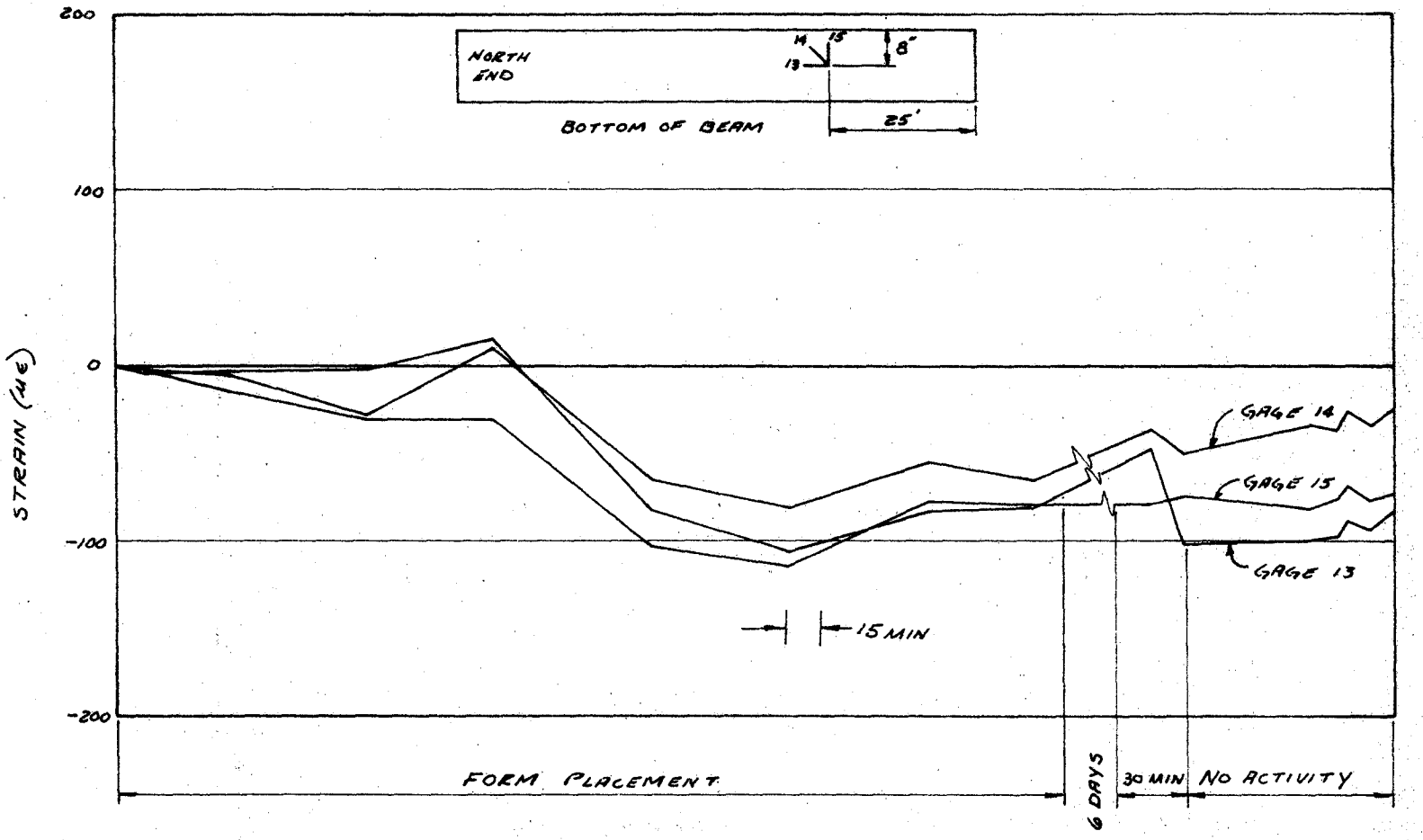

Figure A5. Strain readings, Airport Blvd. Gages 13, 14, and 15.

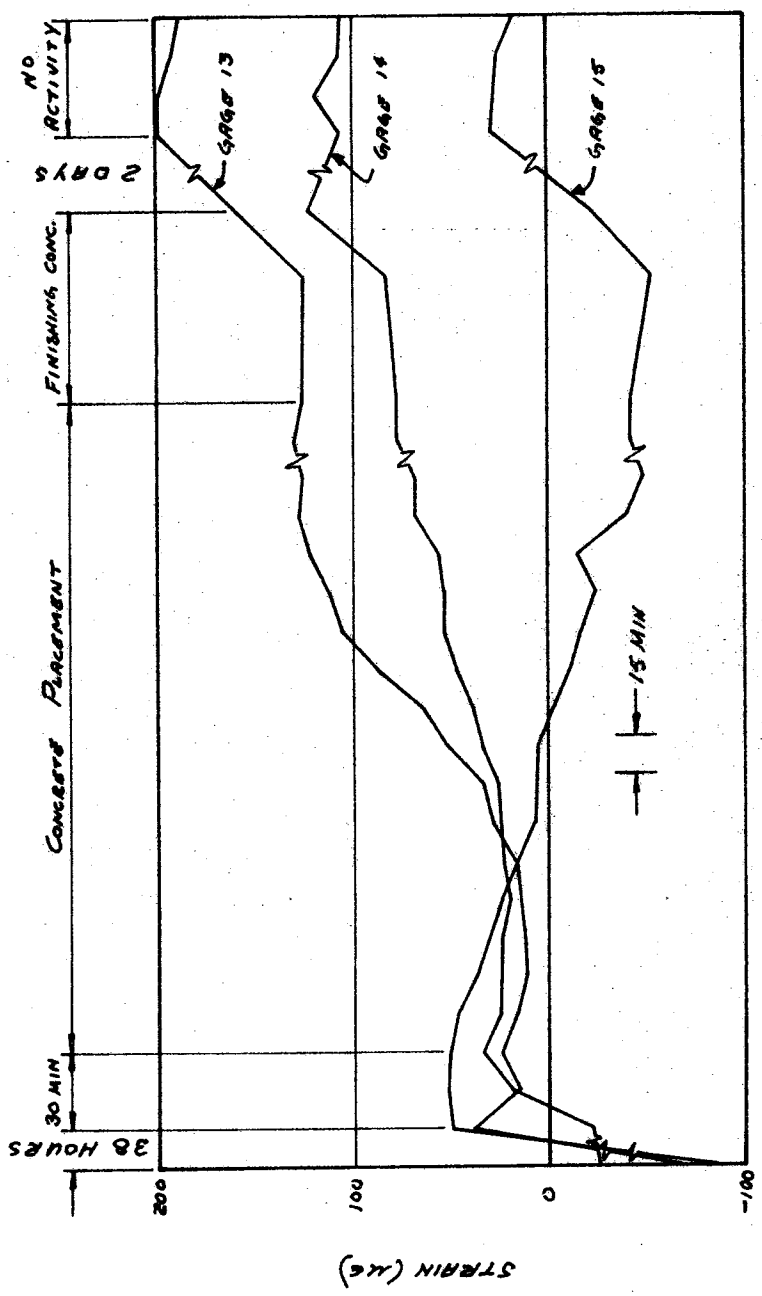

Figure A5. Cont'd.

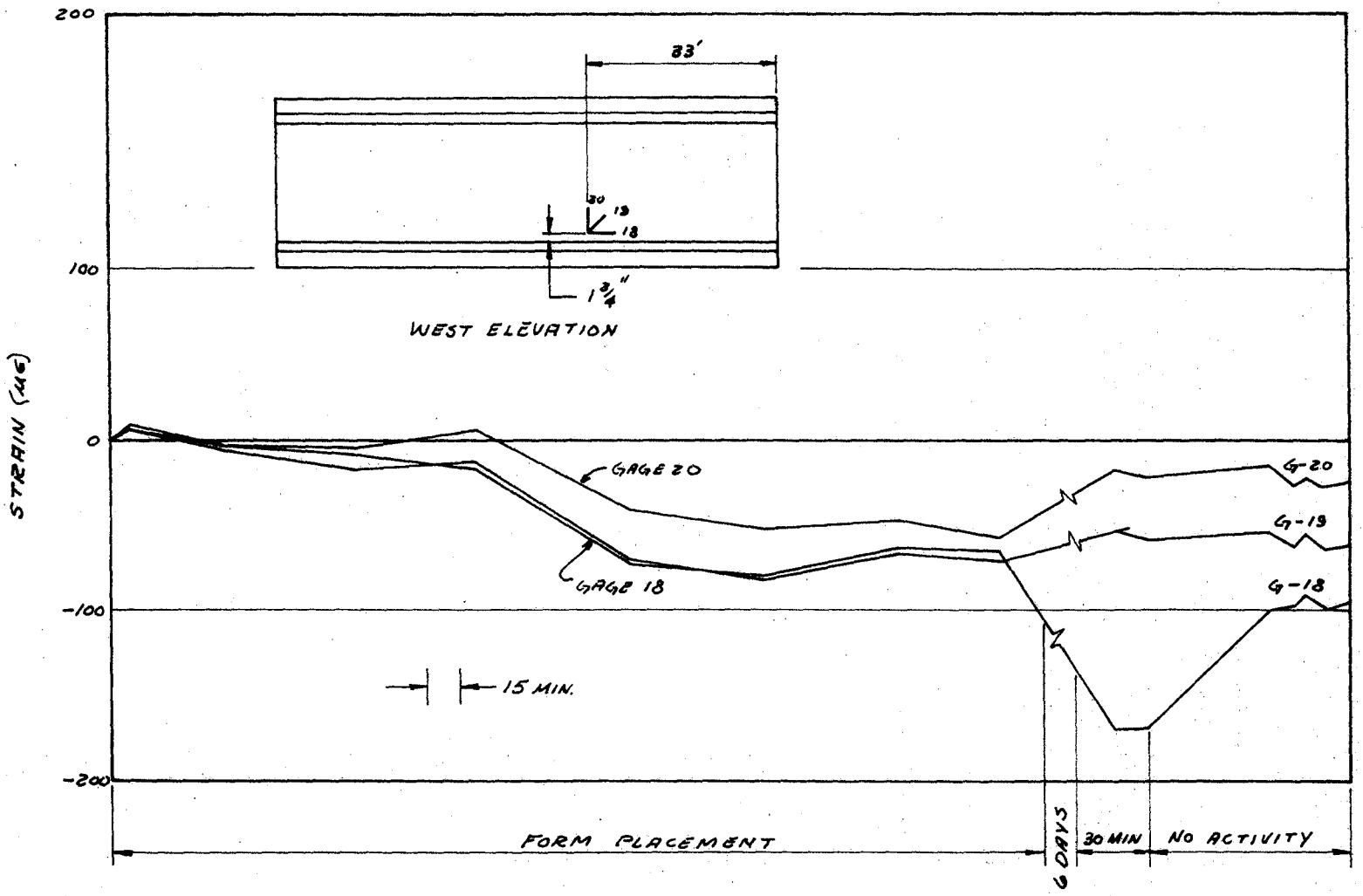

Figure A6. Strain readings, Airport Blvd. Gages 18, 19, and 20.

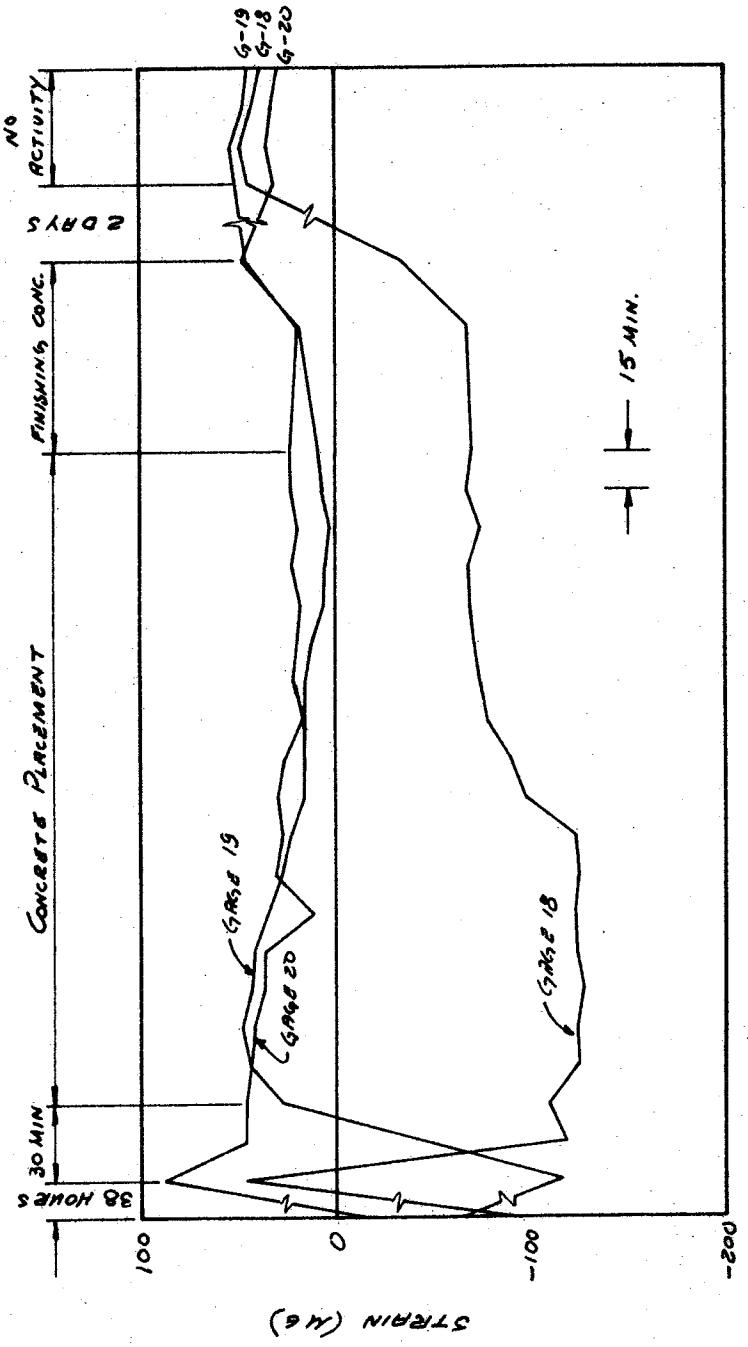

Figure A6. Cont'd.

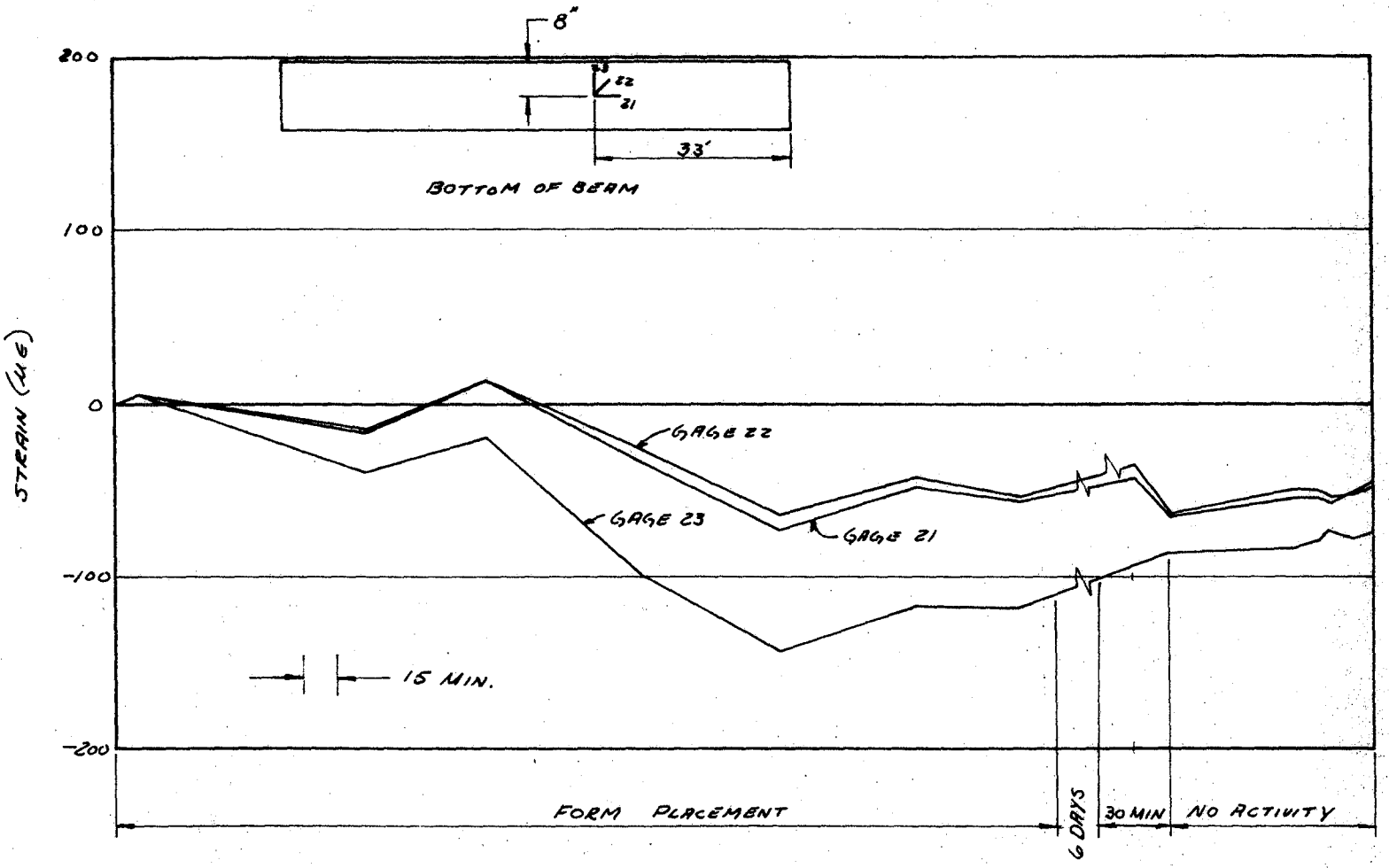

Figure A7. Strain readings, Airport Blvd. Gages 21, 22, and 23.

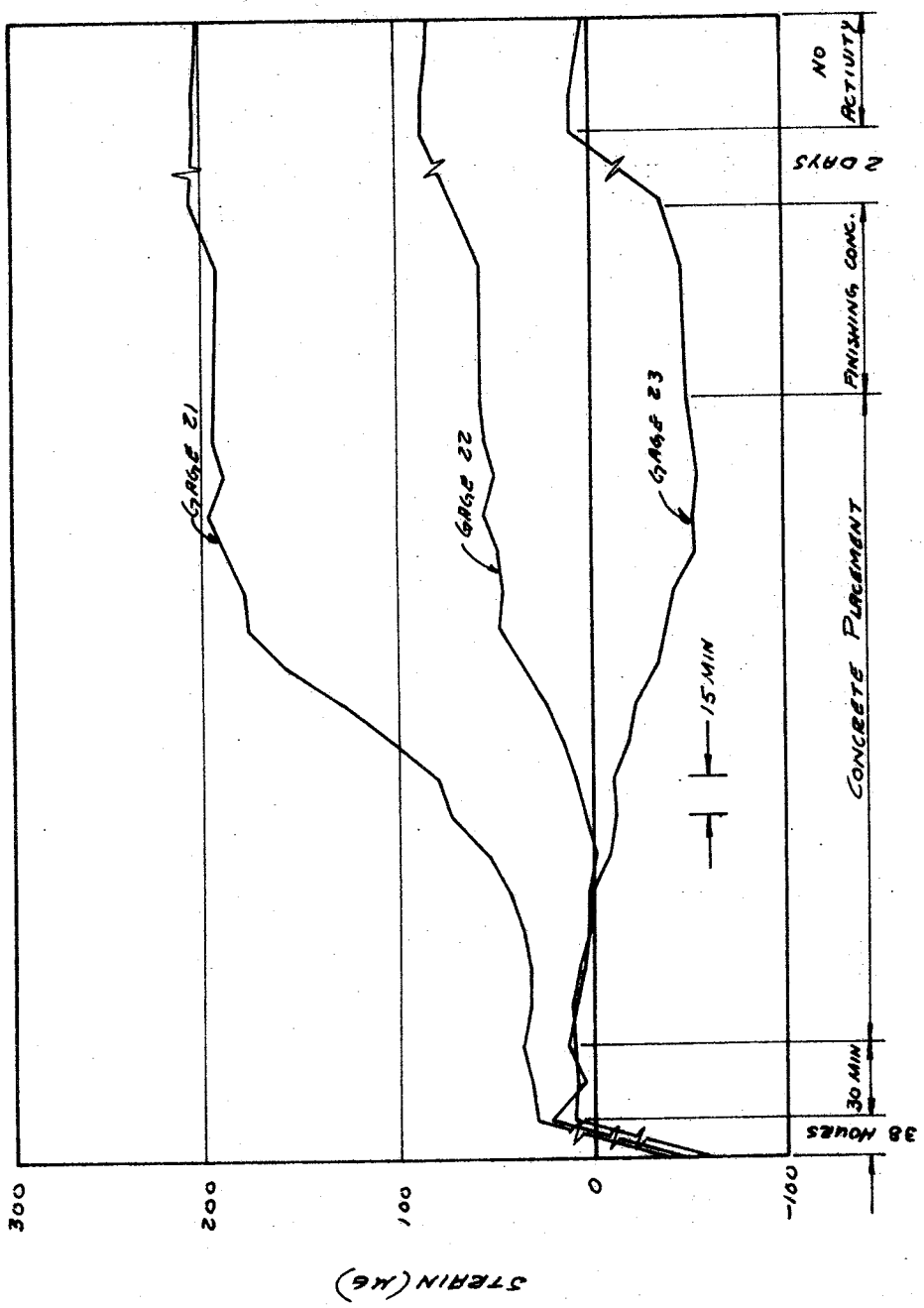

Figure A7. Cont'd.

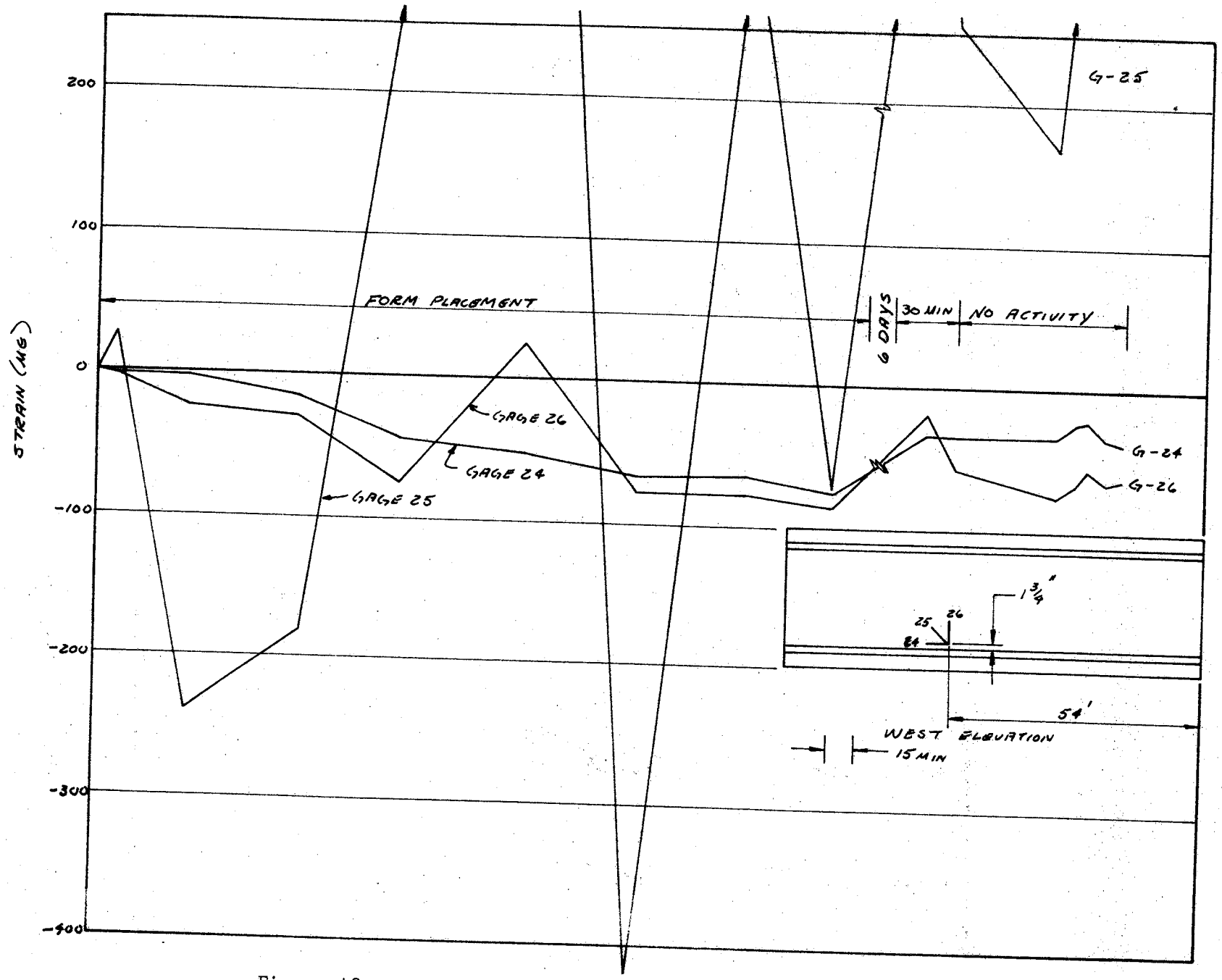

Figure A8. Strain readings, Airport Blvd. Gages 24, 25, and 26.

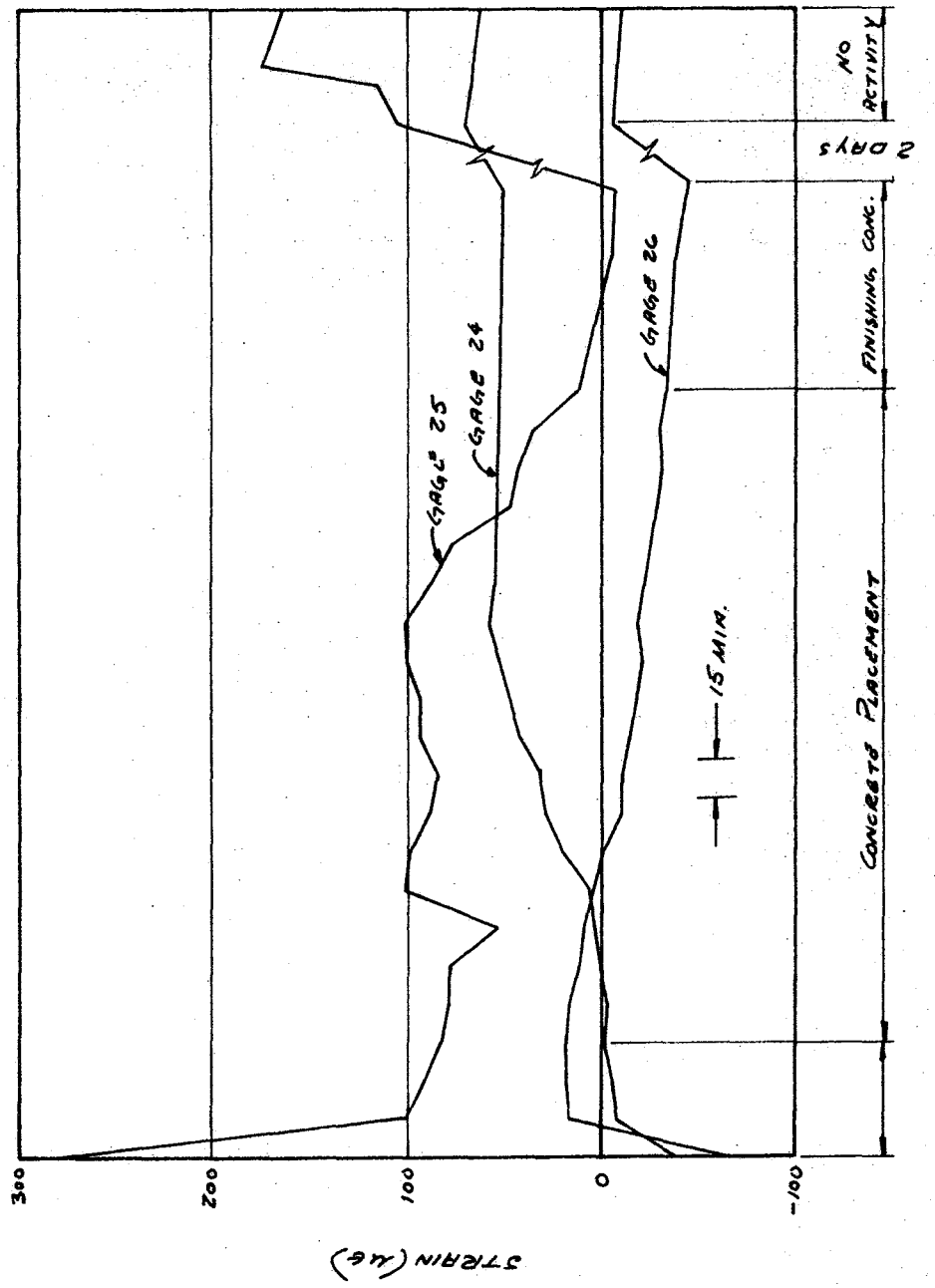

Figure A8. Cont'd.

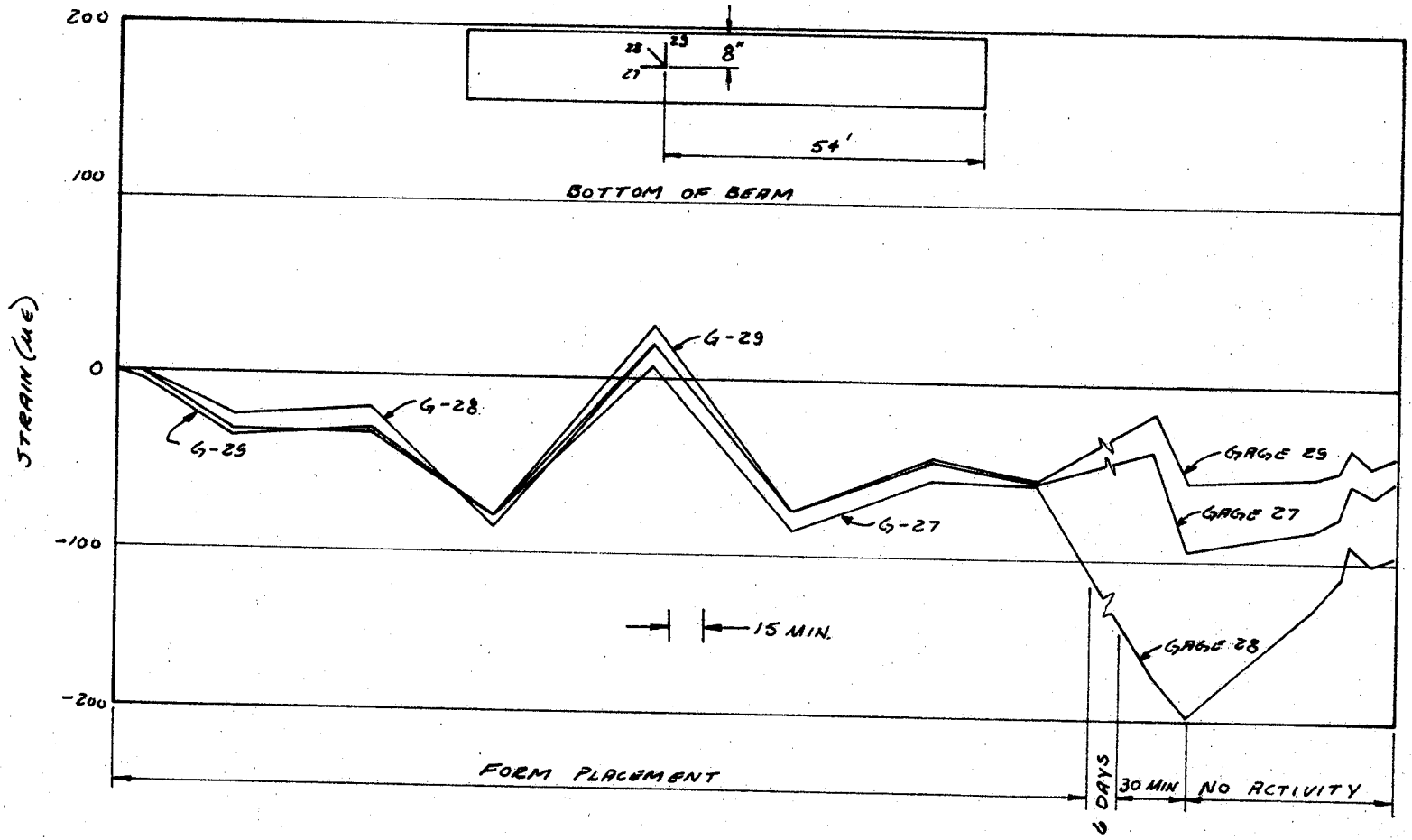

Figure A9. Strain readings, Airport Blvd. Gages 27, 28, and 29.

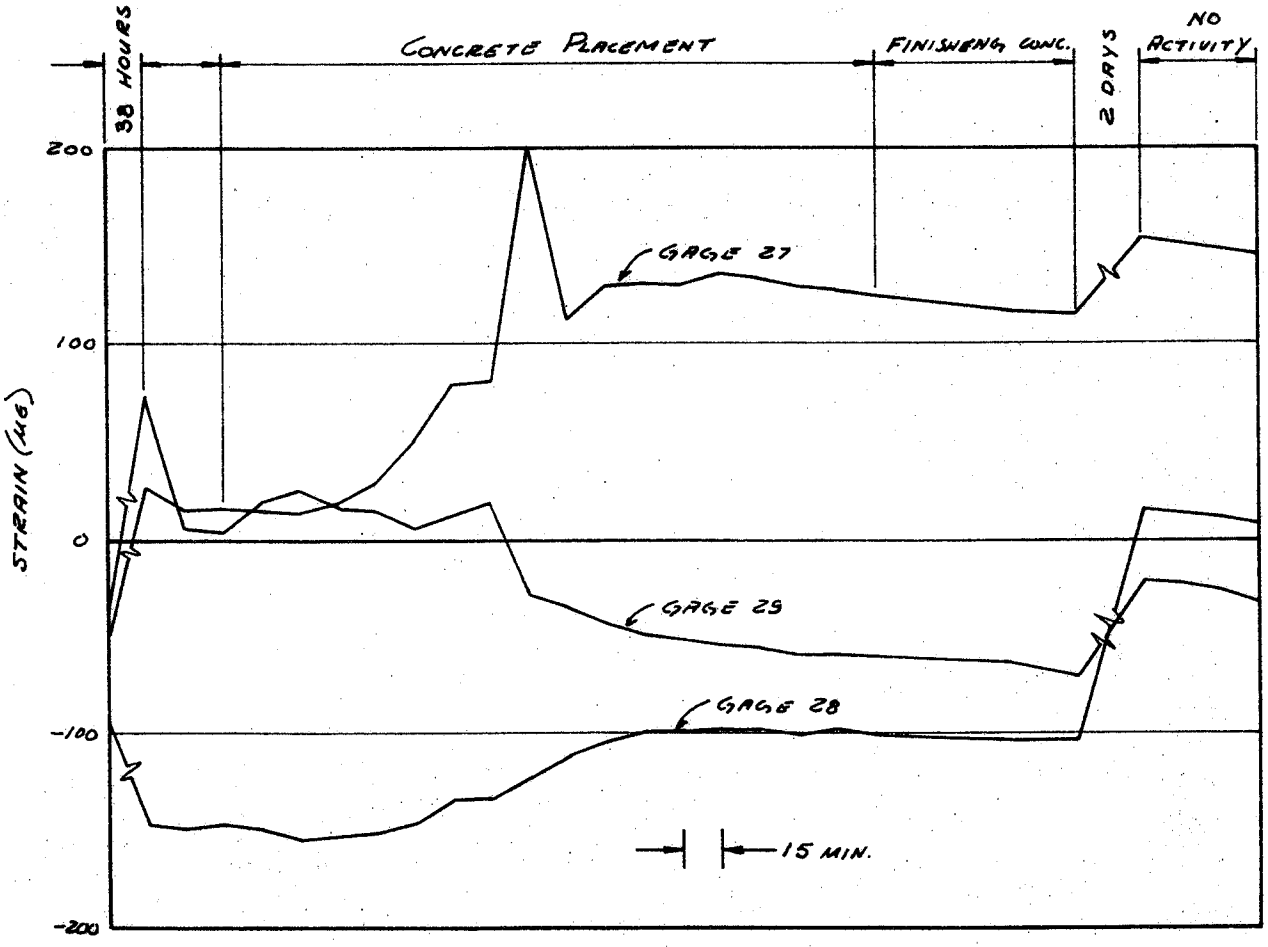

Figure A9. Cont'd.

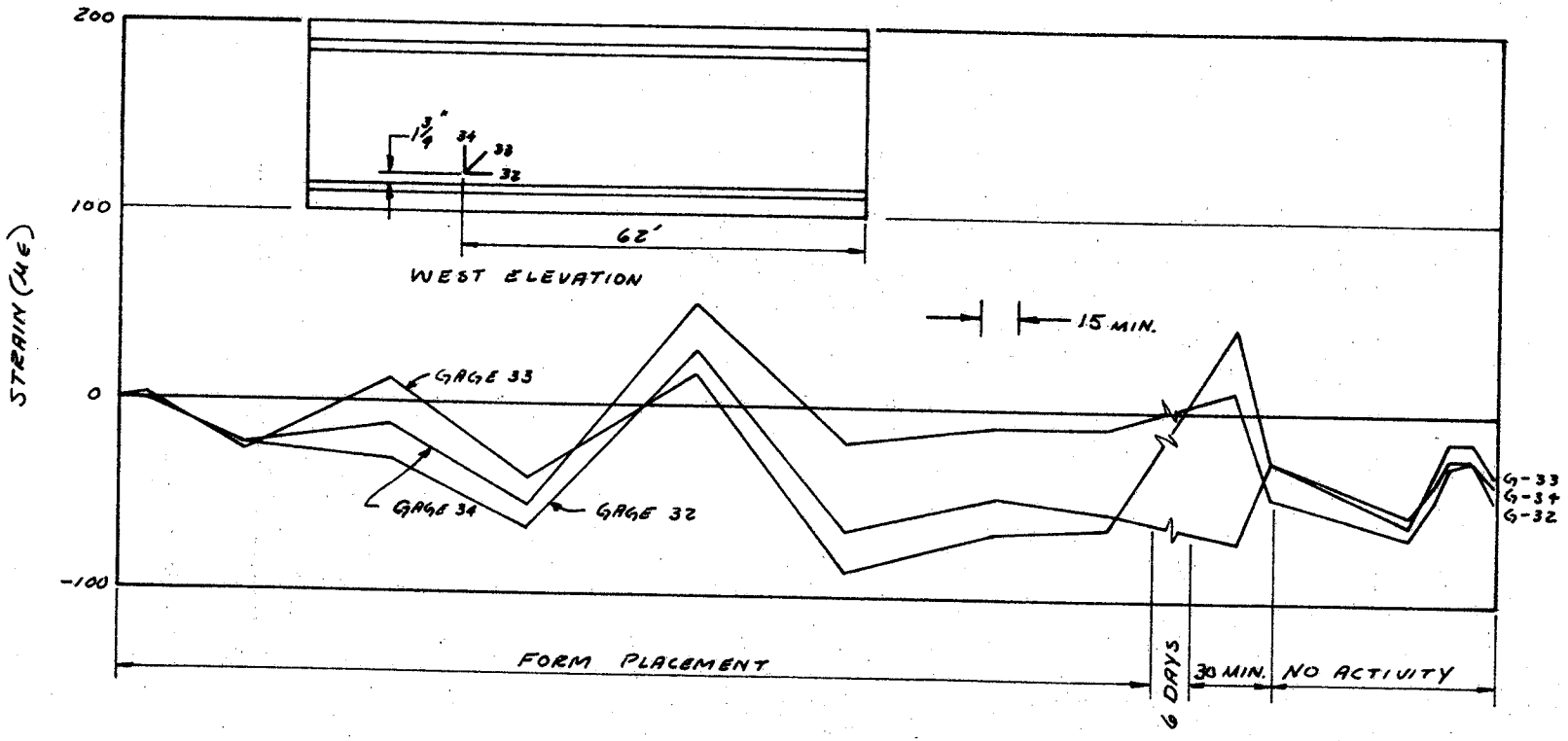

Figure A10. Strain readings, Airport Blvd. Gages 32, 33, and 34.

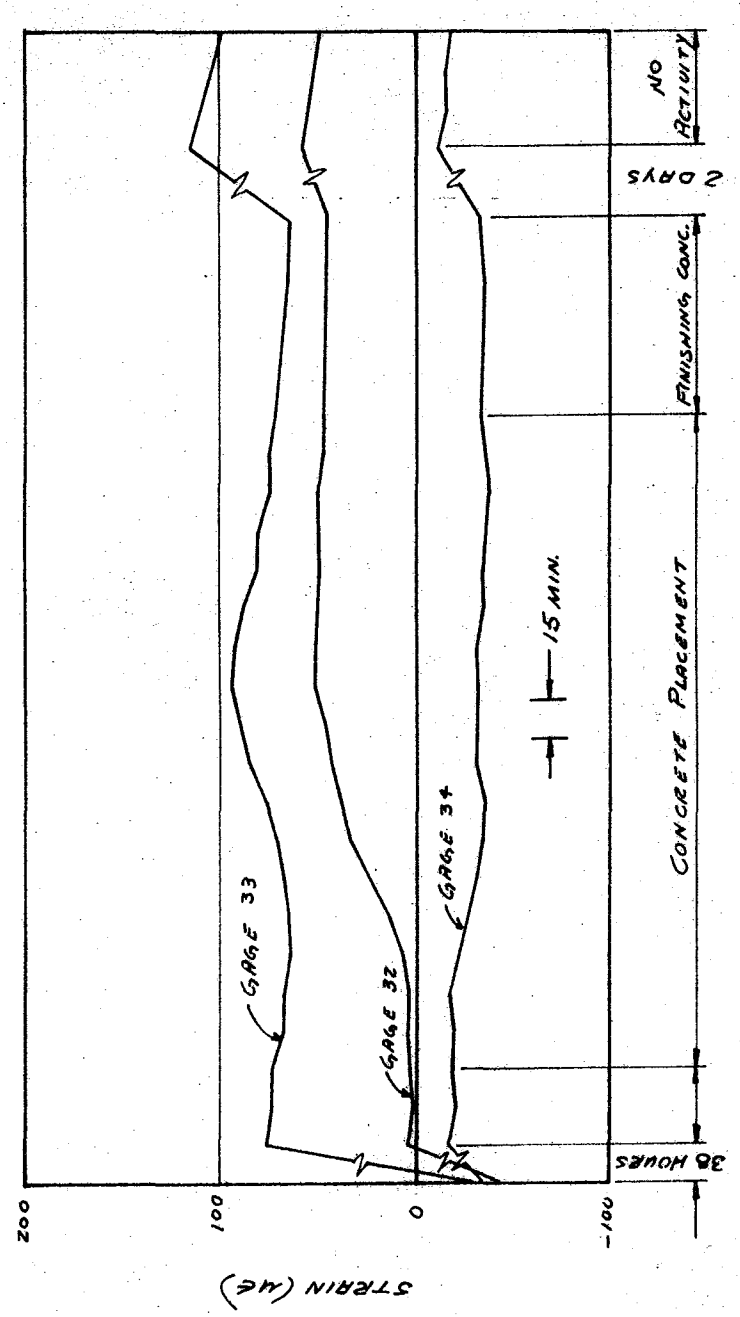

Figure A10. Cont'd.

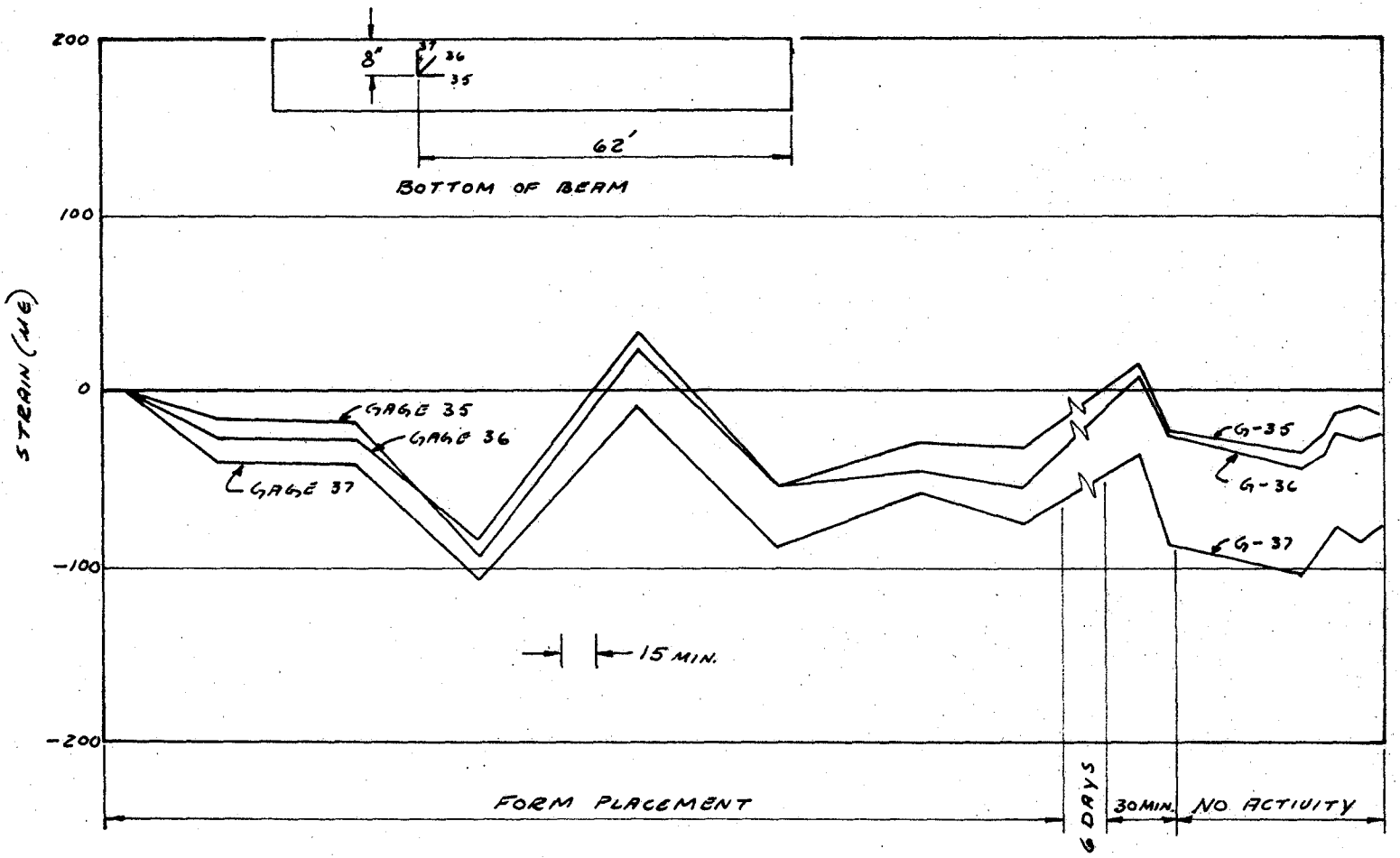

Figure All. Strain readings, Airport Blvd. Gages 35, 36, and 37.

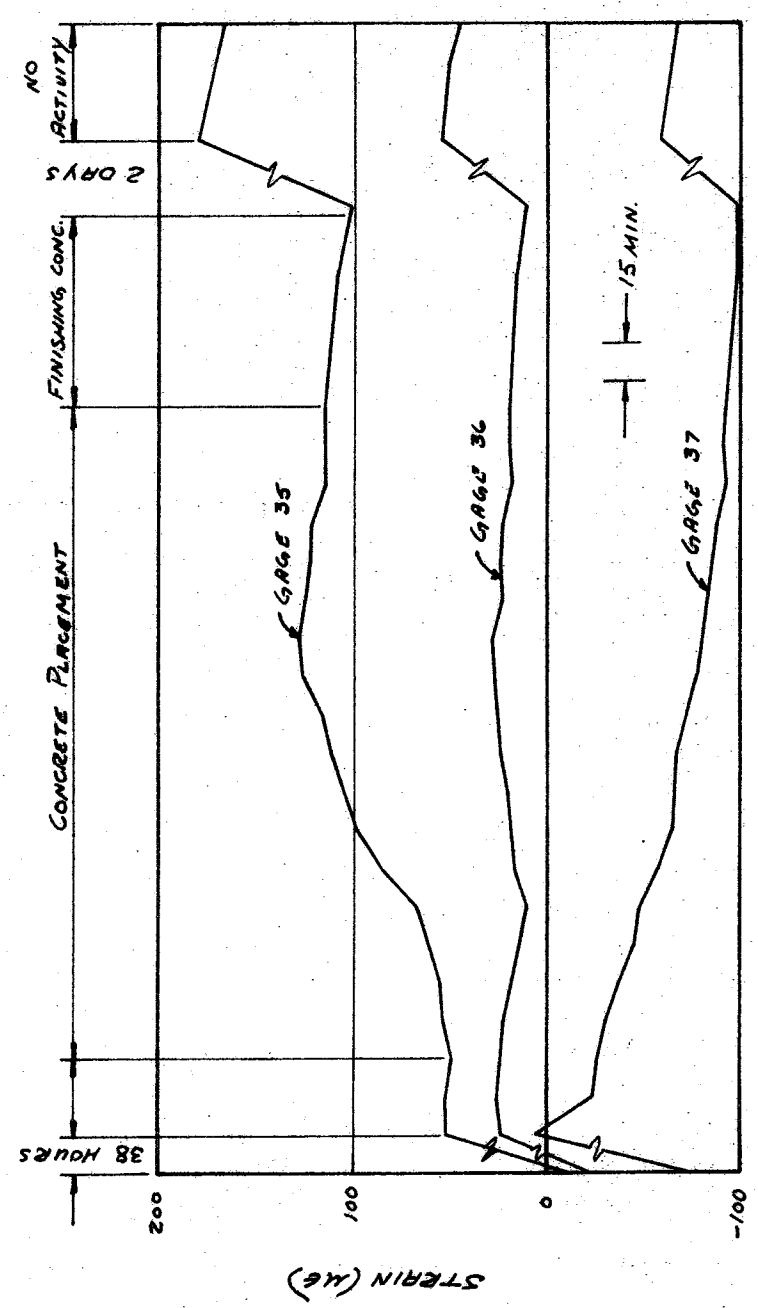

Figure A11. Cont'd.

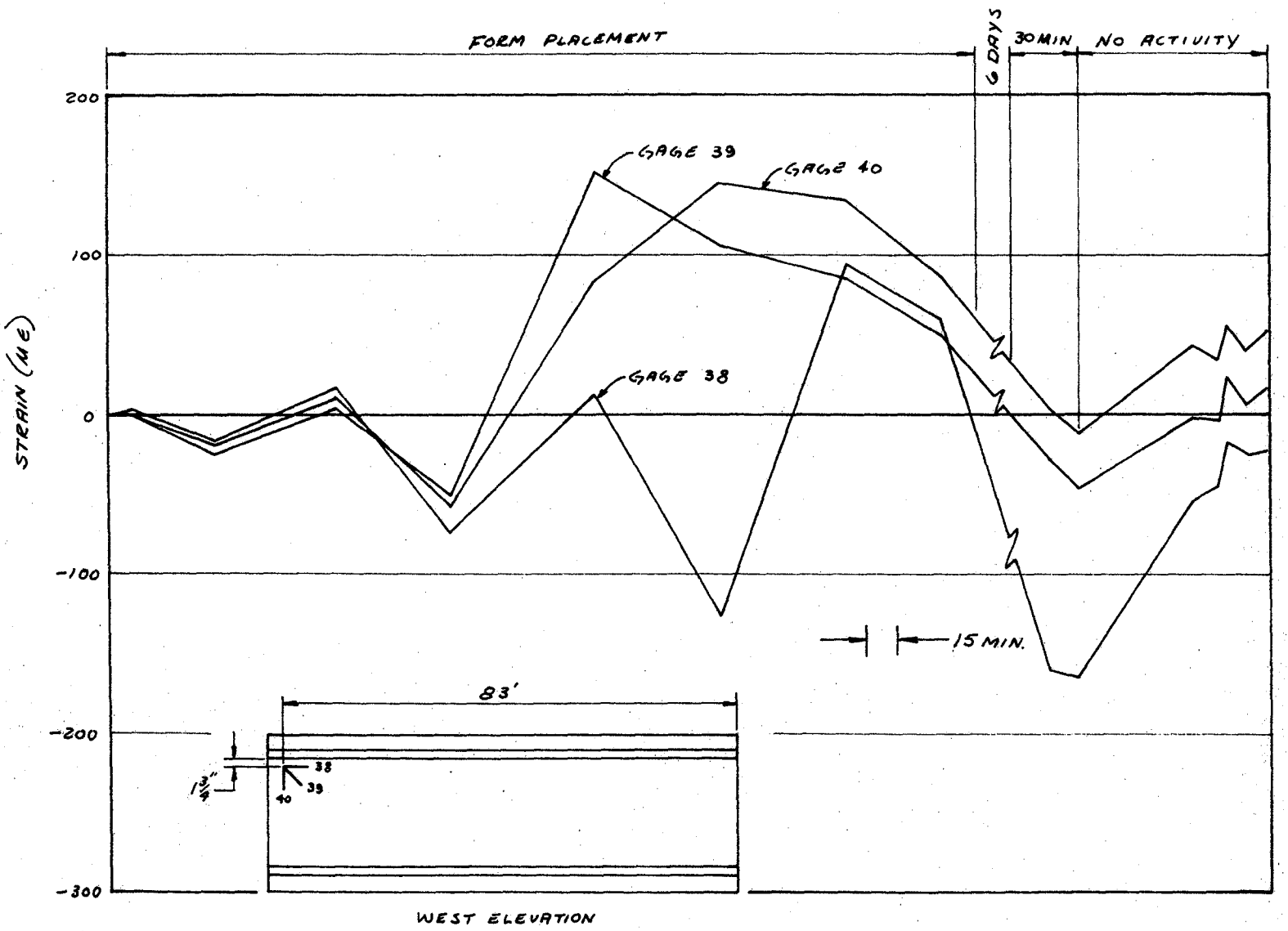

Figure A12. Strain readings, Airport Blvd. Gages 38, 39, and 40.

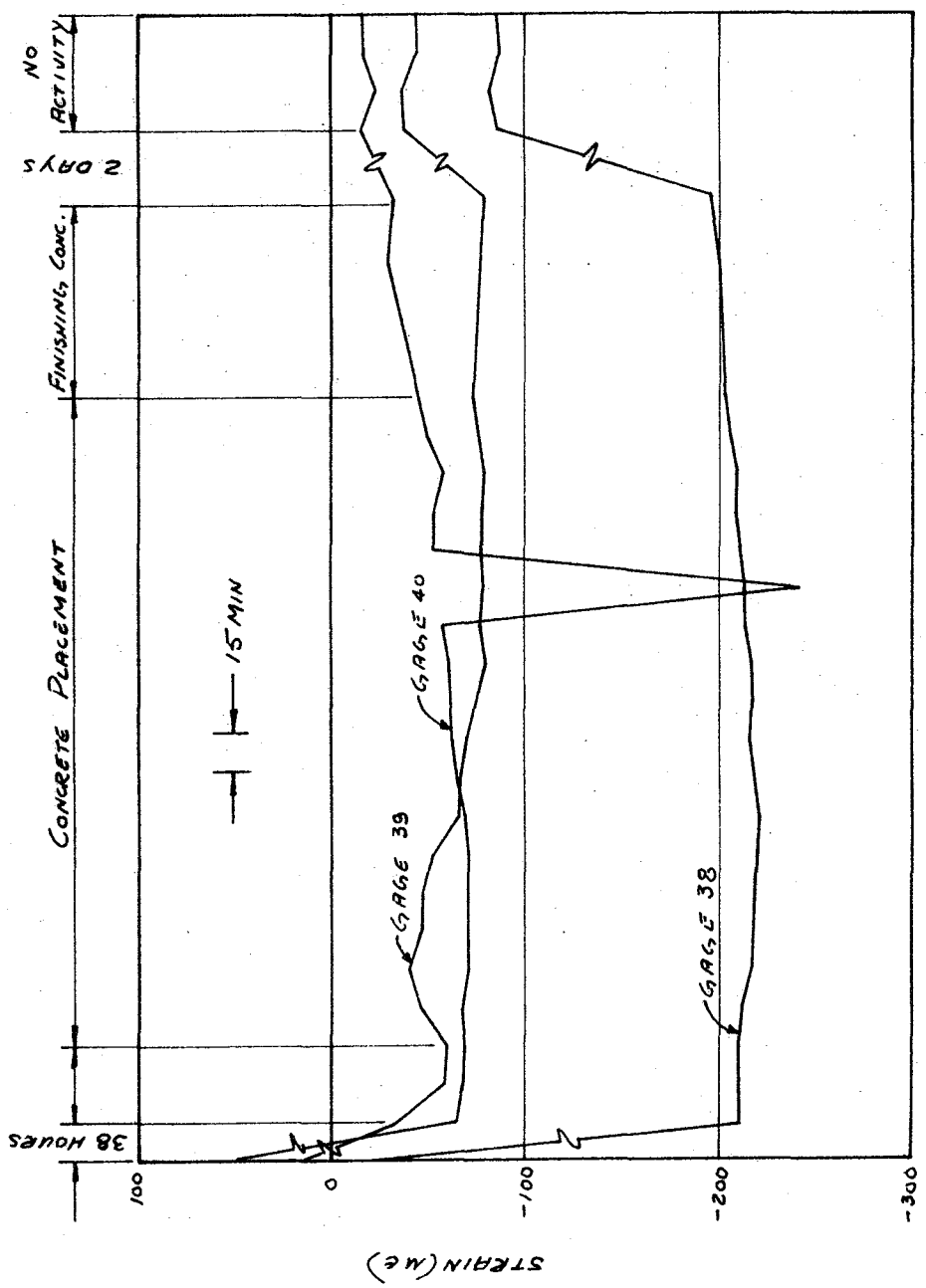

Figure A12. Cont'd.

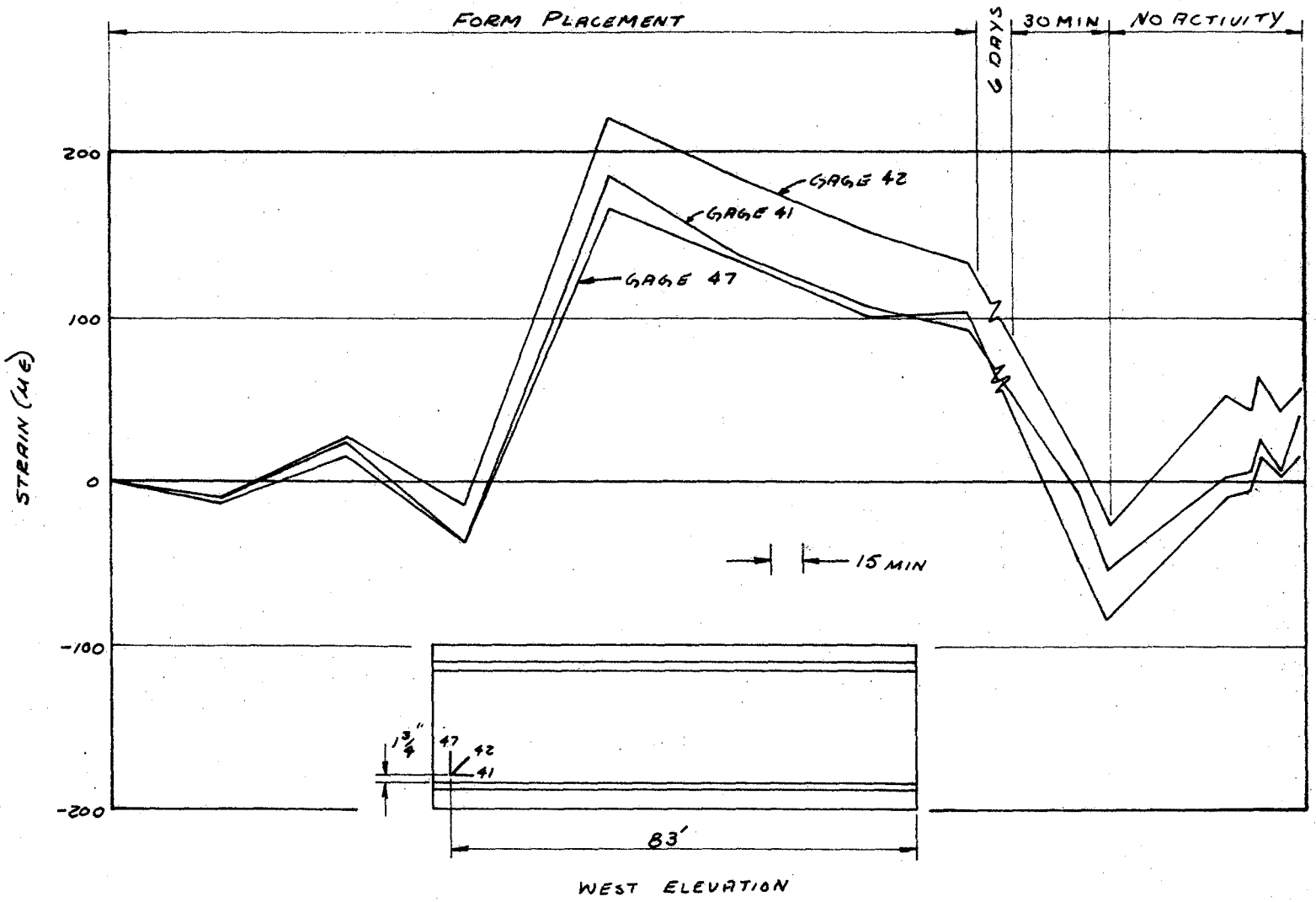

Figure A13. Strain readings, Airport Blvd. Gages 41, 42, and 47.

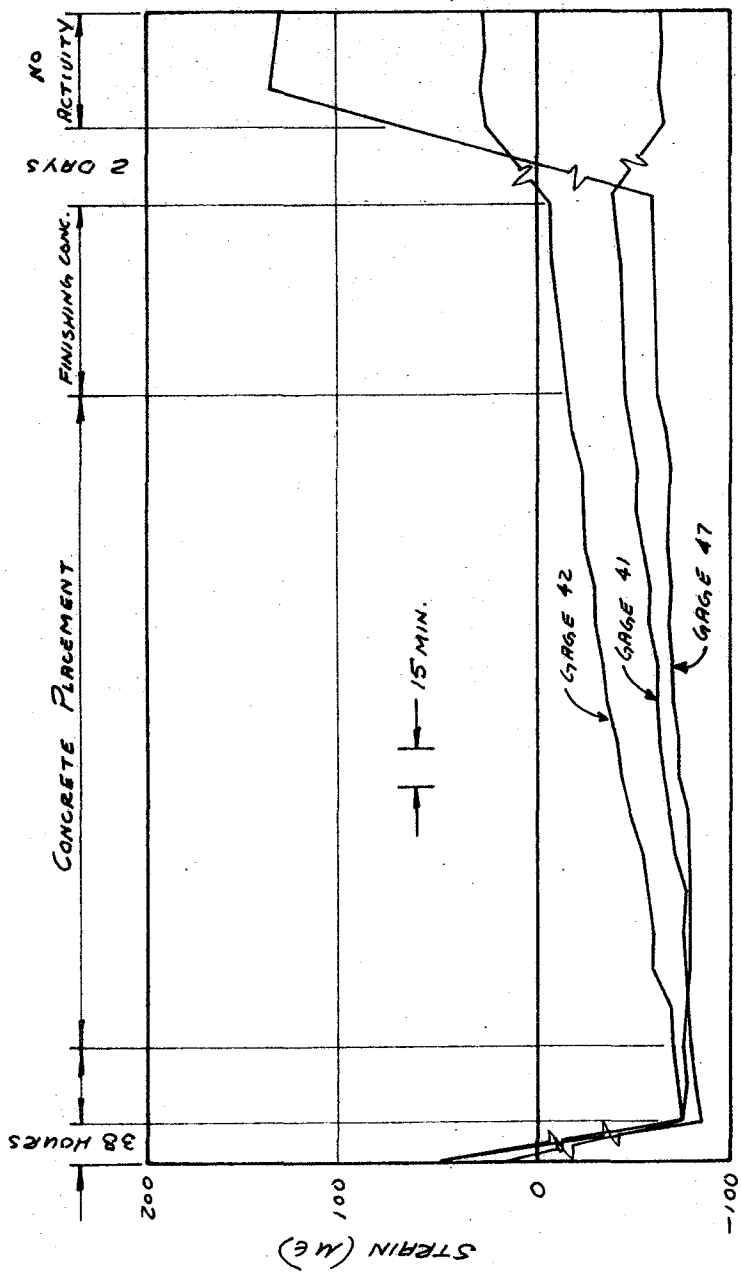

Figure A13. Cont'd.

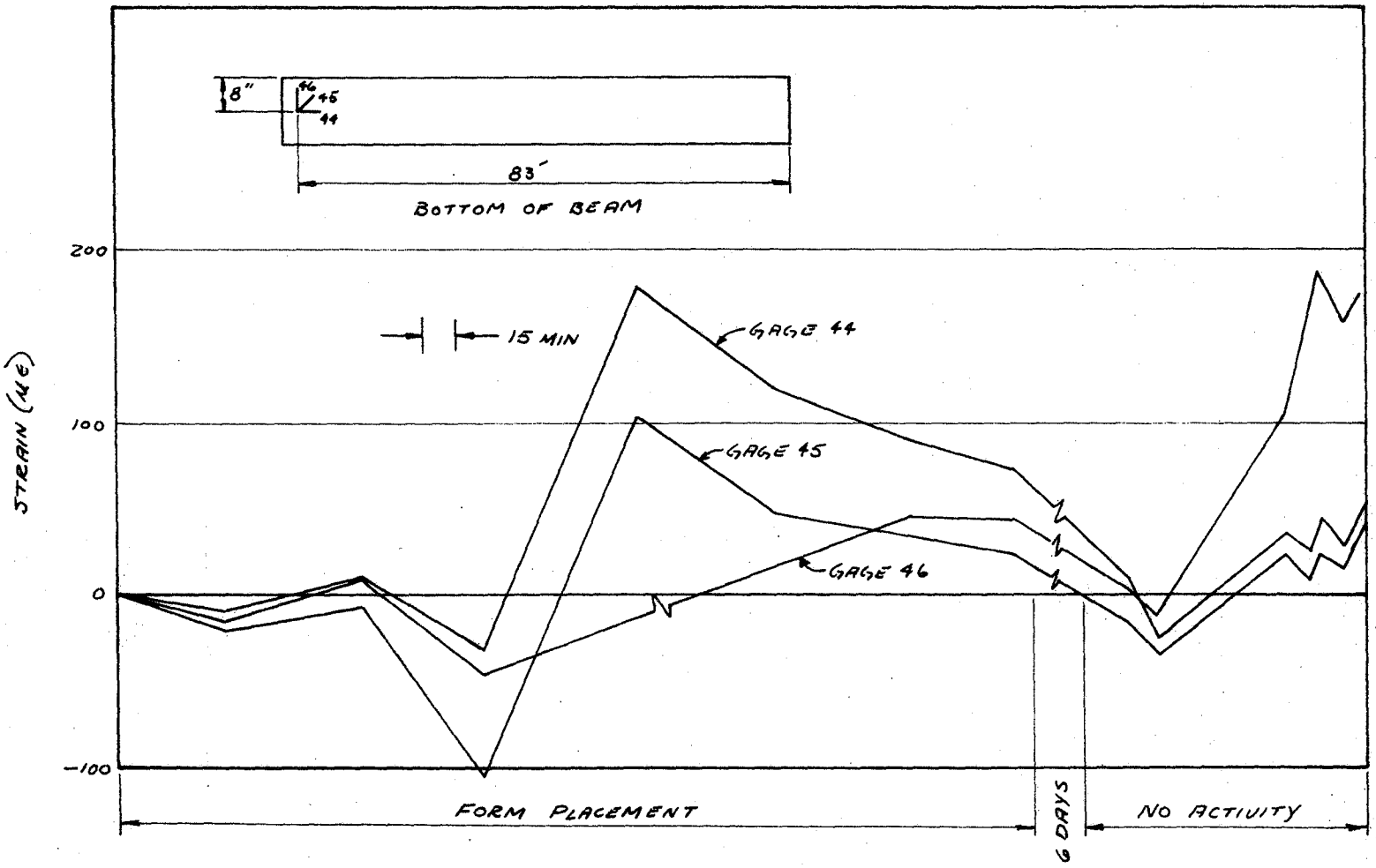

Figure A14. Strain readings, Airport Blvd. Gages 44, 45, and 46.

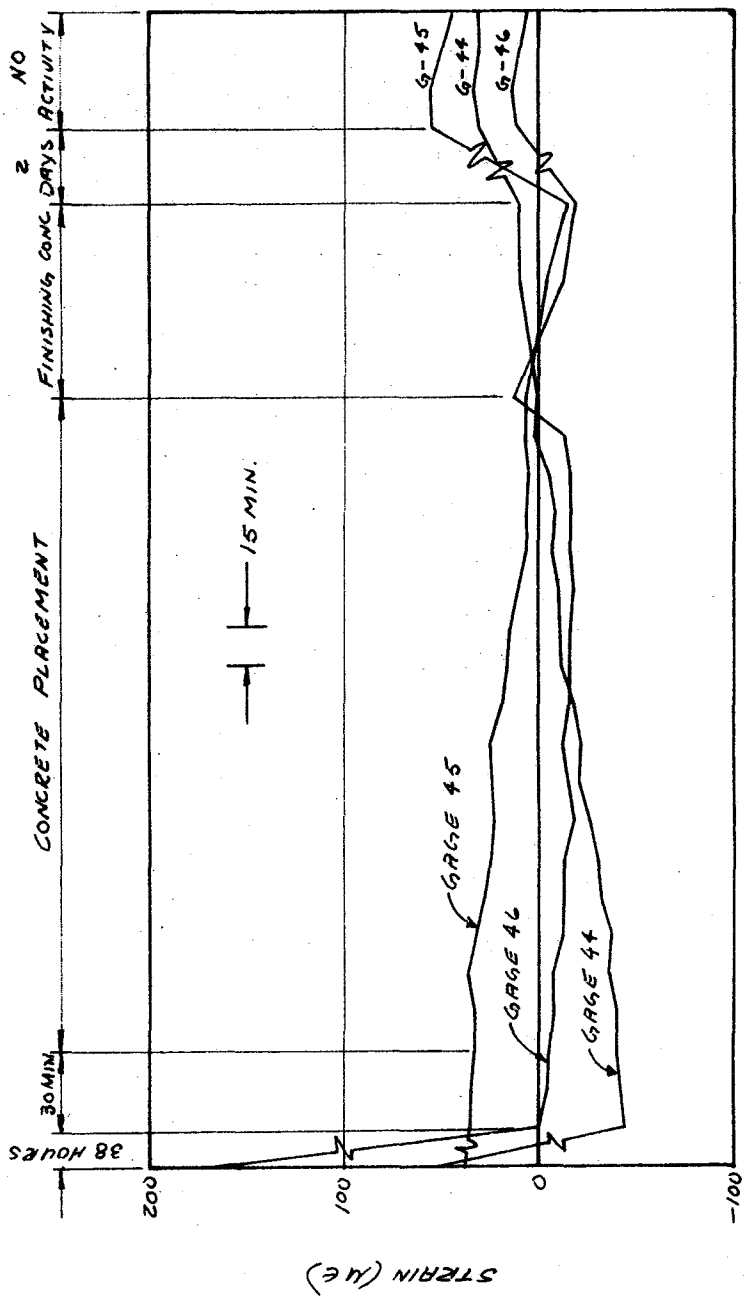

Figure A14. Cont'd.

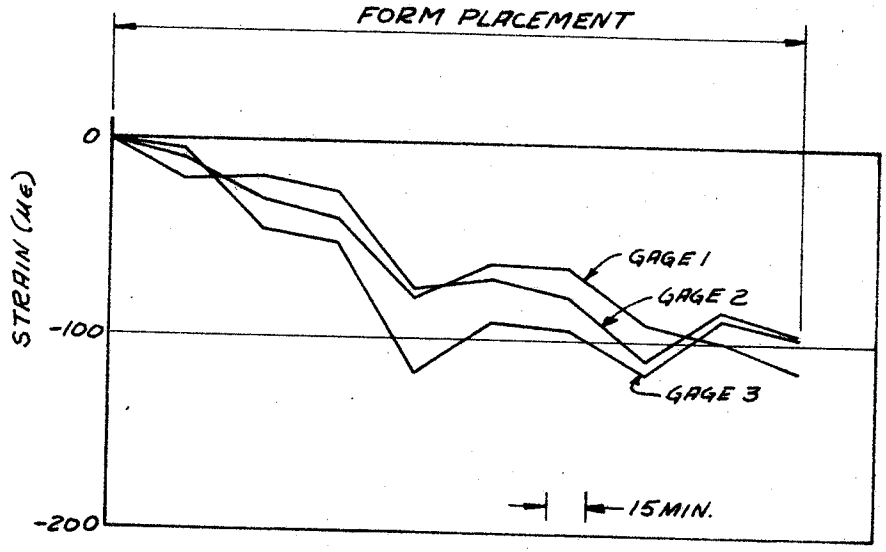

Figure A15. Strain readings, Columbus Drive Gages 1, 2, and 3.

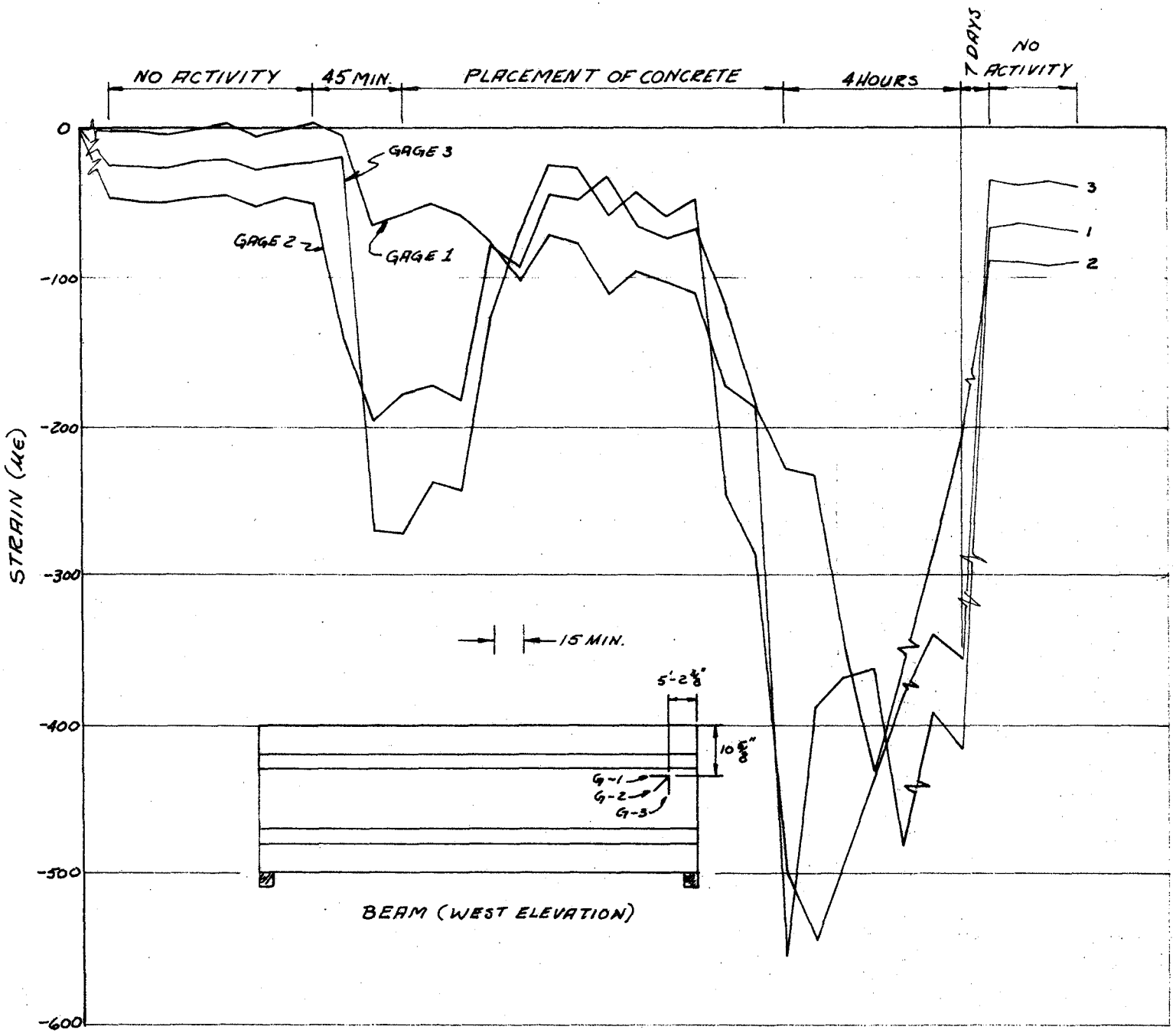

Figure A15. Cont'd.

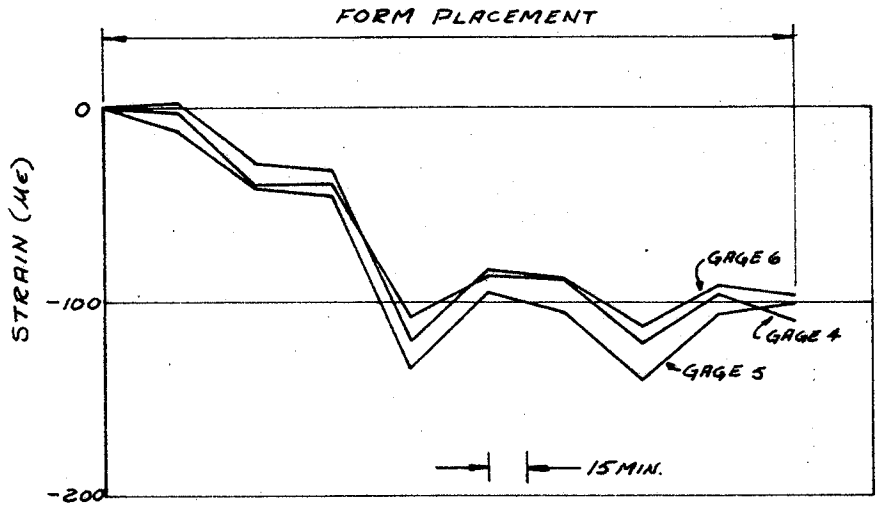

Figure A16. Strain readings, Columbus Drive Gages 4, 5, and 6.

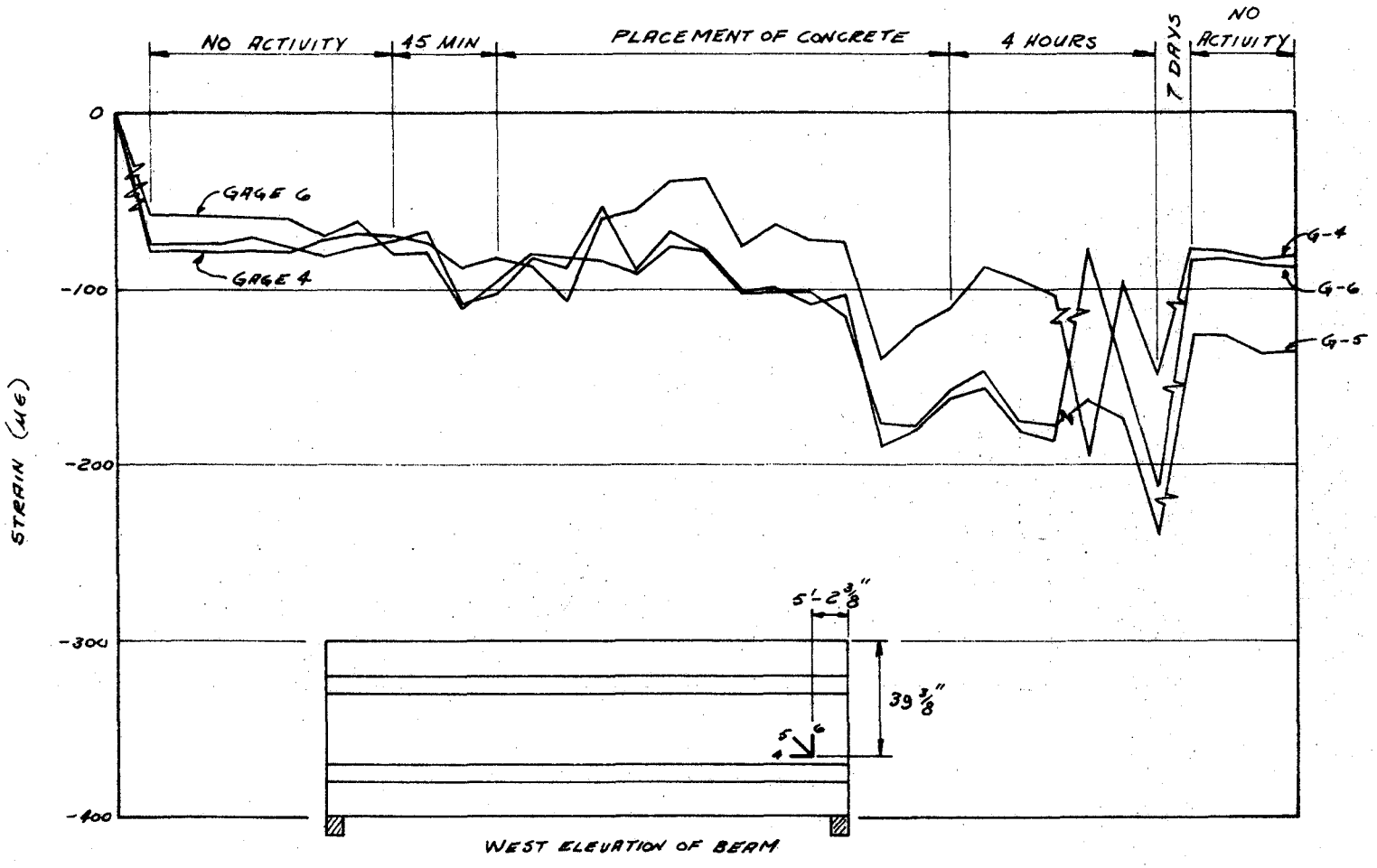

Figure A16. Cont'd.

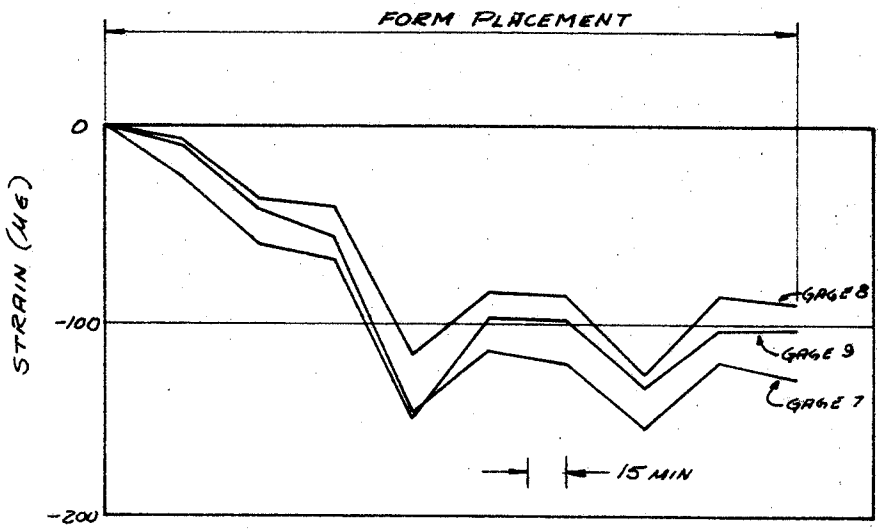

Figure A17. Strain readings, Columbus Drive Gages 7, 8, and 9.

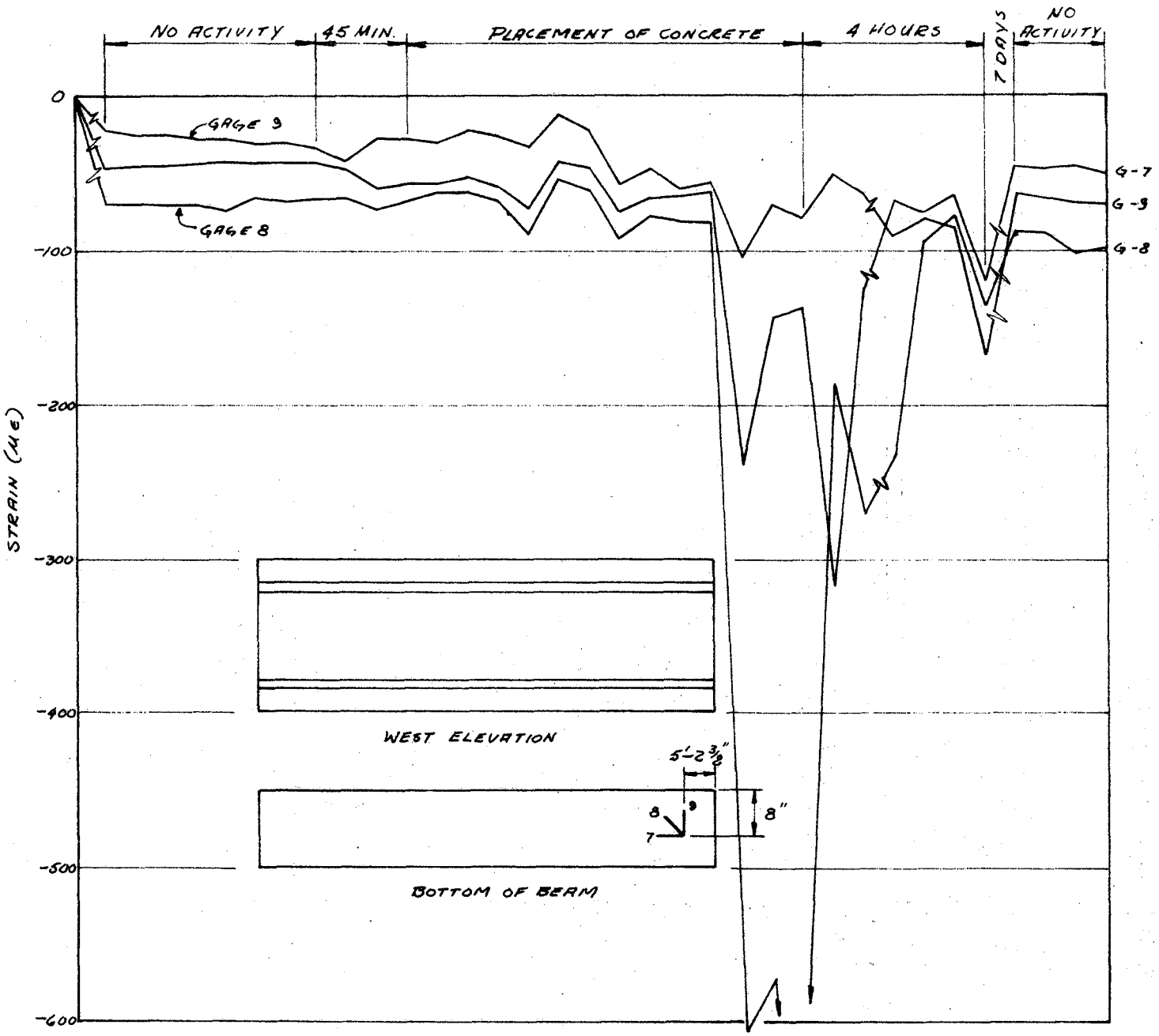

Figure A17. Cont'd.

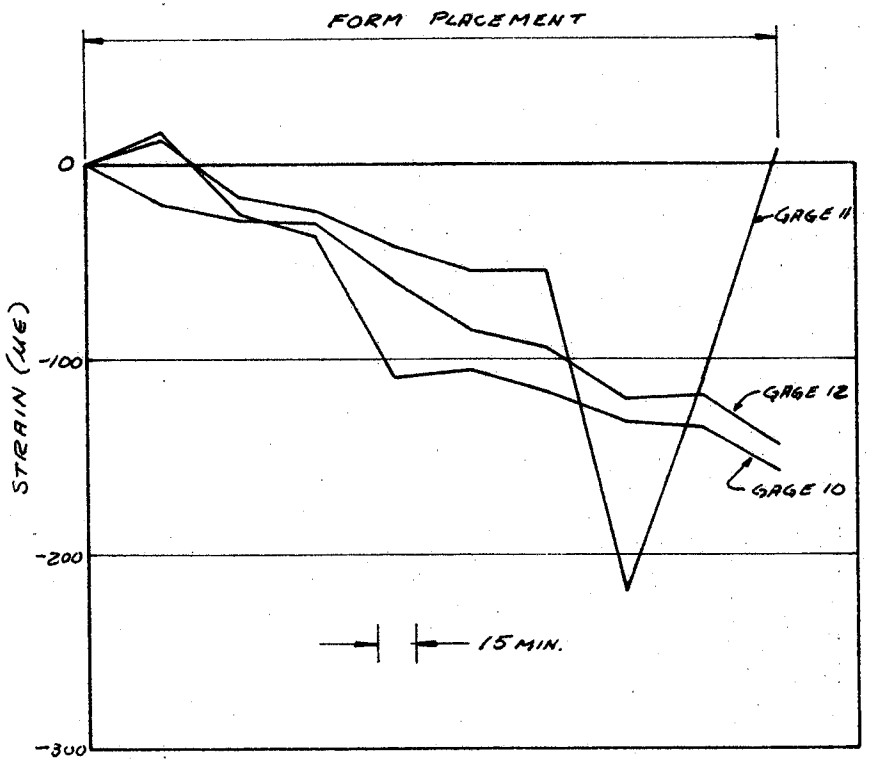

Figure A18. Strain readings, Columbus Drive Gages 10, 11, and 12.

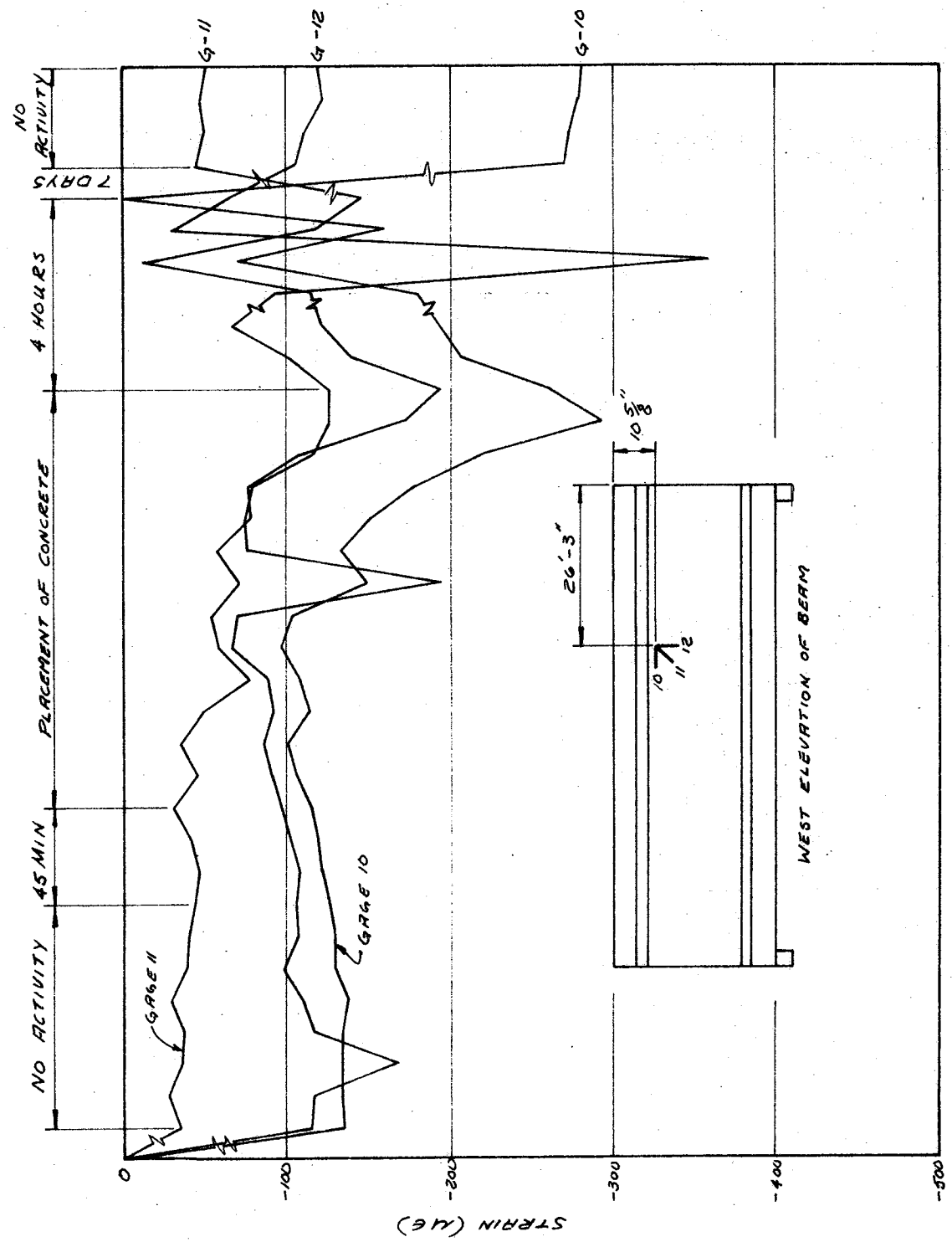

Figure A18. Cont'd.

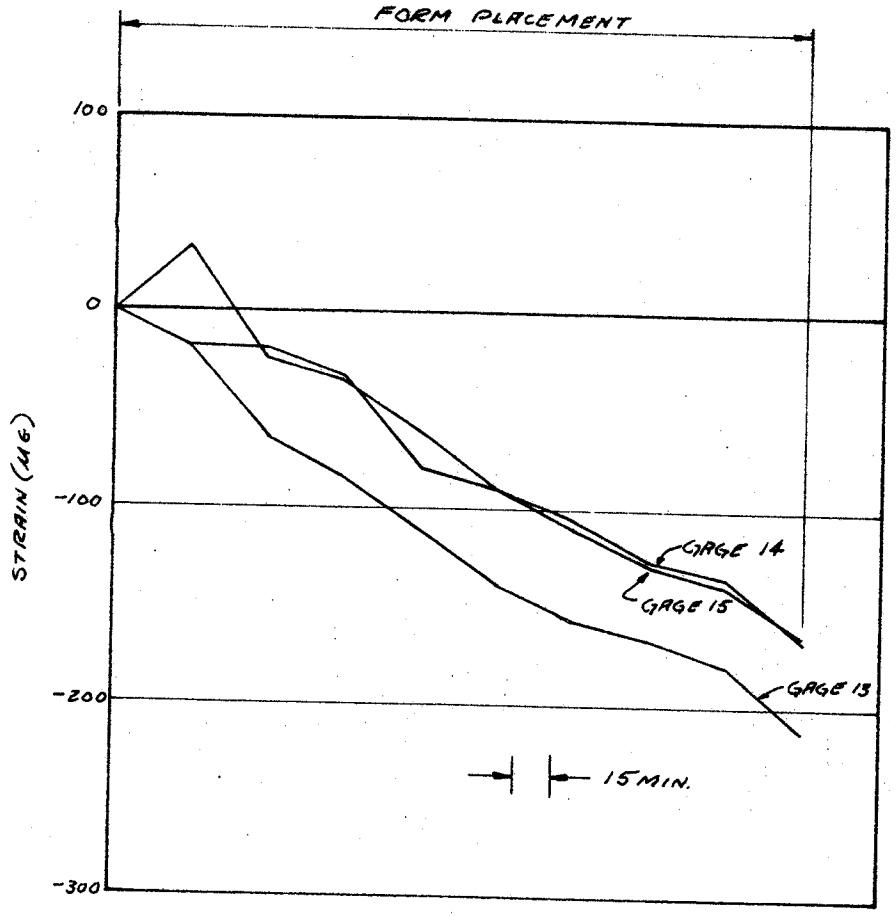

Figure A19. Strain readings, Columbus Drive Gages 13, 14, and 15.

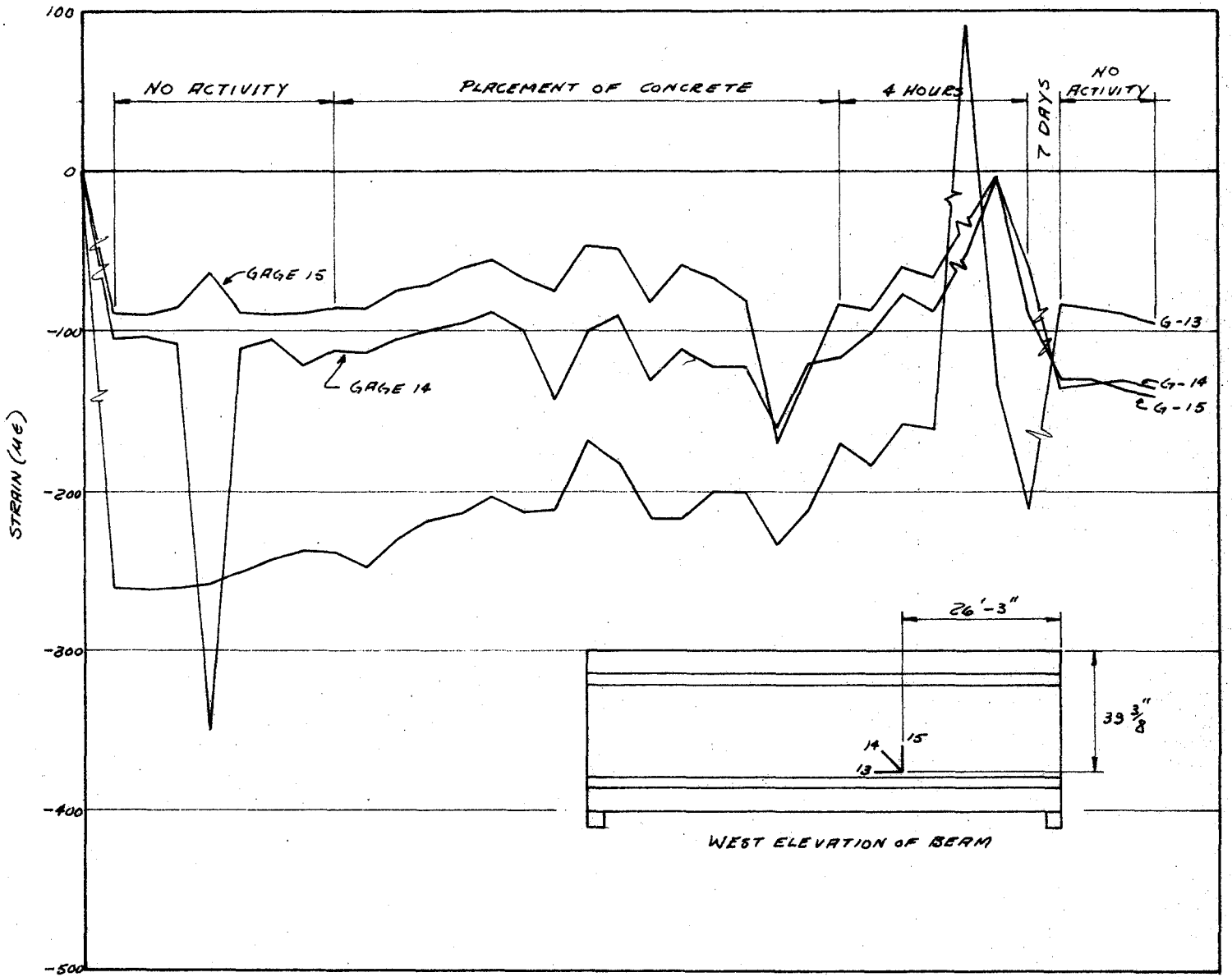

Figure A19. Cont'd.

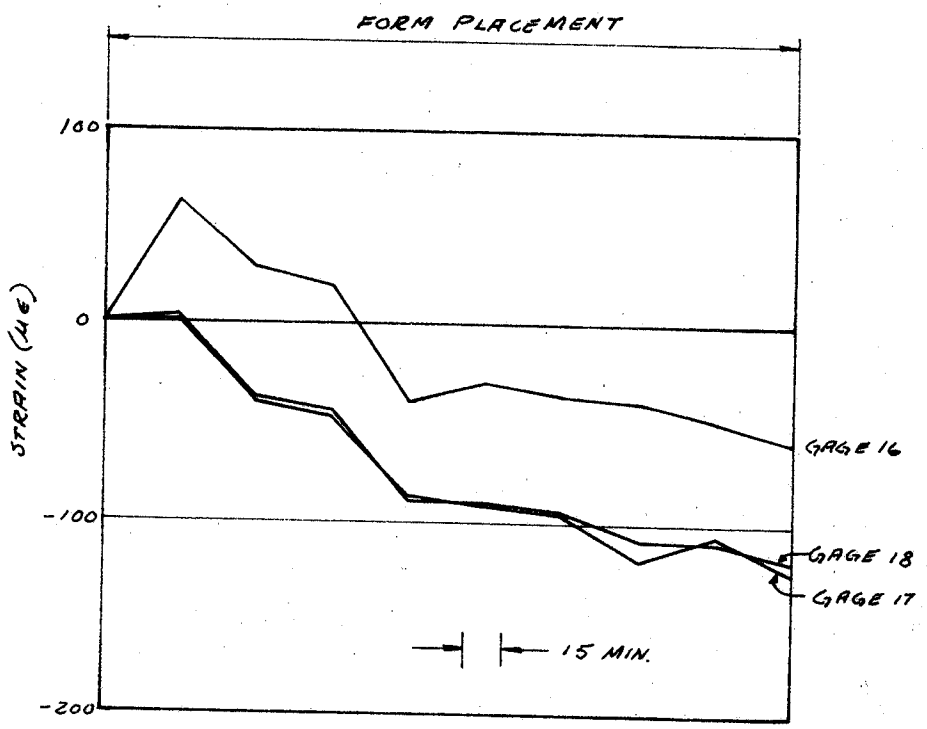

Figure A20. Strain readings, Columbus Drive Gages 16, 17, and 18.

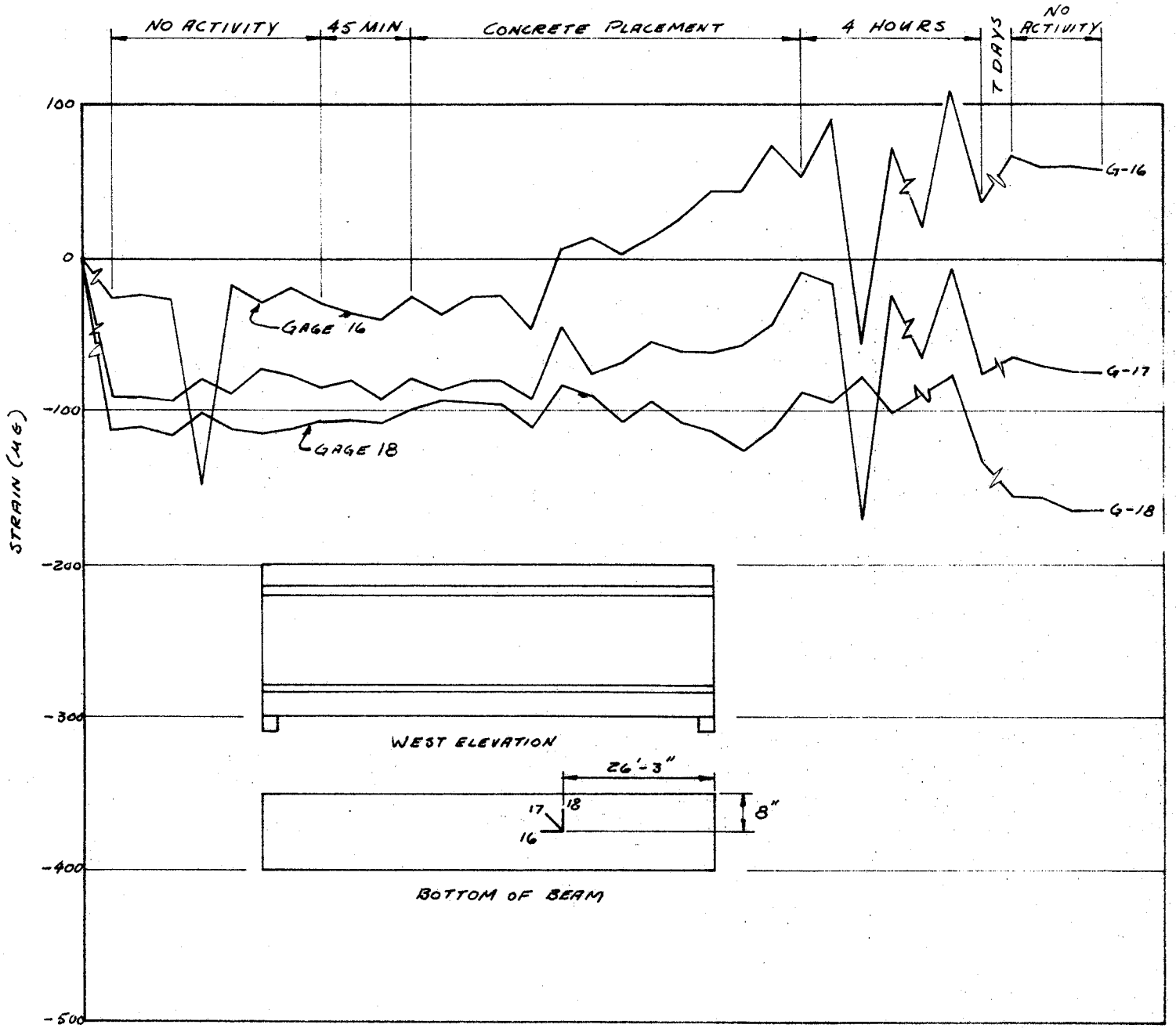

Figure A20. Cont'd.

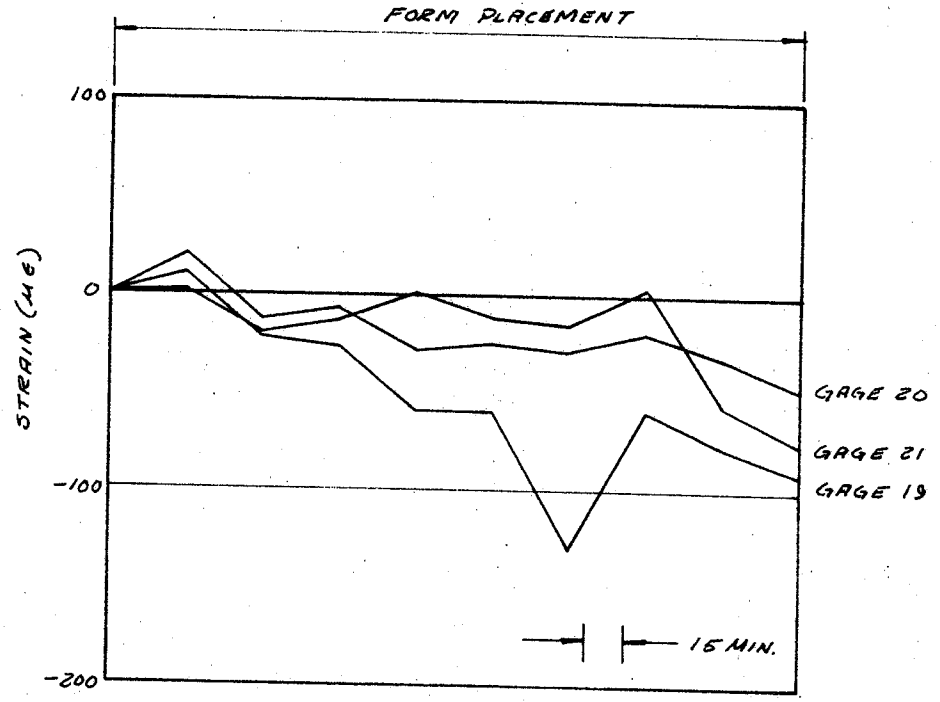

Figure A21. Strain readings, Columbus Drive Gages 19, 20, and 21.

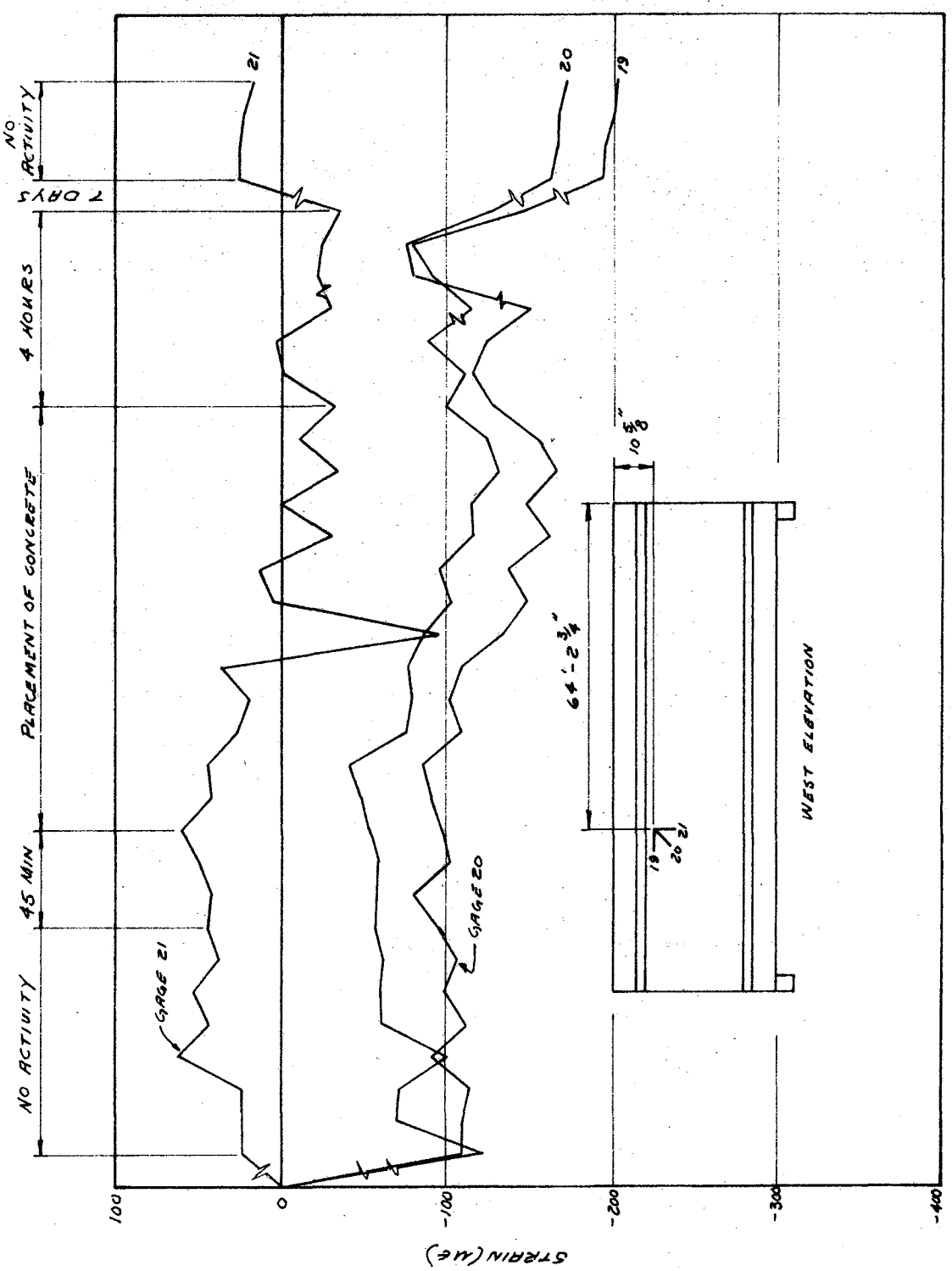

Figure A21. Cont'd.

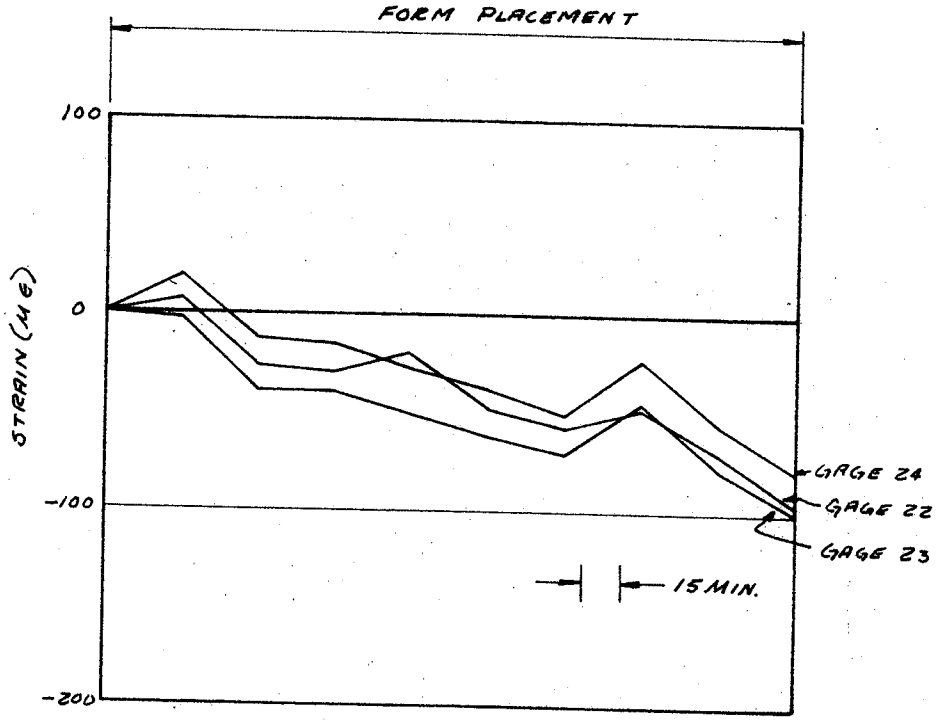

Figure A22. Strain readings, Columbus Drive Gages 22, 23, and 24.

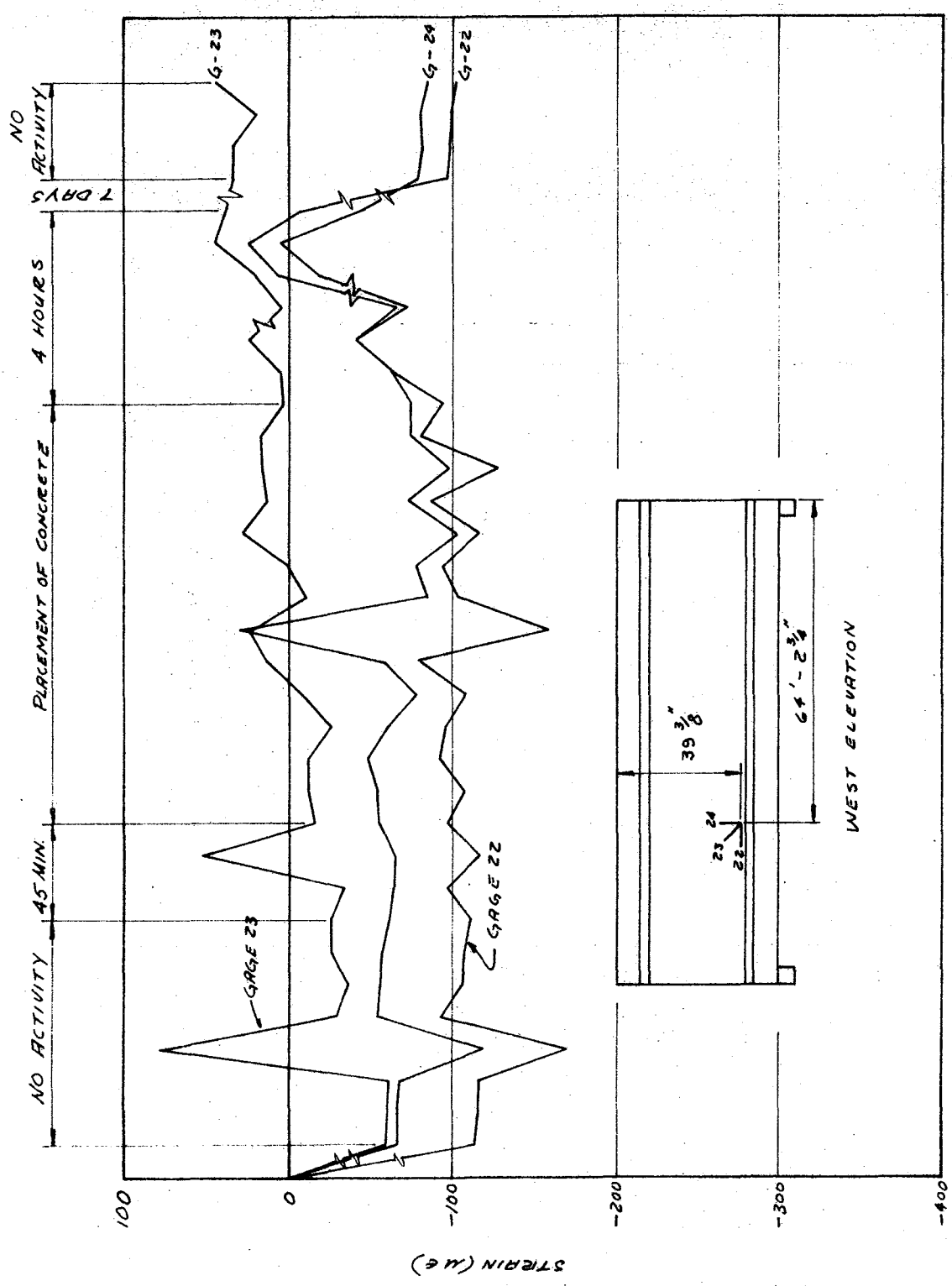

Figure A22. Cont'd.

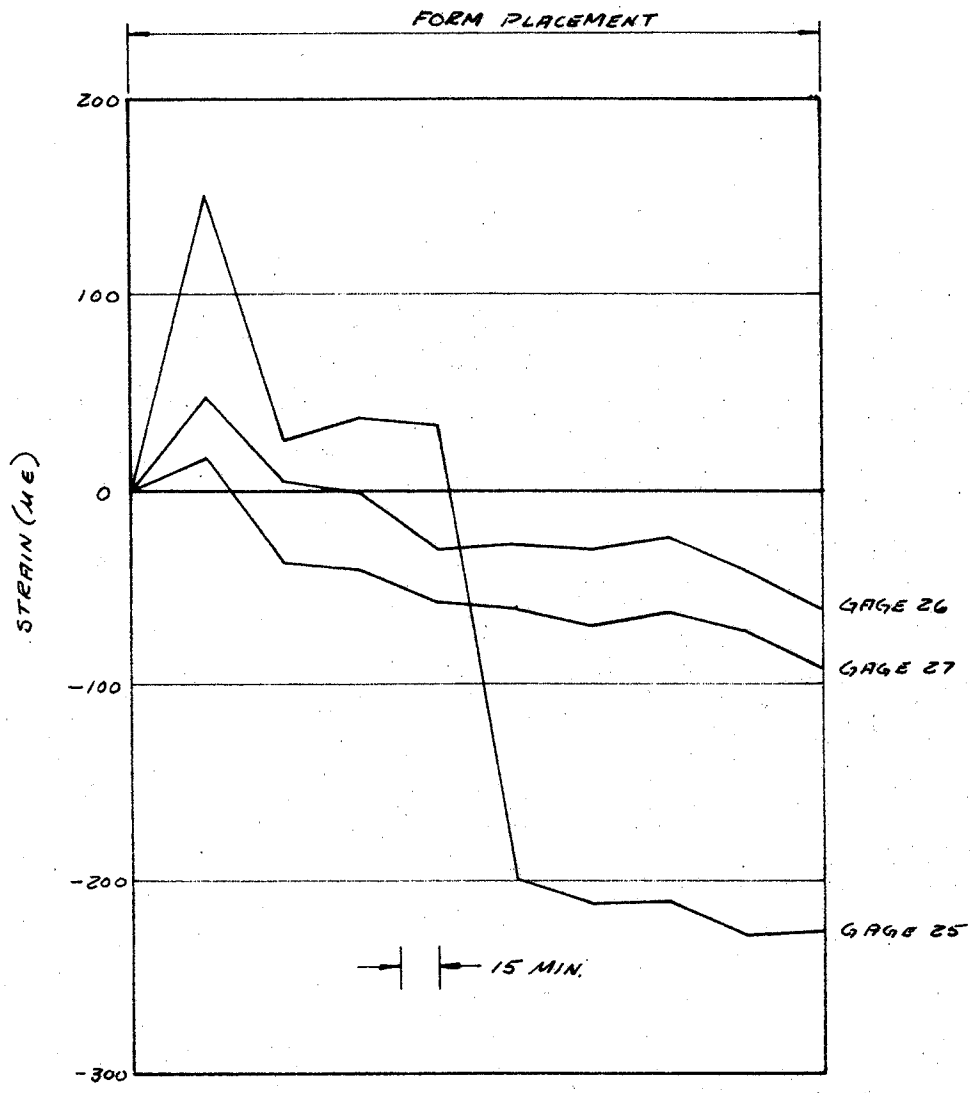

Figure A23. Strain readings, Columbus Drive Gages 25, 26, and 27.

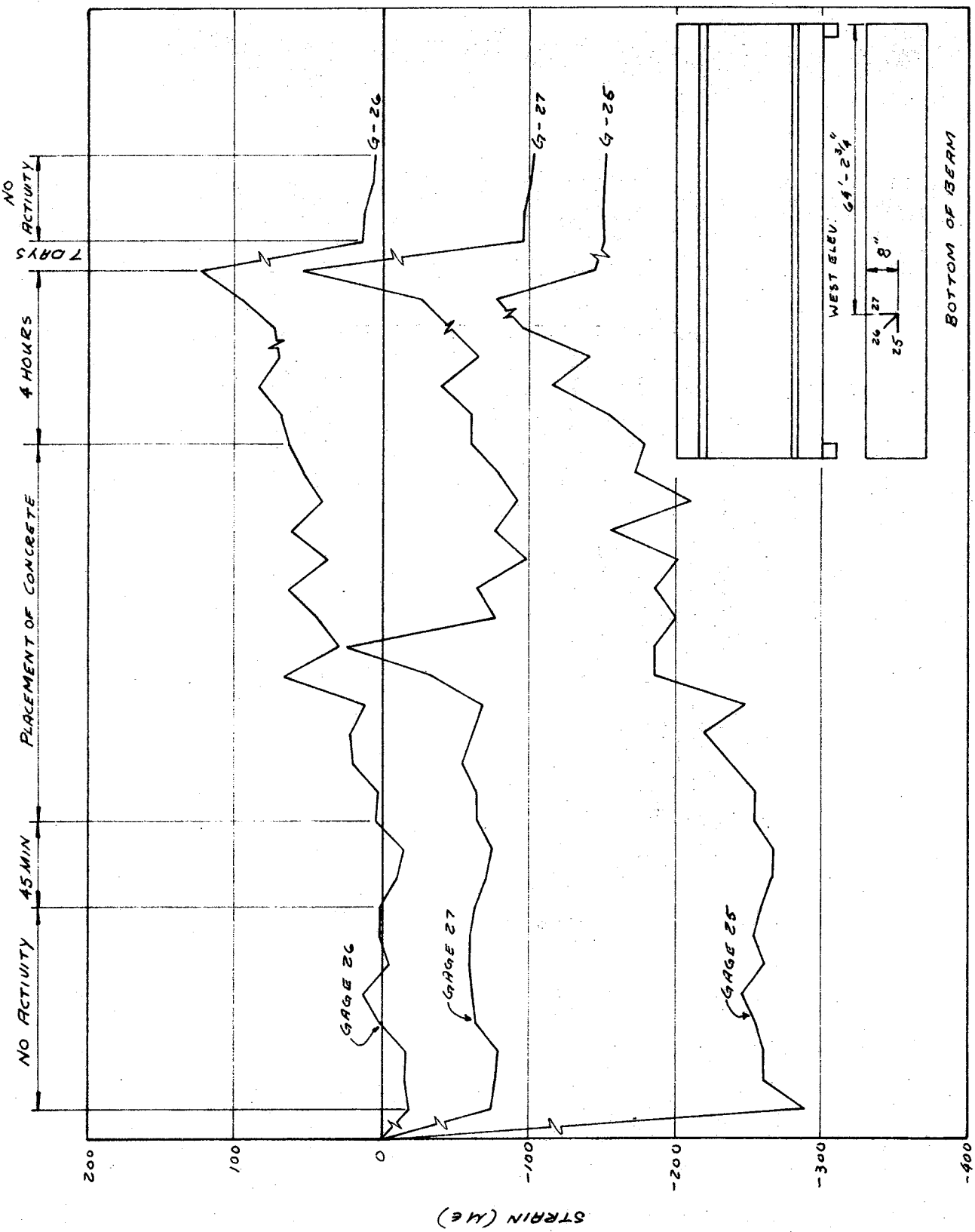

Figure A23. Cont'd.

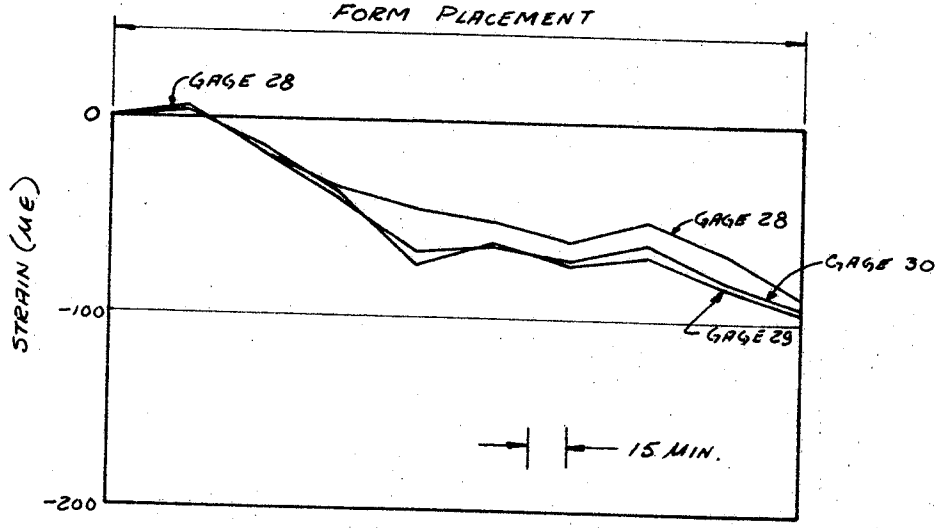

Figure A24. Strain readings, Columbus Drive Gages 28, 29, and 30.

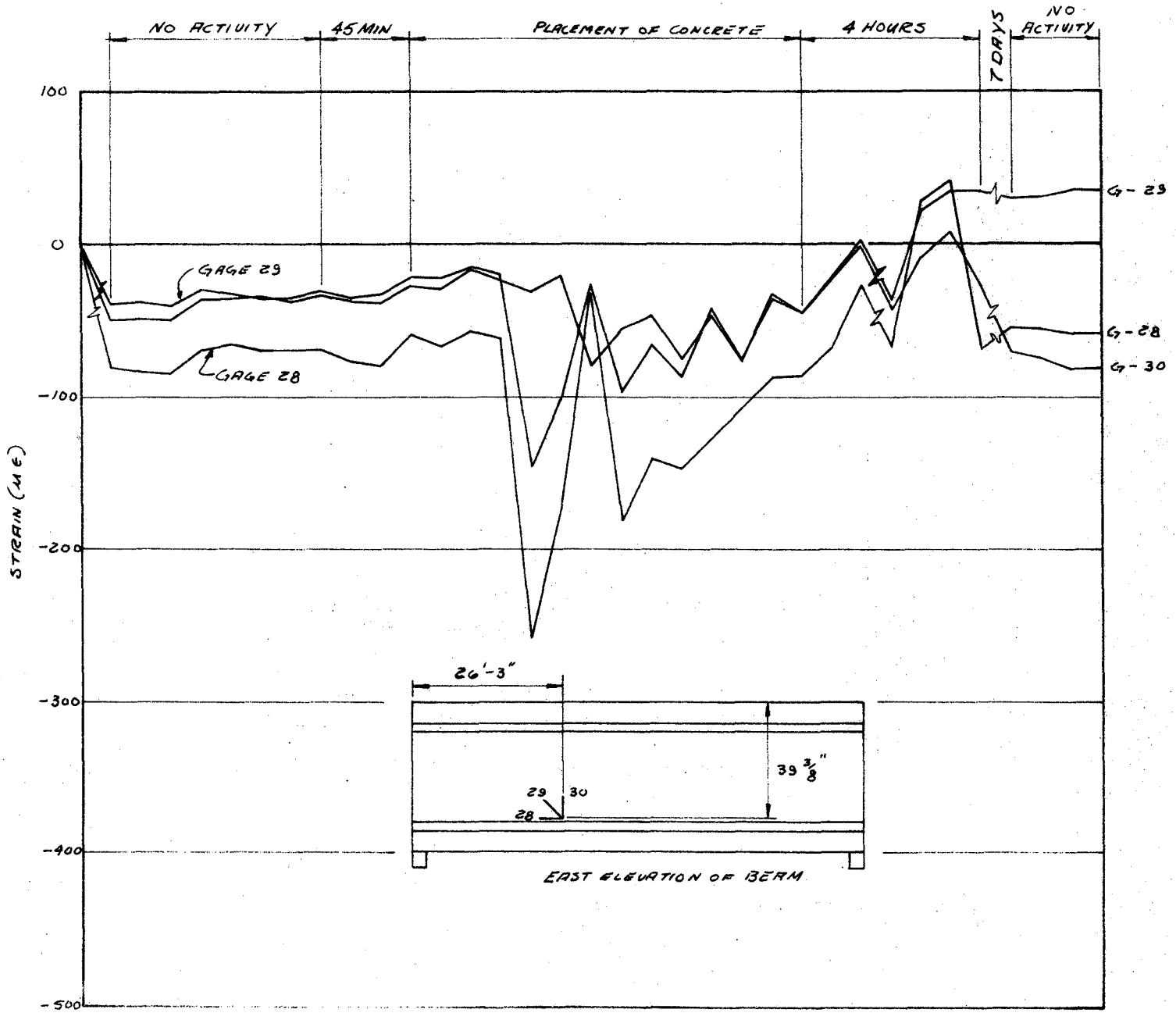

Figure A24. Cont'd.

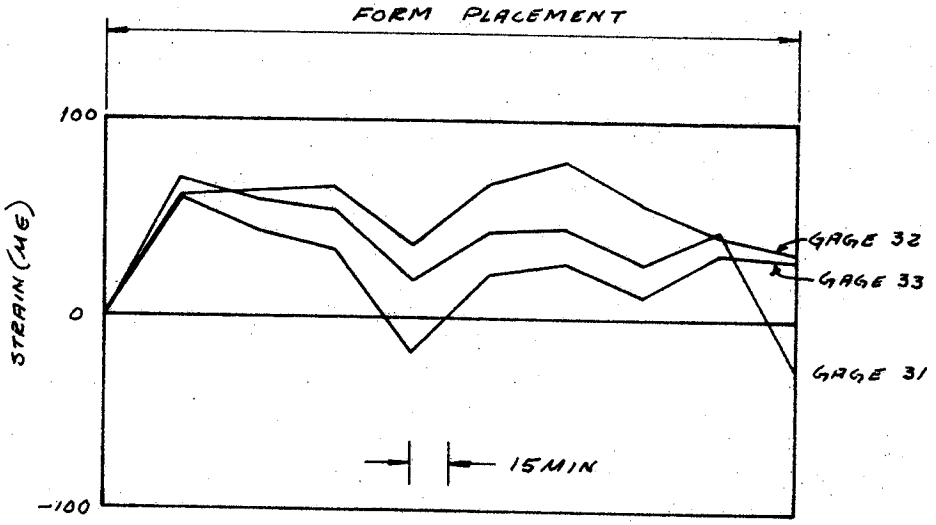

Figure A25. Strain readings, Columbus Drive Gages 31, 32, and 33.

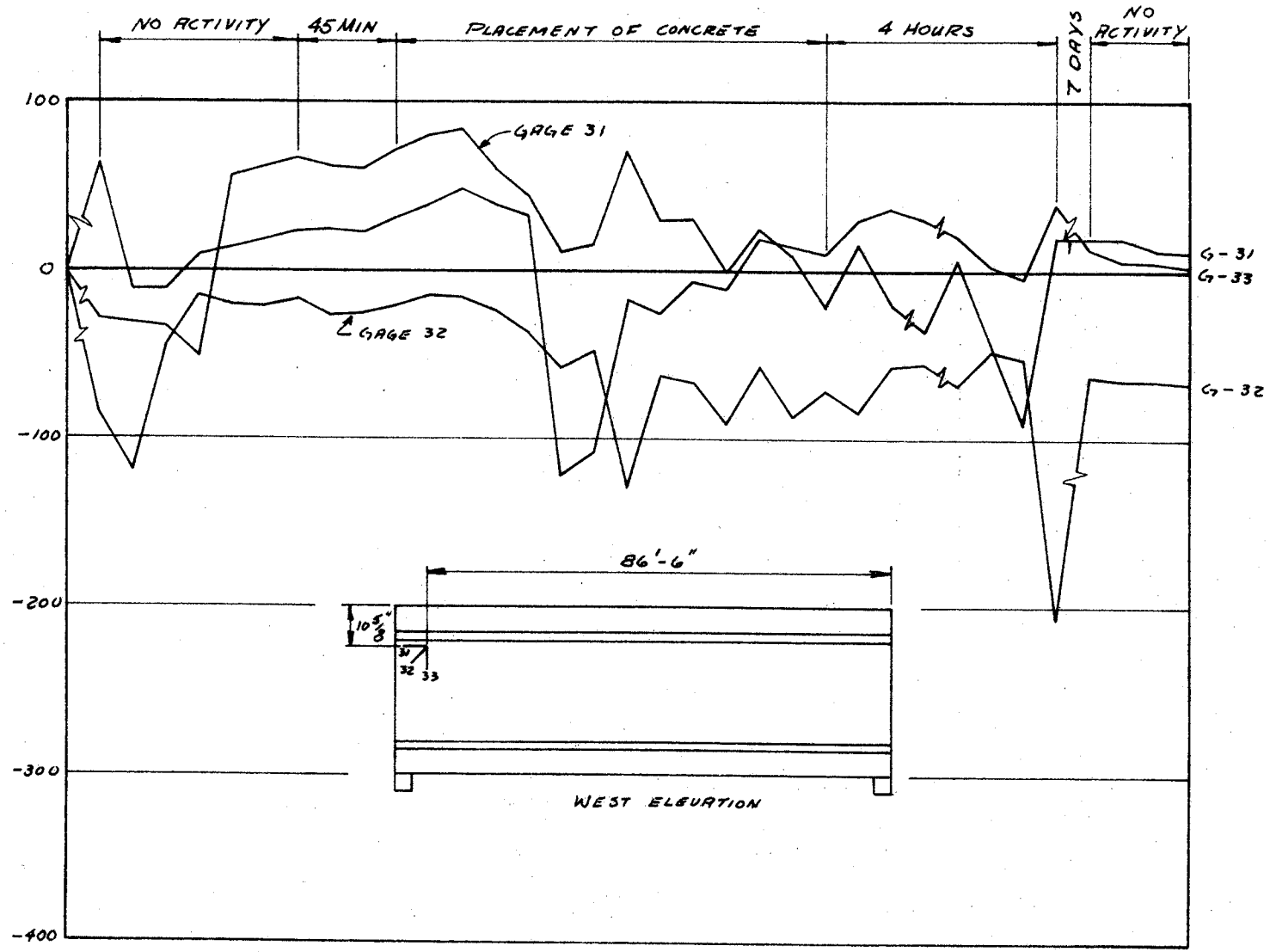

Figure A25. Cont'd.

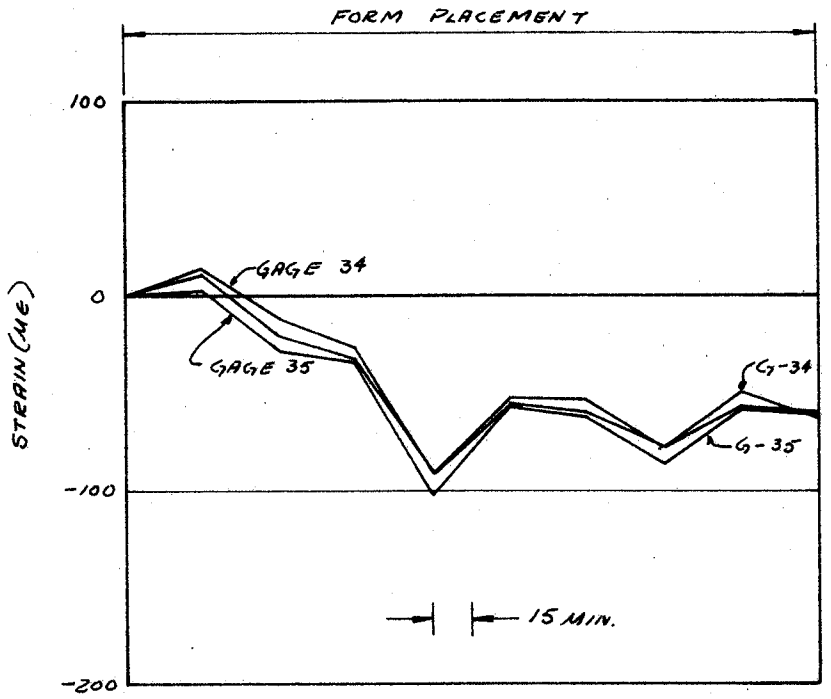

Figure A26. Strain readings, Columbus Drive Gages 34, 35, and 36.

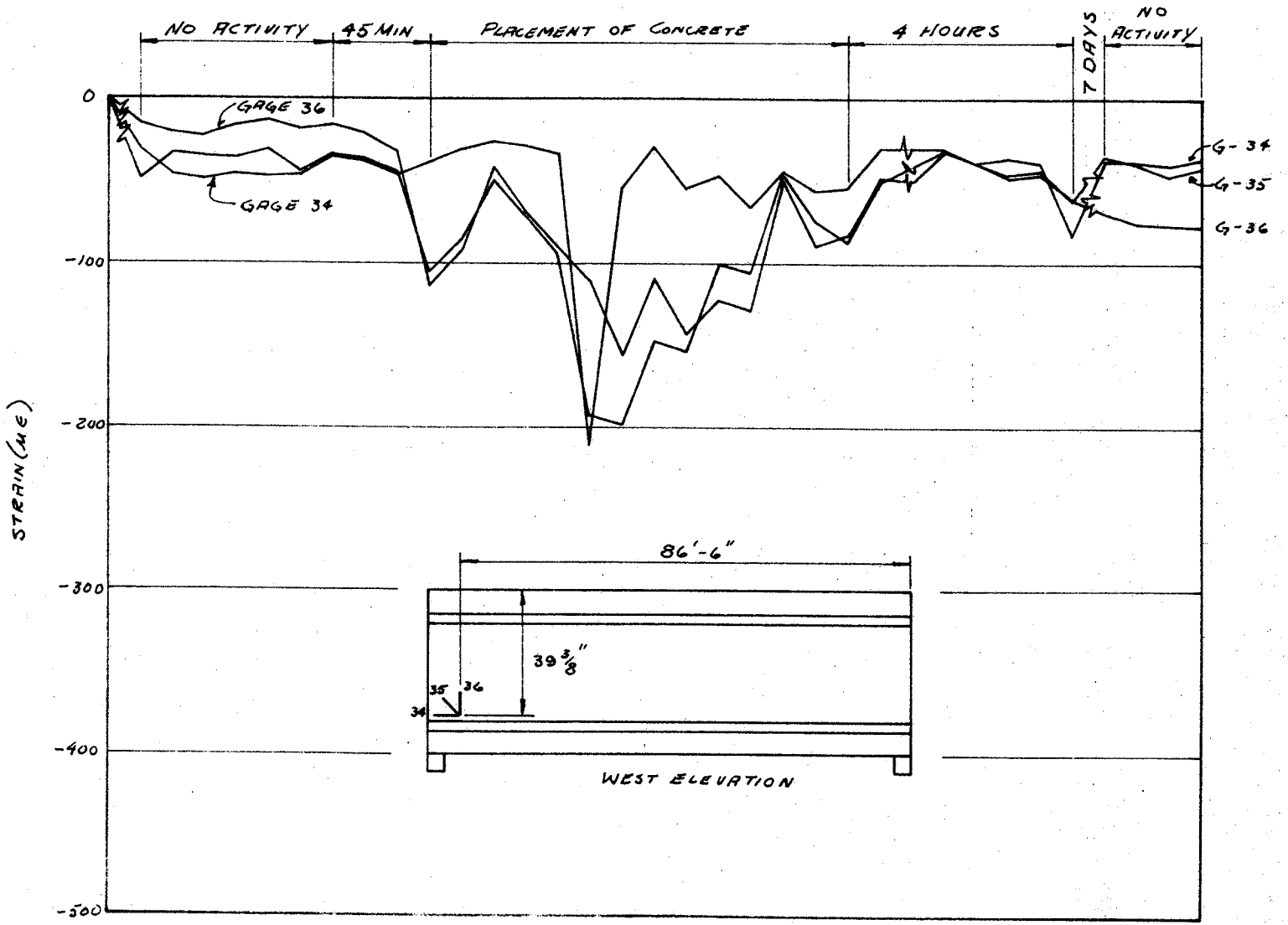

Figure A26. Cont'd.

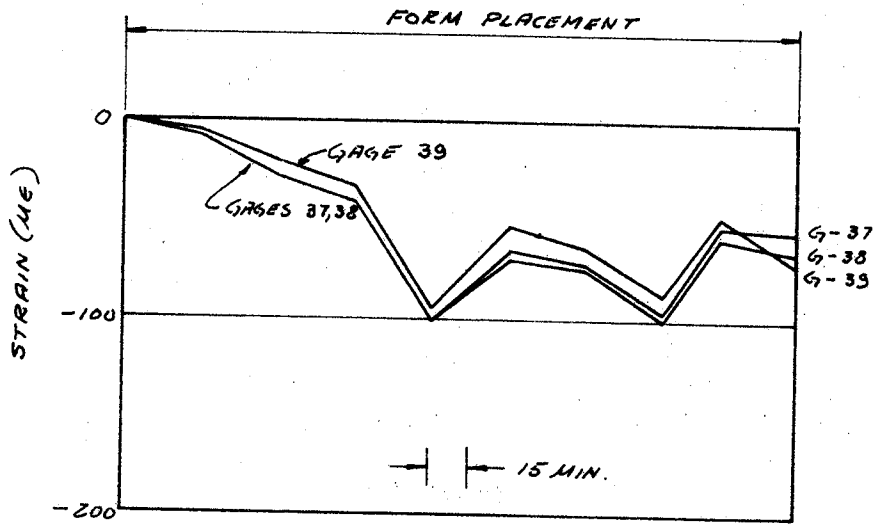

Figure A27. Strain readings, Columbus Drive Gages 37, 38, and 39.

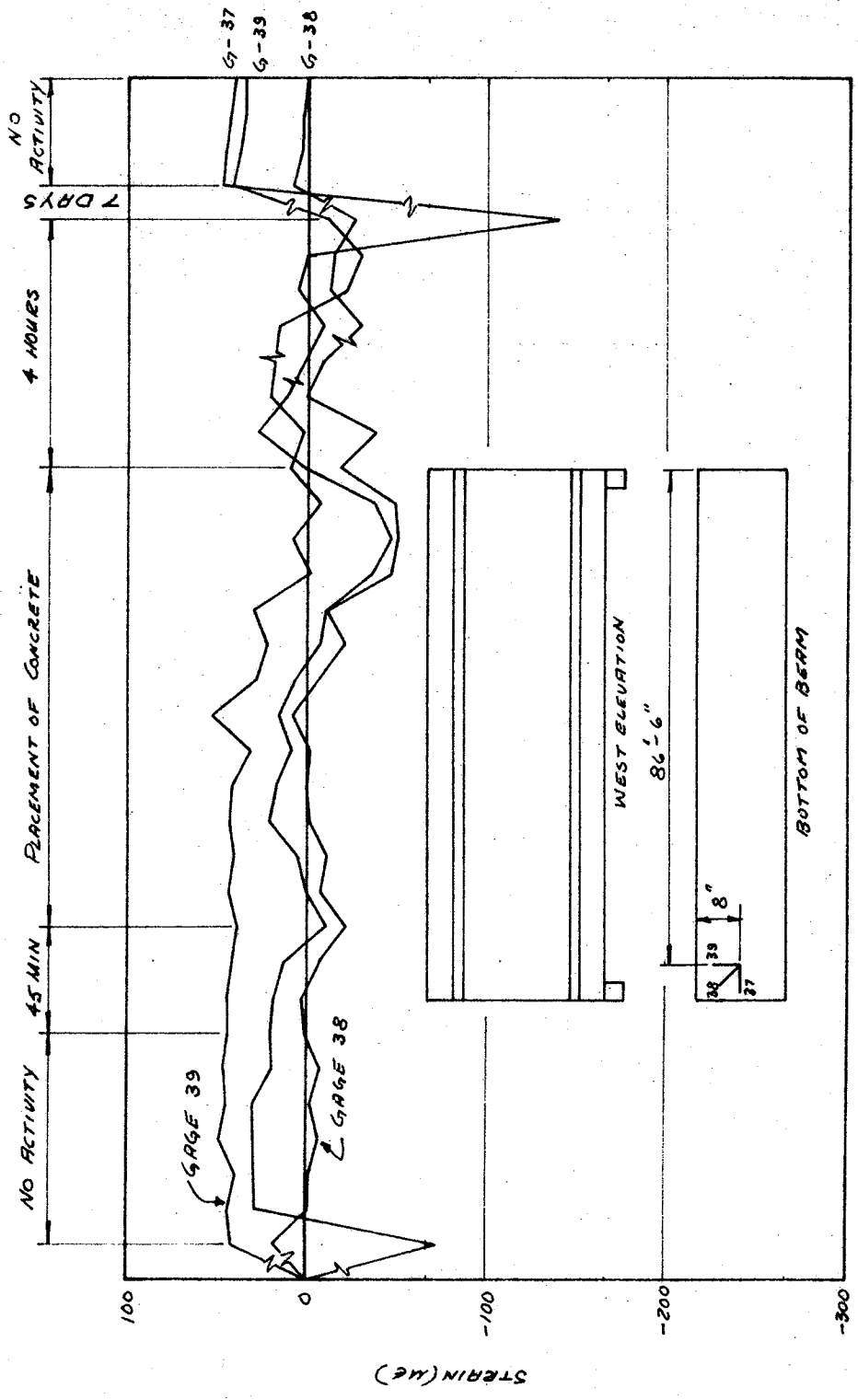

Figure A27. Cont'd.

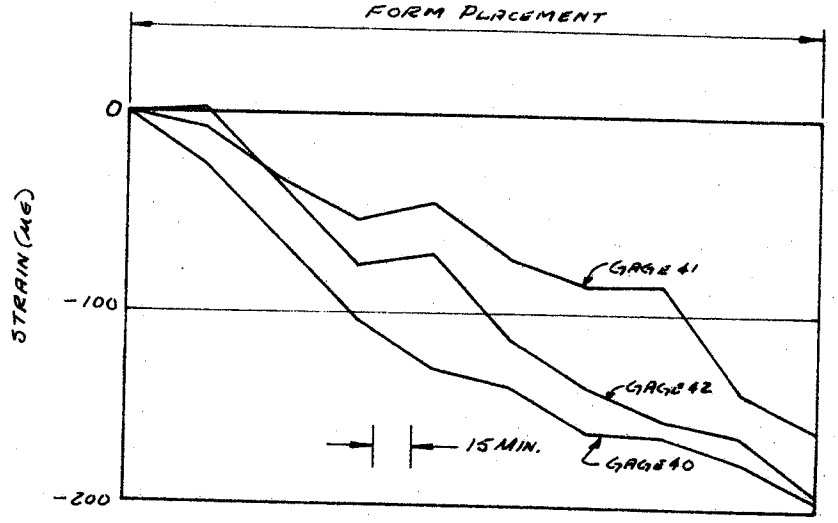

Figure A28. Strain readings, Columbus Drive Gages 40, 41, and 42.

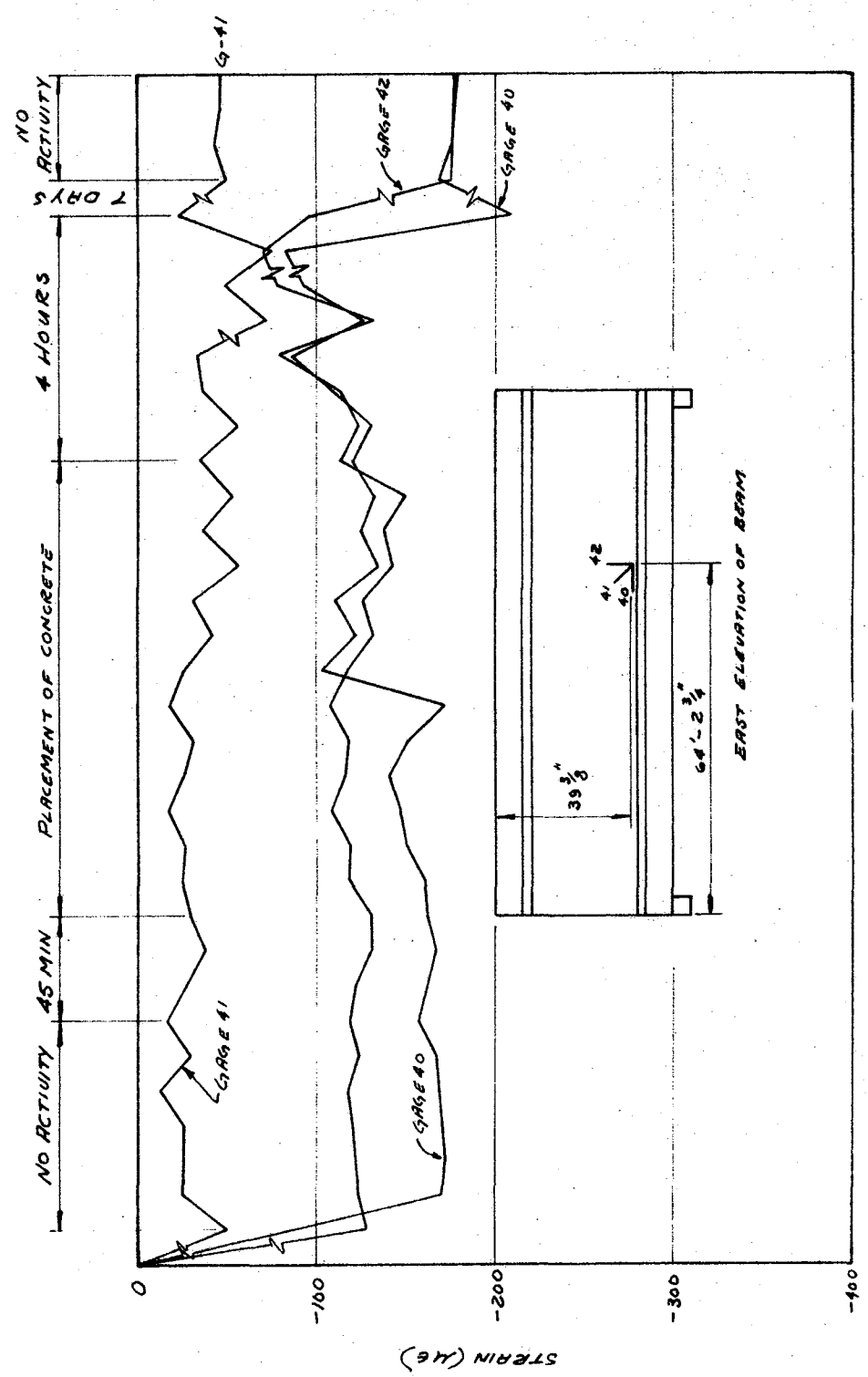

Figure A28. Cont'd.

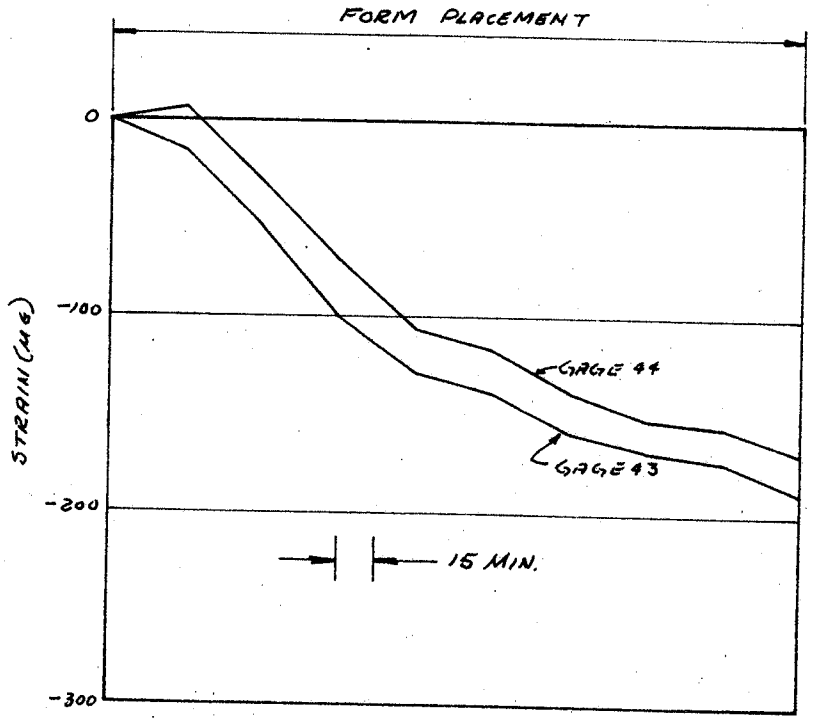

Figure A29. Strain readings, Columbus Drive Gages 43, and 44.

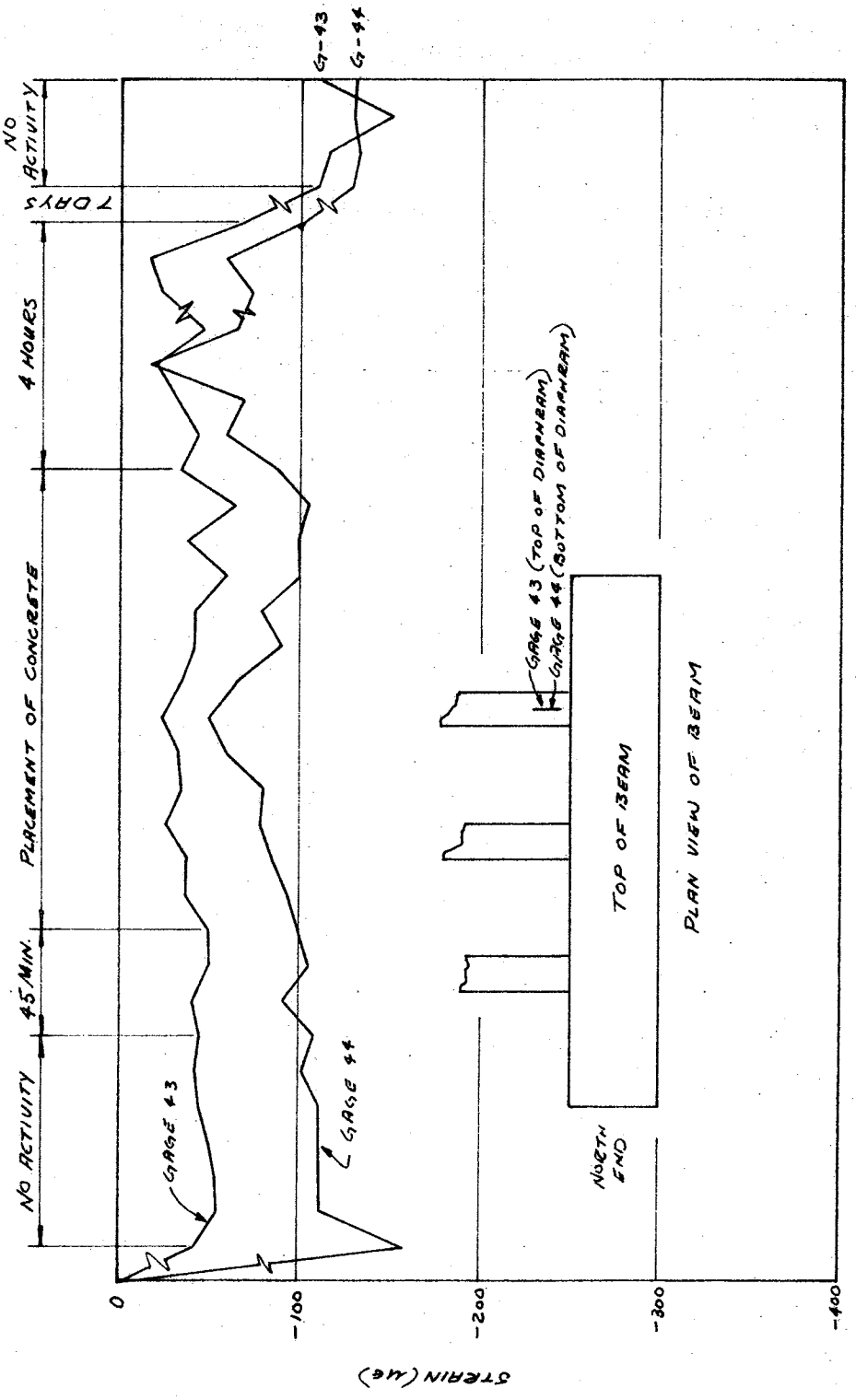

Figure A29. Cont'd.

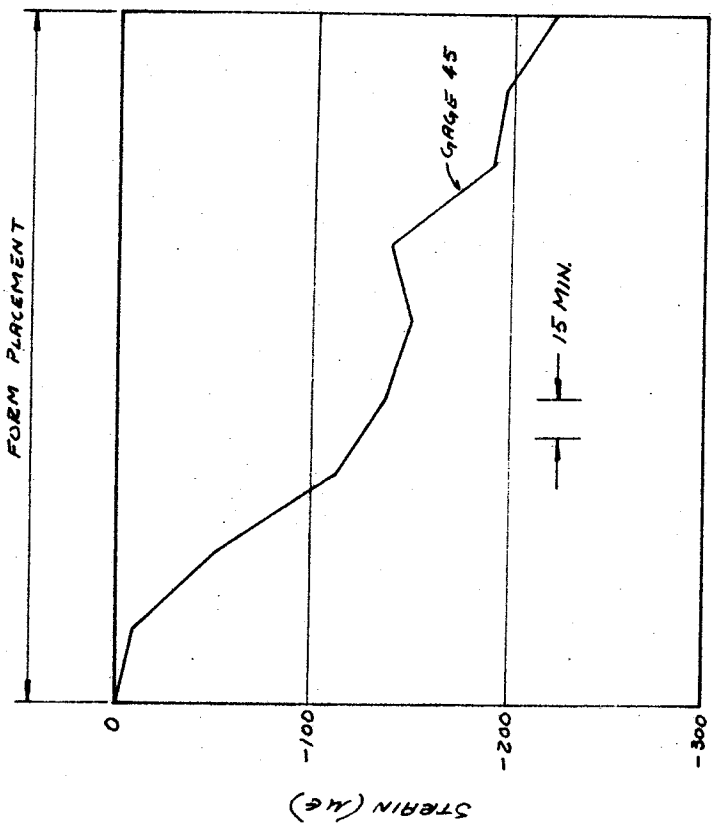

Figure A30. Strain readings, Columbus Drive Gage 45.

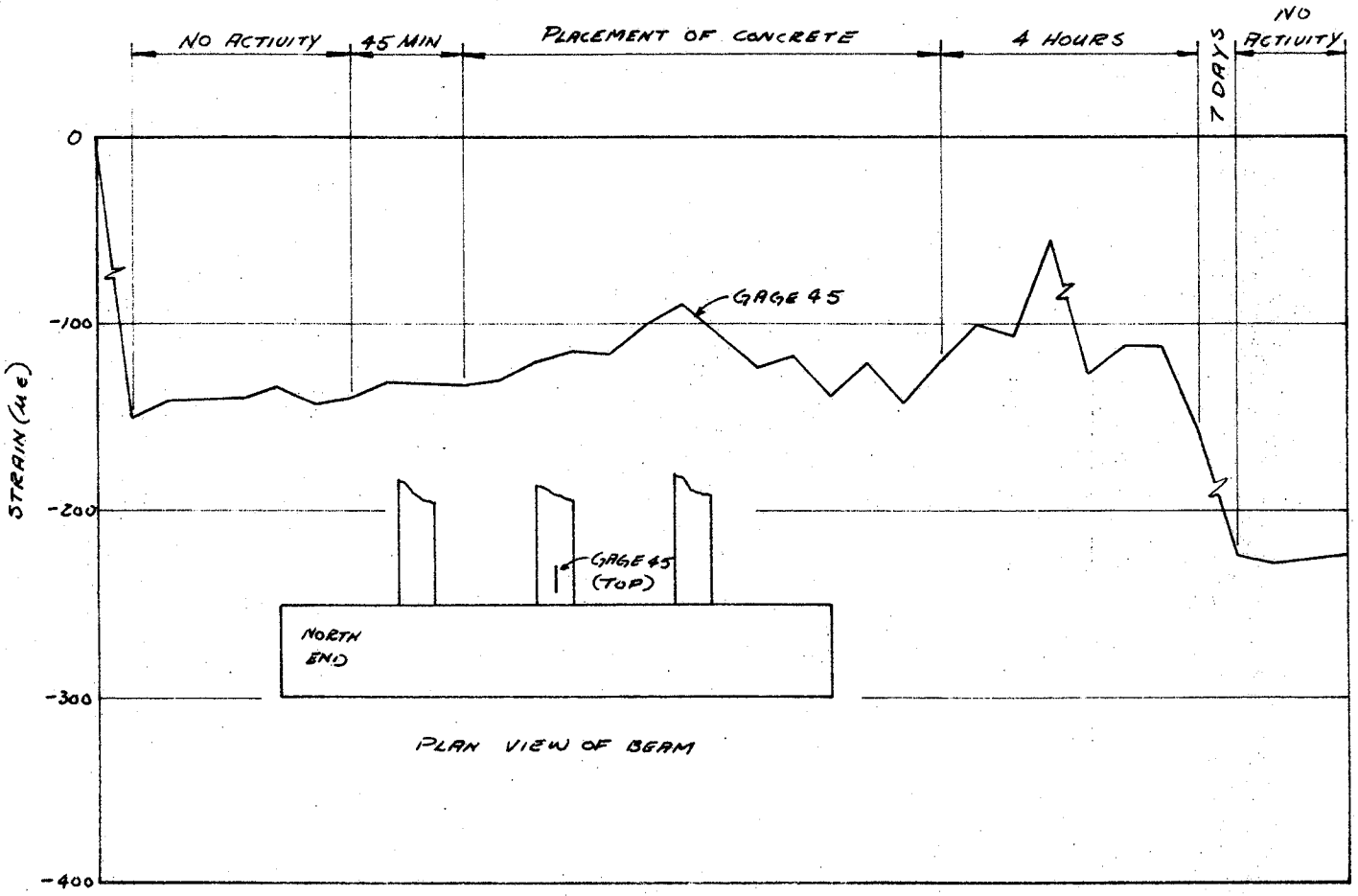

Figure A30. Cont'd.

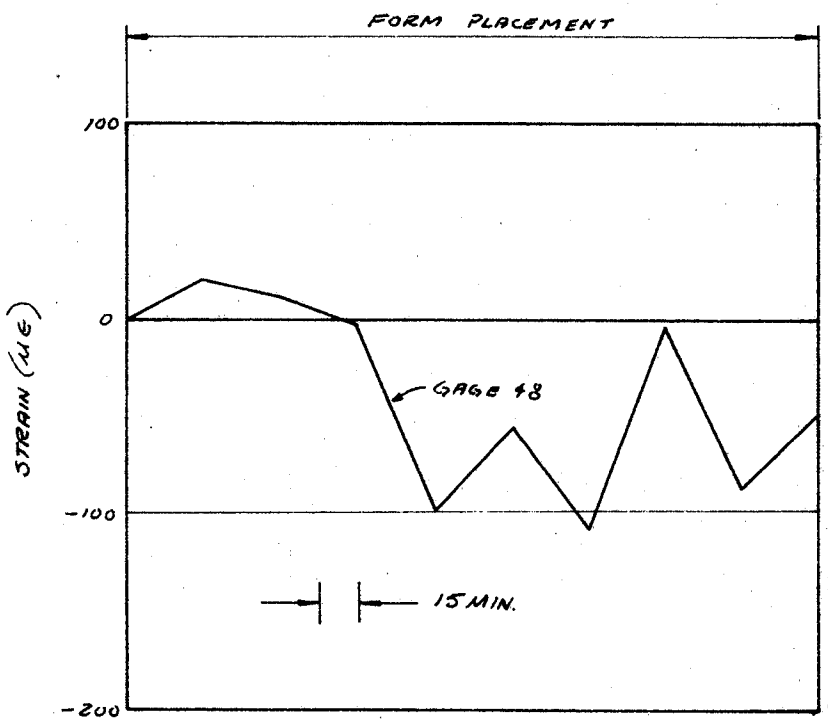

Figure A31. Strain readings, Columbus Drive Gage 48.

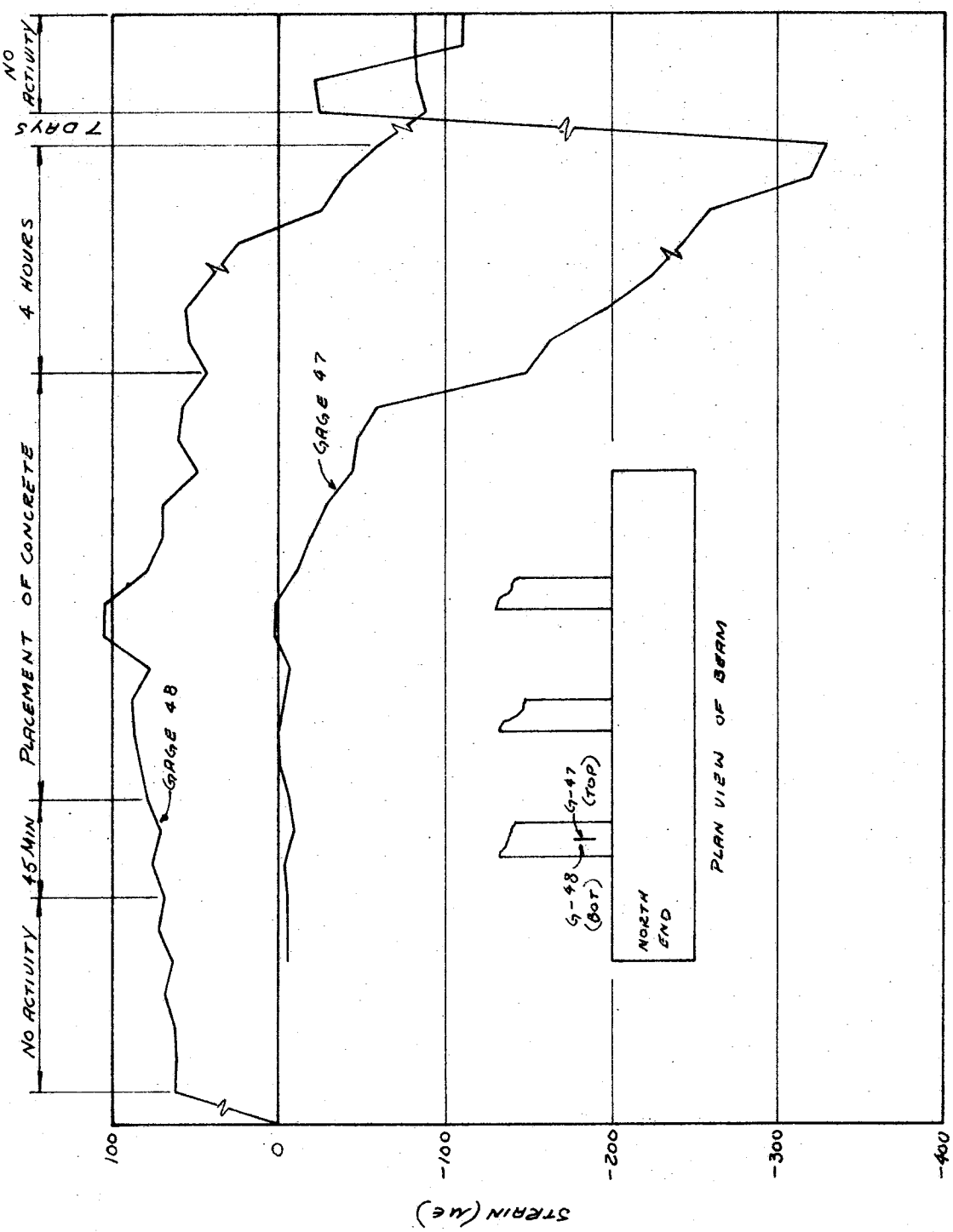

Figure A31. Cont'd.